DOT/FAA/DS-89/36

Criteria For The Use of Lime-Cement-Flyash on Airport Pavements

Research and Development Service
Washington, D.C. 20591

December 1989

Final Report

U.S. Department of Transportation
Federal Aviation Administration

Technical Report Documentation Page

1. Report No.	2. Government Accession No.	3. Recipient's Catalog No.
DOT/FAA/DS-89/36		

4. Title and Subtitle	5. Report Date
Criteria For The Use of Lime-Cement-Flyash on Airport Pavements	December, 1989
	6. Performing Organization Code
7. Author(s)	8. Performing Organization Report No.
William Pailen	
9. Performing Organization Name and Address Pailen- Johnson Associates, Incorporated 8601 Westwood Center Drive Vienna, Virginia 22182	10. Work Unit No. (TRAIS)
	11. Contract or Grant No. DTFA01-85-01047
12. Sponsoring Agency Name and Address U.S. Department of Transportation Federal Aviation Administration Research & Development Service 800 Independence Avenue, N.W., Washington,D.C.	13. Type of Report and Period Covered
	14. Sponsoring Agency Code ARD-240
15. Supplementary Notes	

16. Abstract

A laboratory LCF assessment program was conducted in which samples were fabricated using LCF materials from Ohio, Pennsylvania, Oregon, and Texas sources. The samples were analyzed for the effects of LCF ingredient variations on modulus of resilience, unconfined compressive strength, fracture toughness, tensile strength, and fatigue. Effects of de-icing chemicals on modulus of resilience, unconfined compressive strength, fracture toughness, and tensile strength were analyzed.

A field testing program was conducted in which core samples were obtained from Newark, Portland, and JFK airports. The samples were tested for modulus of resilience and unconfined compressive strength.

A search was conducted of pertinent recent literature on pavement design and analysis, especially LCF pavements.

The report develops design criteria for the use of LCF as a base course in civil aviation pavements. The criteria are based on methods developed by the Port Authority of New York, with adjustments and improvements that resulted from the testing, analysis and literature search. Recommendations are made for improved fatigue testing methods, and for systematic evaluation of the effects of age on the performance of existing LCF pavements.

17. Key Words	18. Distribution Statement
Airport Pavements, Lime-Cement-Flyash.	Document is available to the public through the National Technical Information Service, Springfield, Virginia 22151

19. Security Classif. (of this report)	20. Security Classif. (of this page)	21. No. of Pages	22. Price
Unclassified	Unclassified	128	

Form DOT F 1700.7 (8-72) Reproduction of completed page authorized

ACKNOWLEDGMENT

This report resulted from a three year effort to accumulate and analyze information on the performance of lime-cement-flyash (LCF) in airport pavements and to develop criteria for the design of LCF pavements. The work was performed under Federal Aviation Administration (FAA) contract number DTFA01-85-01047. The FAA Technical Officer on this effort was Dr. Aston L. McLaughlin, ADS-240. His guidance, assistance, advice, and critical review were invaluable and are gratefully acknowledged.

Construction, testing, and analysis of laboratory samples were performed by Resource International, Inc., in Columbus, Ohio under the leadership of V.R Kumar, Director of Construction Services. Analysis of samples obtained in the field was performed at Tuskegee University in Tuskegee, Alabama by graduate student Subdoh C. Biswas under the guidance and direction of Dr. Shaik Jeelani.

TABLE OF CONTENTS

LIST OF TABLES

LIST OF FIGURES

CHAPTER 1 -- INTRODUCTION AND BACKGROUND

1.1 GENERAL

1.1.1 INTRODUCTION

In recent years energy and environmental considerations have brought about an increased interest in the use of LCF in pavement construction. A well-developed technology now exists for the stabilization of bases and subbases with these materials. However, LCF is not always used when it might be appropriate because technical information has not been conveniently available. The following factors are likely to influence the future use of LCF as a base material for varied types of pavement construction:

- Increase in use of coal for fuel (i.e., increase in flyash supply),
- Low energy requirements for producing LCF mixes,
- New technology for LCF use, and
- Widespread availability of lime and flyash.

The primary factors affecting the performance of pavements with LCF base and/or subbase[7] are:

- Loading,
- Interrelationships between load, pavement thickness, and material strength,
- Durability of the material as related to the environment it must serve,
- Quality of construction including uniformity of the final product, and
- Subsurface drainage of the pavement system.

Performance of pavement with LCF as a base/subbase has been studied by the FAA[22] and others.[6,8,15,21,27,28] They have found that LCF base courses are viable materials for use in the construction of pavement. LCF has been used when conventional materials or subgrades require stabilization. Because it can sometimes be purchased inexpensively, use of LCF may provide a basis for very cost-effective pavement construction.

Advantages of using LCF mixtures in pavement construction includes ease in construction and the ability to use conventional construction equipment. The essential requirements for use of LCF mixtures are thorough mixing, uniform spreading, and compaction to a high density.

Administrators, engineers, and researchers recognize the need for technical information on the use of LCF as a base course material for pavement construction. A well-developed laboratory methodology to determine the effects of environment and external loading is an essential step in establishing the physical and mechanical properties of LCF mixtures. These properties could be used as an attempt to determine the short-term effects of environment and external loading on LCF base course materials.

1.1.2 TECHNICAL BACKGROUND AND OBJECTIVES

The subgrade soil supports the pavement and the loads imposed on the pavement surface. The pavement serves to distribute the imposed load to the subgrade over an area greater than that of the tire contact area. The greater the thickness of pavement, the greater the area over which the load on the subgrade is distributed. Therefore, the more unstable the subgrade soil, the greater the required area of load distribution and consequently the greater the required thickness of pavement.

The soils having the best engineering characteristics encountered in the grading and excavating operations should be incorporated in the upper layers of the subgrade if economically feasible. Because of these considerations, soil conditions and the local prices of suitable construction materials are the most important items affecting the cost of construction of landing areas and pavements.[29]

In certain locations of the country where airports are situated, native materials for subgrade and/or base construction may be unsuitable. In view of this, efforts are being made to stabilize the subgrade and base courses by using cement, lime, and flyash in various combinations with the existing

subgrade and/or base material. This recourse to construction of base and/or subgrade is being taken in view of the fact that it would be prohibitively expensive to replace the unsuitable material by obtaining standard graded material.

The use of lime, cement, and flyash in various combinations with the available subgrade and/or base materials has helped to increase the bearing strength of runways and taxiways used by heavy commercial aircraft. However it is not known how the strength is effected on a long-term basis by ingress of chemicals, rainwater, etc., and other environmental effects.

One purpose of this investigation is to develop a methodology to establish material properties depending on optimal proportioning of lime, cement, and flyash in different combinations, chemical activity, etc. Another purpose is to study the long-term changes in the behavior of the combination of materials that may occur as a result of pozzolanic activity and environmental forces.

Mix designs have been developed by the Port Authority of New York and New Jersey[25] for improvement of the base course using certain mixes of lime, cement, and flyash. The design approach developed in this report follows that of the Port Authority. But it also extends it by including stress/strain characteristics of LCF mixtures from several regions of the United States, by expanding the equations for prediction of maximum stress in a pavement slab, and by providing some measurement data that may be helpful in assessing the effects of aging.

The research included performing tests in the laboratory on trial mixes using lime, cement, and flyash. The materials were obtained from four widely dispersed geographic locations, and three water samples having different pH values were used.

It is clear from literature and experience that LCF is a viable base course material for airport pavements. However, the complex, long-duration nature of the chemical reactions that occur within the mixture as well as the effect of external loading, climatic and environmental conditions is not well

understood, especially with regard to LCF pavement performance.

Destabilizing effects on lime and flyash due to chemical reactivity and loss of cementing properties are major factors in the performance characteristics of the LCF mix. Measurement of physical and mechanical properties may provide insight into short term effects, and distress function parameters may be used as indicators for indicators for long-term effects.

By proper experimental design both short-term and long-term parameters will reflect not only chemical and cementing effects but also loading, temperature, and environmental effects.[22]

The objective of this study is to develop a design criteria and construction procedure for using LCF as a base course in civil aviation pavements. Included in the scope of the effort is an evaluation of the mix designs and performance characteristics of existing pavements as well as a laboratory study to quantify the short and long term changes in material behavior as a result of pozzolanic activity and environmental factors.

This report documents the activities and findings of Pailen-Johnson Associates, Inc. (PJA) and its subcontractors in conformance with the work plan submitted to the FAA. The subcontractors are Resource International, Inc., in Ohio and Tuskegee University in Alabama.

1.2 CURRENT PAVING PRACTICES

Present FAA design practices for runways and taxiways consider two types of pavements: (1) flexible, and (2) rigid. LCF however exhibits the characteristics of a flexible pavement immediately after construction, and of a rigid pavement as it matures. Hence, there is a need to develop a set of design guidelines that is specific to LCF.

Flexible pavements consist of a bituminous wearing surface placed on a base course and, when required by subgrade conditions, a subbase. The entire flexible pavement structure is ultimately supported by the subgrade.

The bituminous surface or wearing course must prevent the penetration of surface water, fuel or other solvents to the base course, provide a smooth, well-bonded surface free from loose particles which might endanger aircraft or personnel, resist the shearing stresses occasioned by aircraft loads, and furnish a texture of nonskid qualities, without causing undue wear on tires.

The base course is the principal structural component of the flexible pavement. It has the function of distributing the imposed wheel load pressures to the pavement foundation, the subbase and/or subgrade. The base course must be of such quality and thickness to prevent failure in the subgrade, withstand the stresses produced in the base itself, resist vertical pressures tending to produce consolidation and resulting in distortion of the surface course, and resist volume changes caused by fluctuations in its moisture content.

Rigid pavements for airports are composed of portland cement concrete placed on a granular or treated subbase course that rests on a compacted subgrade. Under certain conditions of soil classification, drainage and frost, a subbase is not required.

The concrete surface must provide an acceptable nonskid surface, prevent the infiltration of surface water, and provide structural support to the aircraft.

The use of LCF in highway and selected aviation pavements has been an accepted practice for over 20 years. In many instances the long term strength gain of these pavements has exceeded the initial design goals of the projects. Little data has existed, however, on the effects of environmental situations such as the ingress of chemicals with rainwater on the pavement. In the aviation environment, these problems have been further complicated by the lack of design guidelines directly applicable to LCF.

1.3 SYNOPSIS OF STUDY ACTIVITIES

The approach used in developing the specification results from the following activities:

- A search for pertinent recent literature on pavement design and analysis, especially LCF pavements,

- Conduct of a laboratory LCF assessment program in which samples were fabricated using LCF materials from four areas and were analyzed for the effects of LCF ingredient variations on modulus of resilience, unconfined compressive strength, fracture toughness, tensile strength, and fatigue, and

- Conduct of a field testing program in which core samples were obtained from four airports and were analyzed for the effects of pavement age on modulus of resilience and unconfined compressive strength.

- Adaptation of design methods developed by the Port Authority of New York with adjustments and improvements that resulted from the testing, analysis and literature search. The following adjustments and improvements were made:

  - LCF strength characteristics that resulted from the tests are available for preliminary design and planning.

- Equations for calculation of the maximum tensile and compressive stresses imposed by an aircraft load on a pavement slab are expanded to take into account the location of the load relative to the edges of the pavement.

CHAPTER 2 - DESIGN AND CONDUCT OF LABORATORY TESTS

2.1 GENERAL

The purpose of the laboratory test activities was to investigate short-term and long-term properties of LCF as they are affected by pozzolanic activity, environmental forces, chemical activity, and optimal proportions of ingredients. From the investigation a database of information was acquired to serve as a baseline to develop a design methodology and construction procedure for the use of LCF as a base course.

The work effort was divided into two parts, sample preparation and sample testing. Two factorial designs were used in sample preparation. The full factored design varied four (4) mixes (varying proportions of LCF sand), three (3) pH values (basic, normal, acidic), and five (5) ages for a total of 60 different combinations. The smaller design varied three (3) ages (varying maturity), three (3) pH levels (acidic, normal, basic), and two (2) de-icing chemicals (urea and glycol) for a total of eighteen (18) different combinations.

The investigation of LCF mix designs which meet FAA design requirements was performed to resolve the following questions for four different LCF sources.

- What are the effects of aging on the mechanical properties and performance of the mix?
- What are the effects of mixing water pH on the mechanical properties and performance of the mix?
- What are the effects of occasional exposure to de-icing chemical?

2.2 DESCRIPTION OF MATERIALS USED

Four sources for LCF materials were investigated. They were Ohio, Pennsylvania, Oregon and Texas. Cement, sand, and water were procured from Ohio, while lime and flyash were procured from the four sources suggested above. The physical properties of the material were to conform to the specifications detailed below:

2.2.1 LIME

In general the term lime refers to oxides and hydroxides of calcium and magnesium, but not to carbonates. There are various types of lime commercially available. The type of lime used in this research study was Type N, and obtained from four different sources/regions, as stated earlier.

2.2.2. FLYASH

Flyash is the finely divided residue that results from the combustion of ground or powdered coal and is transported from the boiler by flue gases. Flyash is collected from the flue gases by either mechanical or electrostatic precipitation devices.[7]

Flyash is a pozzolan and is defined as "a siliceous or siliceous and aluminous material, which in itself possesses little or no cementious value but which, in finely divided form and in the presence of moisture, reacts chemically with calcium hydroxide at ordinary temperatures to form compounds possessing cementious properties."[22]

Flyash is available in different conditions. "Dry" flyash is taken directly from the precipitator or from dry storage. If the flyash is stockpiled in the open atmosphere, it is normally conditioned by adding water to prevent dusting. Some conditioned stockpiled flyashes may develop cementious properties and "set up" in the stockpile. If the flyash has set up, crushing and screening may be required prior to use in stabilized mixtures. In some

instances the collected flyash is slurried into storage pond areas and must subsequently be reclaimed from the pond for use.[7]

Typical ranges of values for the chemical composition of flyash are:

Principal Constituents	Percent
$Si0_2$	28-52
Al_20_3	15-34
Fe_20_3	3-26
CaO	1-10
MgO	0-2
SO_3	0-4
Loss on Ignition	1-30

2.2.3 CEMENT

The type of cement used in this study was Type I Portland Cement conforming to ASTM C150.

2.2.4 WATER

The type of water used in this study was potable water from city water supply system with a pH value of 7. As samples of LCF were to be tested for determination of the effect of pH value, "pH down" chemical manufactured by Aquarium Pharmaceuticals was used to bring the pH value of water to 5 (make water acidic) and lime was added to water to bring the pH value to 9 (make water basic). Lime from the four sources was used to make the water basic for preparation of respective samples.

2.2.5 SAND

The type of sand used was natural sand obtained from river sources, with not more than 10 percent by weight passing the #200 sieve. The other material properties of sand are listed below:

- Sieve analysis

Sieve Size	Percent Passing
#4	100
#8	97.5
#50	28.9
#100	8.6
#200	4.8

- Soundness - 6.4 percent.

According to FAA aggregate gradation requirements, a wide range of gradations is permitted for base course construction. FAA also permits the use of clear sand and if a substantial portion passes sieve #4, the combined LCF gradation is to be adjusted to produce the maximum dry density in the compacted mixture.

2.3 MIX OPTIMIZATION CONCEPT

2.3.1 PREVIOUSLY PUBLISHED CONCEPTS

Review of published literature revealed much detailed information on mixture properties of lime-flyash-aggregate (LFA) mixtures and the factors which influence these properties. Although LFA mixtures do not contain cement, which is added to accelerate hardening, analysis of their properties gave some insight into the performance range of lime-cement-flyash-aggregate (LCFA) properties.

Initially, the early strength properties of LCF mixtures may be higher than those of LFA due to the effect of cement, but over the course of time the LFA strength properties approach the strength properties of LCF mixtures due to continued pozzolanic activity. It was noted that the factors having the greatest influence on LFA mixtures are:[1]

- o Proportions,
- o Materials,
- o Processing, and
- o Curing.

A review of the methods used to proportion the total quantity of lime plus flyash and the lime to flyash ratio has not produced a clear answer for the best procedure. It is generally agreed that lime-flyash stabilization is best suited for sands and gravels; and that the quantity of lime-flyash to be added depends upon the gradation of the soil. Some investigators feel that lime and flyash should be added to produce the maximum density mixture, others feel that the best mixture is a function of water content.

The gradation of the soil is the major contributor in determining the total amount of lime plus flyash that is added to the material. The objective is to add enough lime and flyash to the mixture to be able to form a dense mass when compacted. It has been shown, that the ability of a soil to carry loads is related to soil gradation.[3] Narrowing the band of particle size tends to reduce the load carrying capacity of the soil. Hence, the addition of LFA to a poorly graded soil accomplishes two things; the pozzolans react with lime to form a cementious compound, secondly it produces a better graded mixture with improved load carrying capacity.

Flyash reactivity and the amount of fines present in a soil are two important characteristics affecting the ratio of lime to flyash. Reactivity has been shown to be directly related to the fineness of the flyash.[8] Viskochil[4] investigated this relationship and concluded that 1:9 or 2:8 were the optimal ratios for lime to flyash for sand, silt or clayey soils when 25 percent flyash was used. Other investigators[5] have developed different ratios with

the most common being 1:3 and 1:4. Viskochil and Hoover[4] concluded that greater compaction and corresponding high densities result in higher strengths regardless of the lime-flyash ratio. Hollen and Marks[6] went further and suggested a method for determining optimal mixture based upon obtaining the greatest density.

The optimal mixture is frequently referred to as that which produces the greatest density. However, a study done by the Corps of Engineers[5] in 1976 on sandy gravel-lime-flyash and clay gravel-lime-flyash mixtures concluded that the maximum density did not produce the greatest strength. They concluded that strength was dominated by water content, with the highest strengths occurring at 1 to 2 percentage points dry of optimum.

It has been suggested that the optimmal lime to flyash ratio is generally dependent upon the material being stabilized and the reactivity of the flyash. Due to the variability of aggregate and flyash properties, it is very difficult to project optimal lime to flyash ratios without the actual testing of several specimens over a range of LFA proportions.

2.3.2 PROPORTIONS USED FOR LABORATORY TESTS

Proportioning of lime, cement, flyash, and sand was to be made so that the final selected mixture can be used for the designated purpose. For this study, the bases for proportioning the material components by weight were as follows:

- For Ohio, Texas and Oregon sources of lime and flyash, the lime content was to be between 2.5 and 4.0 percent, flyash content from 11 to 15 percent, lime to cement ratio to be kept below 3:1 and the sand content to be varied as necessary. These proportioning standards were to be used to determine the final LCF proportions.

- For the Pennsylvania source of lime and flyash, the chosen mix proportions 3.2 percent lime, 0.8 percent cement, 13 percent flyash, and 83 percent sand.

For the Ohio, Texas and Oregon sources, the percent factors that can be varied in the mixture selection process are the amount of lime, flyash, and cement, but within the guidelines set above, and varying sand content as required. The job mix formula was determined by laboratory mix design procedures, which included selecting the final mix proportion based on: (i) moisture-density relationship and lime + flyash ratio for selection of sand content, and (ii) maximum unconfined compressive strength obtained from a laboratory-developed curve for unconfined compressive strength and lime + flyash ratio.

2.4 SAMPLE PREPARATION FOR OPTIMIZATION OF MIX

Sample preparation for LCF mixes was according to ASTM D1632 with the following modifications.

- Mold size was 2 inches in diameter and 4 inches in height and made out of solid wall construction.
- Manually operated rammer weighing 5.5 lb. was fabricated specially to suit the mold size for specimen preparation.
- Specimens were prepared in three layers, with 7 blows per layer.
- Weight of compacted soil was determined.
- Specimens were wrapped in plastic sheet and aluminum foil, and maintained at $73^{o}\pm3^{o}F$, for later use for unconfined compressive strength tests.

Seventy specimens were prepared for each source; 35 specimens with six spares for establishing the sand content and 27 specimens with two spares for establishing the lime + cement/flyash ratio.

2.5 TEST RESULTS OF SELECTED MIXTURES

Mix proportions for sand content optimization were designed as detailed below.

Case	Cement %	Lime %	Flyash %	Sand %
i	2.25	6.5	26.25	65
ii	1.9	5.6	22.50	70
iii	1.6	4.70	18.70	75
iv	1.25	3.75	15.00	80
v	0.625	1.875	7.50	90

For the moisture-density relationship, samples were fabricated with a water content range of 4 percent to 18 percent at increments of 2 percent. Test results are presented in Figures 2.1, 2.2, 2.3, and 2.4. For sand-content optimization, samples were fabricated with a sand content range of 65 percent to 90 percent. Test results are presented in Figures 2.5, 2.6, 2.7 and 2.8. For sand content optimization at optimal moisture and dry density a total of 35 samples per source were tested and results are tabulated in Table 2.1 and graphically presented in Figures 2.9, 2.10, 2.11, and 2.12. Test results are summarized as follows:

Maximum LCF Density, pcf, for Different Sand Contents

Source	Sand Content (% by weight)				
	65	70	75	80	90
Ohio	127	131	133	136	134
Pennsylvania	129	131.5	135	137	133
Oregon	128.5	130	135	135	137
Texas	138	140	139	137.5	133.5

Table 2.1 LCF moisture-density relationship (γ_d, pcf).

Source	Sand Content	Moisture Content %							
		4	6	8	10	12	14	16	18
Ohio	65%	-	121.5	124.4	127.3	125.1	122.8	120.2	117.7
	70%	-	123.8	127.7	131.0	127.7	122.8	122.3	120.1
	75%	-	127.8	130.5	133.3	130.7	128.0	125.1	125.2
	80%	126.8	129.4	133.2	136.2	131.6	127.8	125.5	-
	90%	127.6	128.3	132.9	134.2	132.9	131.4	128.7	-
Penn	65%	-	120.4	122.4	125.6	128.4	126.5	121.9	120.0
	70%	-	123.0	123.7	128.6	131.5	126.6	122.8	122.2
	75%	-	126.6	128.2	134.5	133.4	129.2	125.9	123.5
	80%	126.2	127.8	129.9	136.9	136.0	131.1	130.8	-
	90%	126.2	127.5	131.4	132.5	133.4	132.0	130.2	-

Table 2.1 LCF moisture-density relationship (γ_d, pcf). (continued)

Source	Sand Content	Moisture Content %							
		4	6	8	10	12	14	16	18
Oregon	65%	-	122.9	128.7	127.0	124.6	119.2	114.4	115.3
	70%	-	126.9	130.1	129.6	127.2	123.7	121.6	122.1
	75%	-	128.5	134.7	133.7	127.9	122.8	125.8	125.1
	80%	128.4	131.6	135.0	135.3	131.9	128.7	125.8	-
	90%	130.8	133.5	136.2	137.7	136.9	134.9	131.1	-
Texas	65%	-	134.3	134.5	138.0	134.9	130.1	123.0	117.1
	70%	-	137.6	137.1	140.8	136.1	130.5	127.8	122.0
	75%	-	134.5	140.2	140.9	137.2	134.3	125.2	121.3
	80%	130.6	133.5	134.3	131.0	129.5	124.0	119.5	-
	90%	126.2	130.0	133.2	136.0	137.1	132.5	129.8	-

MOISTURE-DENSITY
Ohio

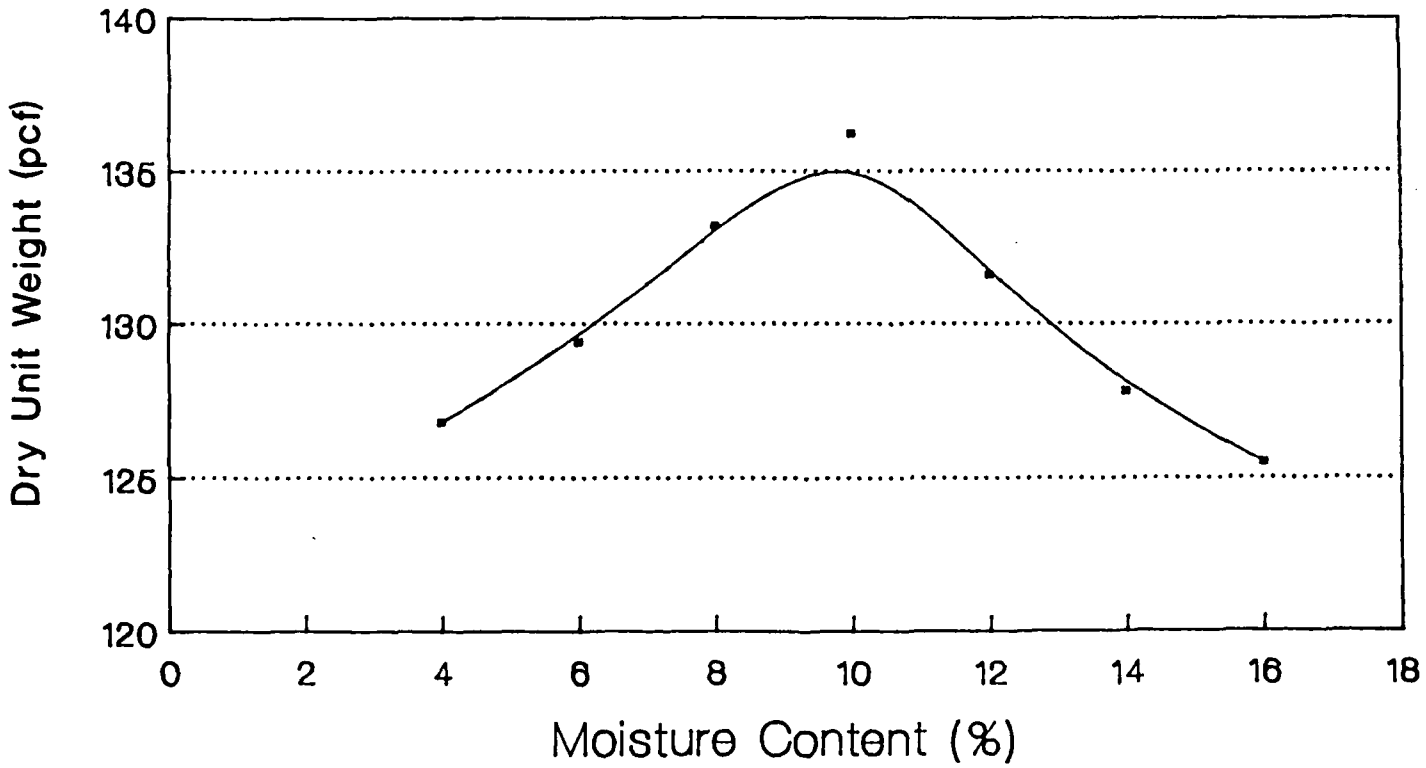

Figure 2.1 Moisture Density, Ohio Source

MOISTURE-DENSITY
Pennsylvania

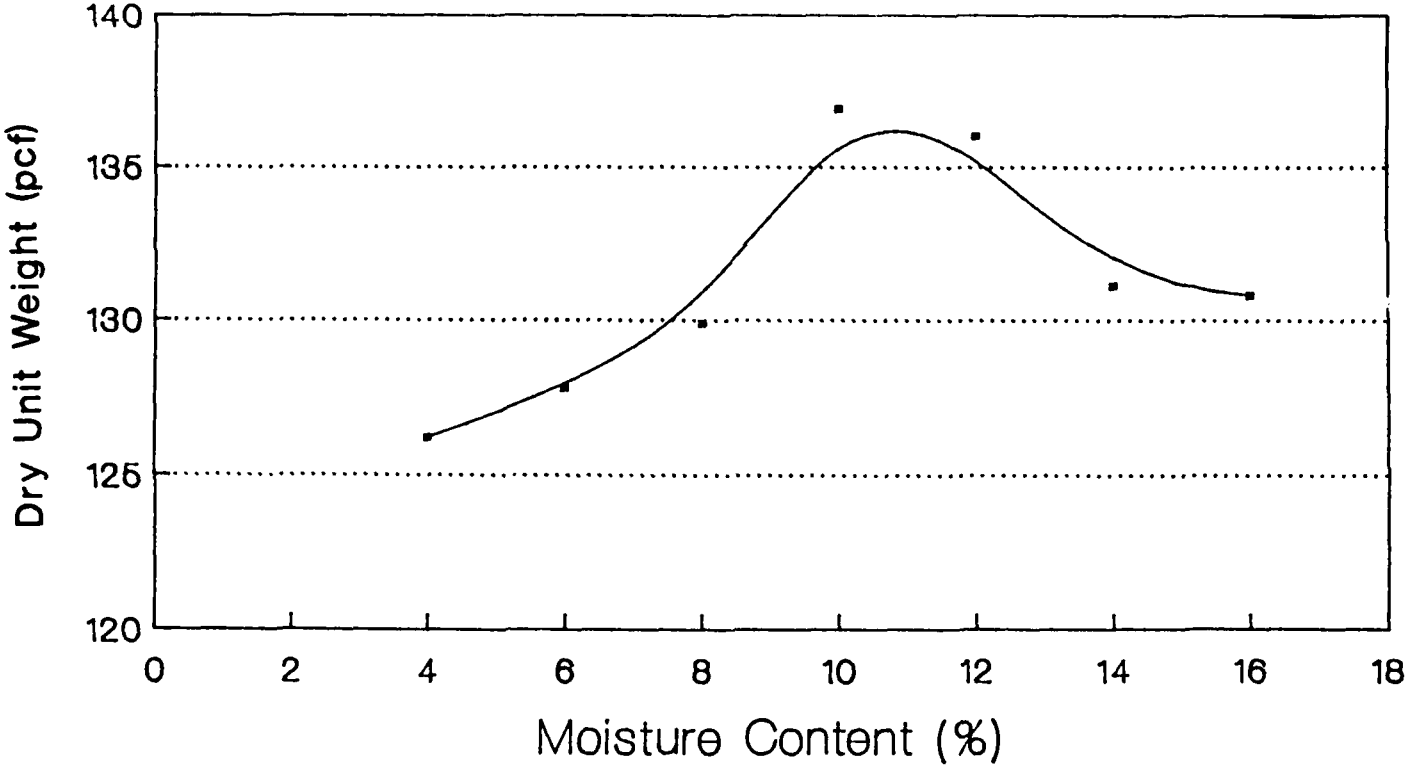

Figure 2.2 Moisture Density, Pennsylvania Source

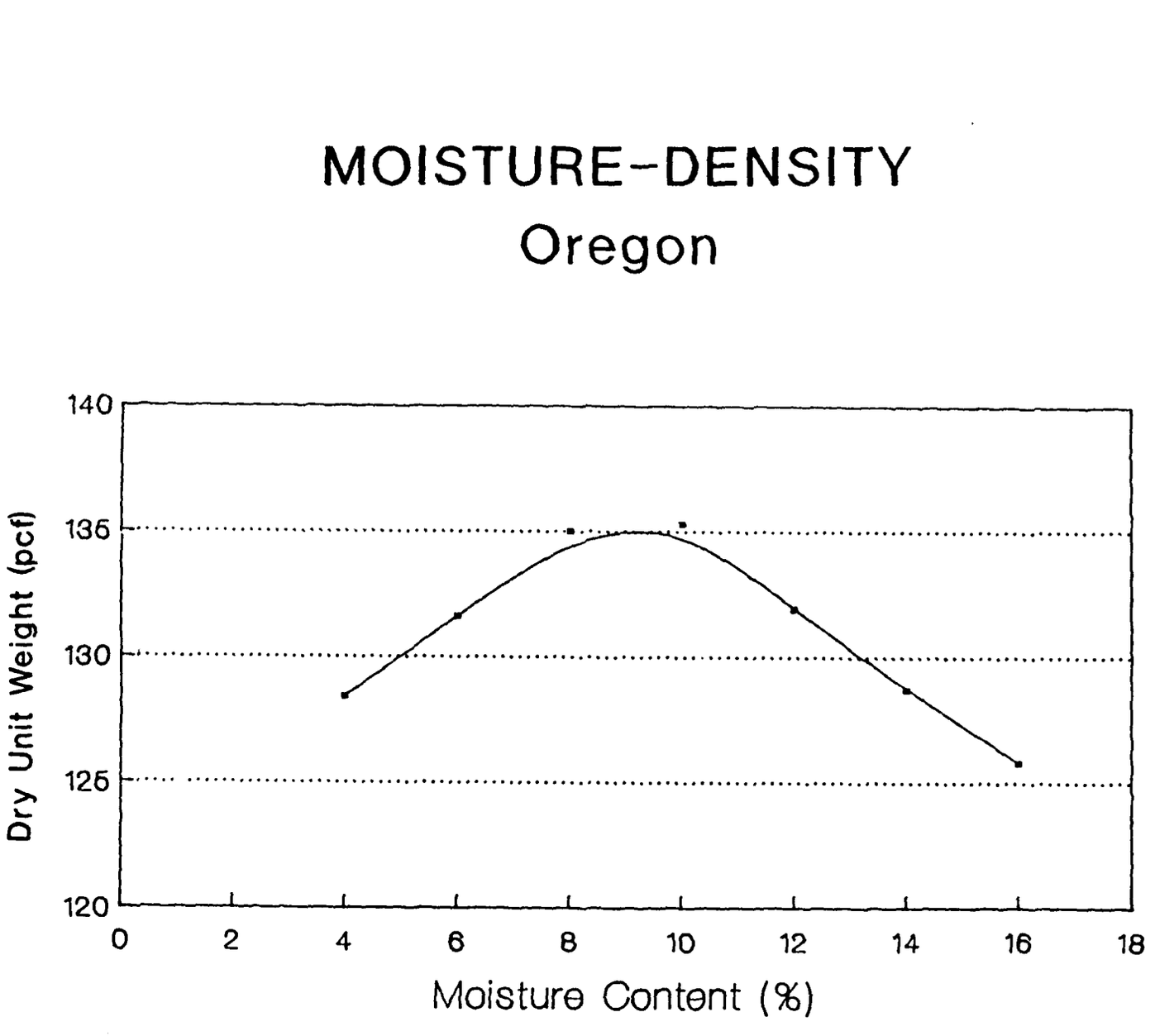

Figure 2.3 Moisture Density, Oregon Source

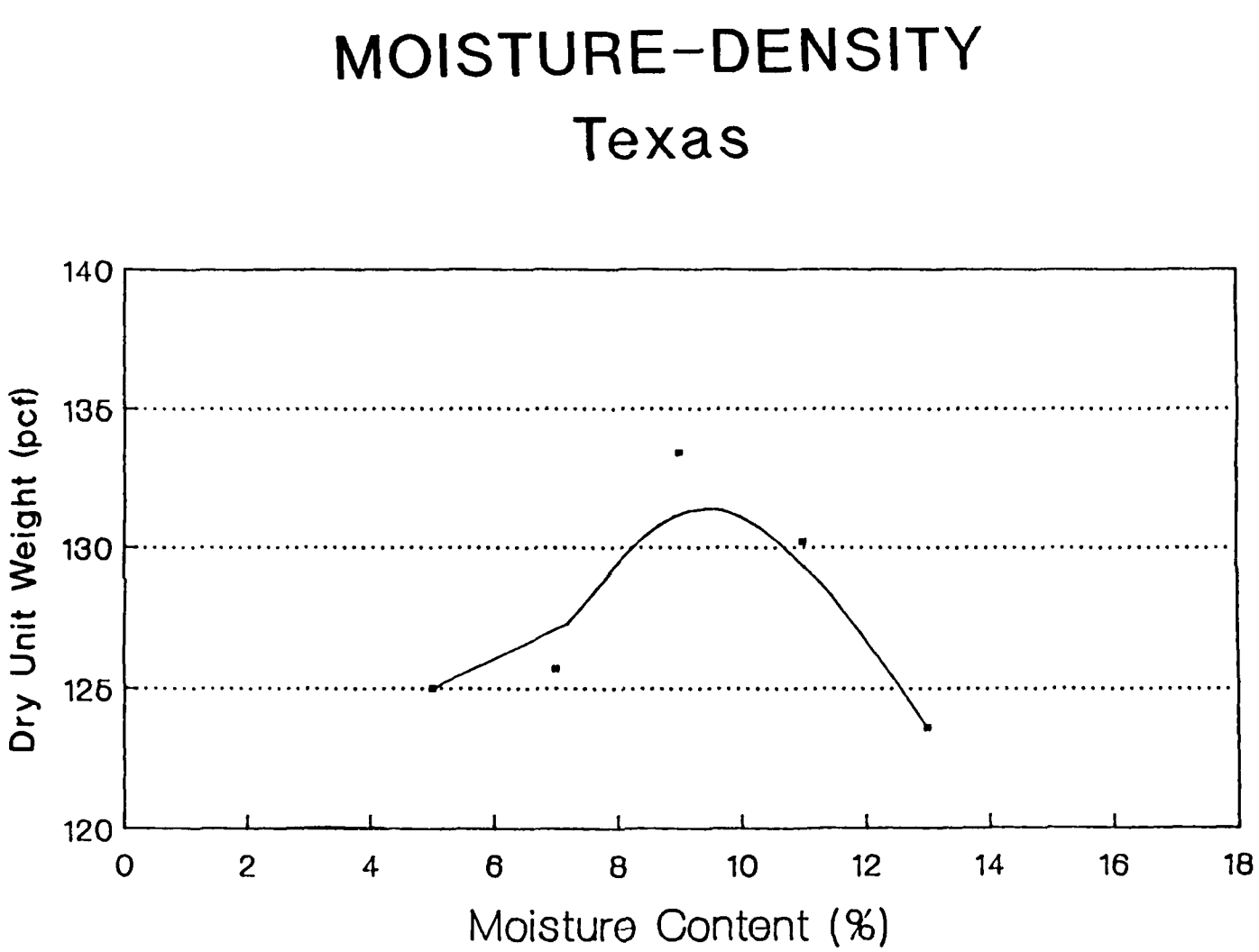

Figure 2.4 Moisture Density, Texas Source

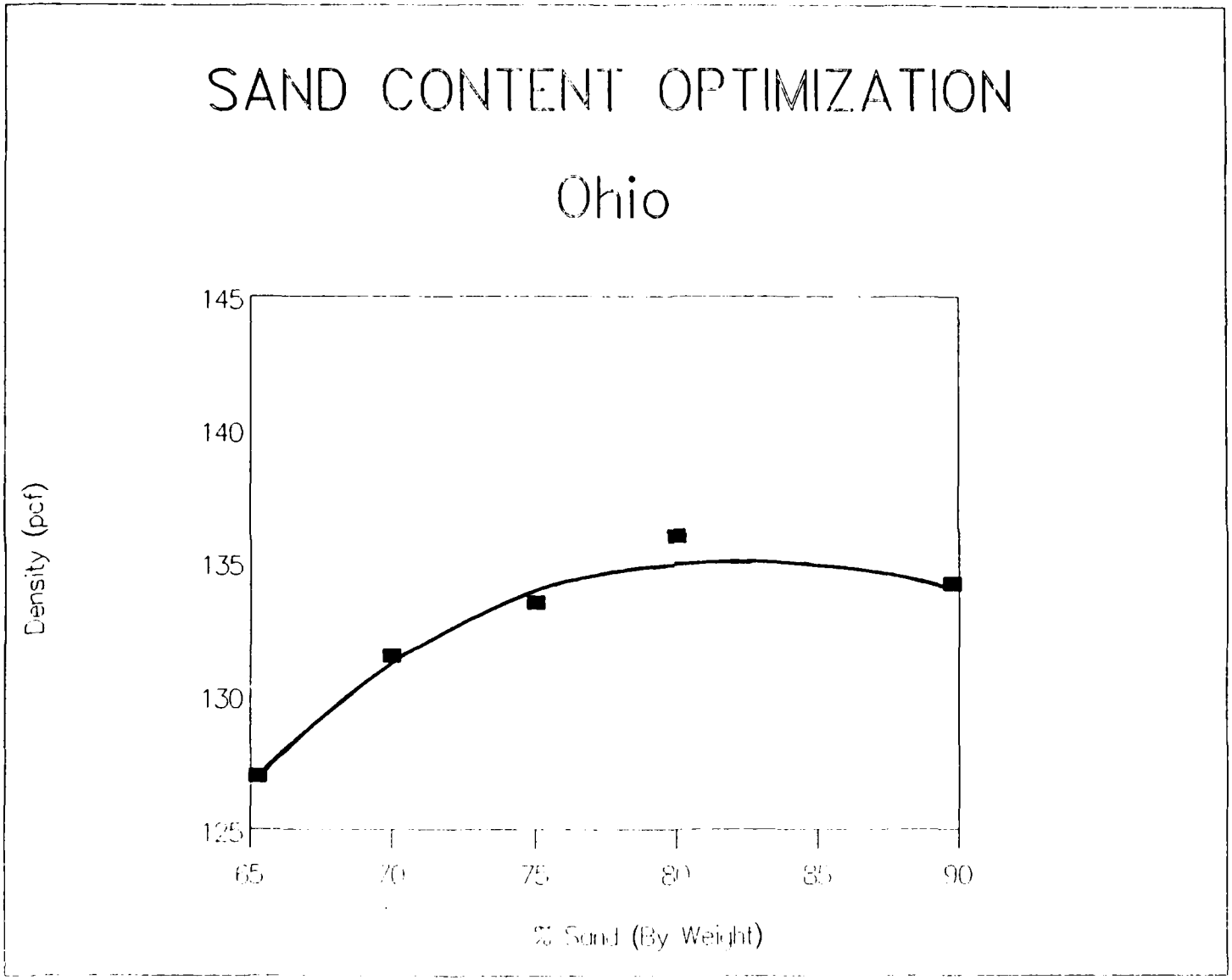

Figure 2.5 Sand Content Optimization, Ohio Source

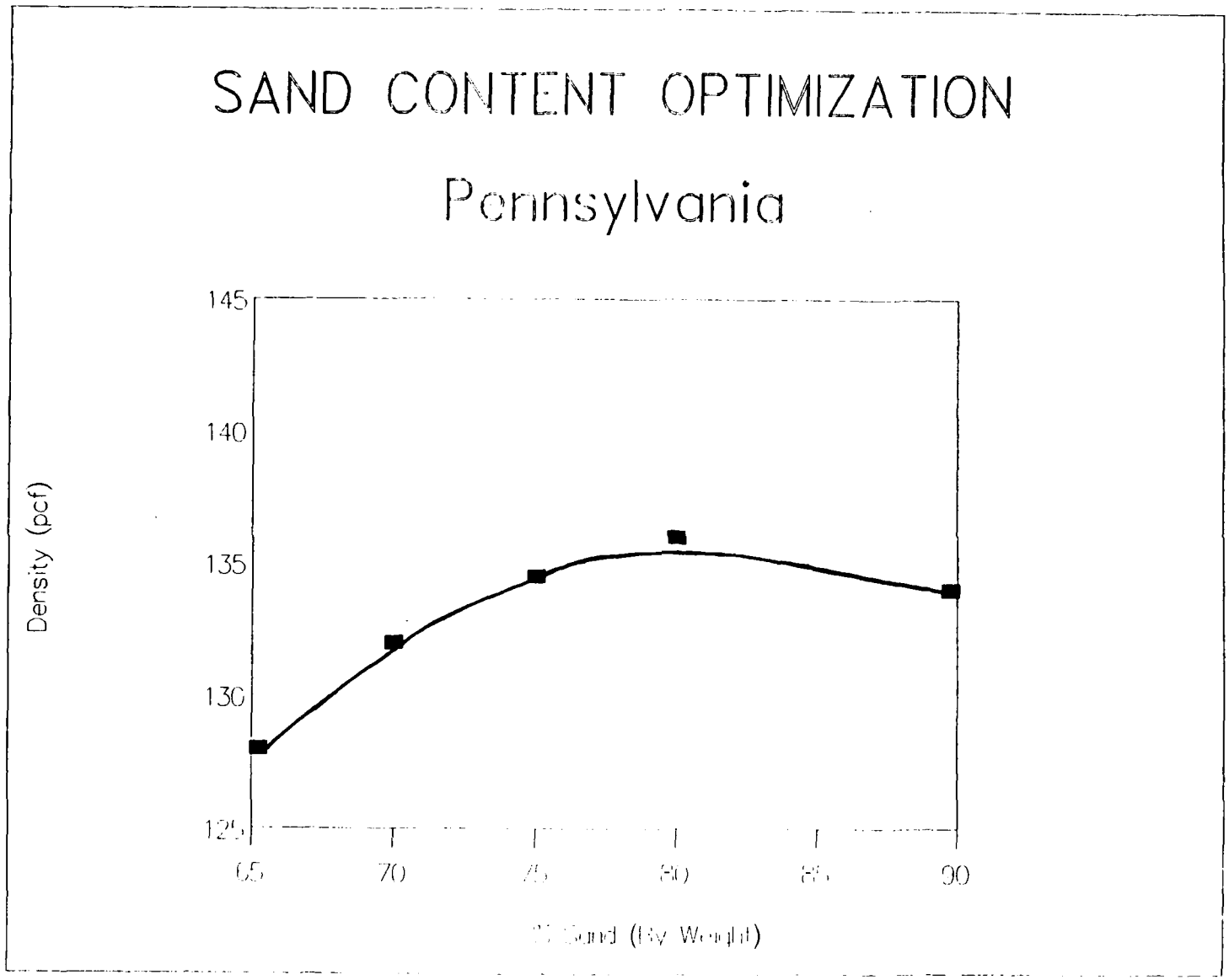

Figure 2.6 Sand Content Optimization, Pennslyvania Source

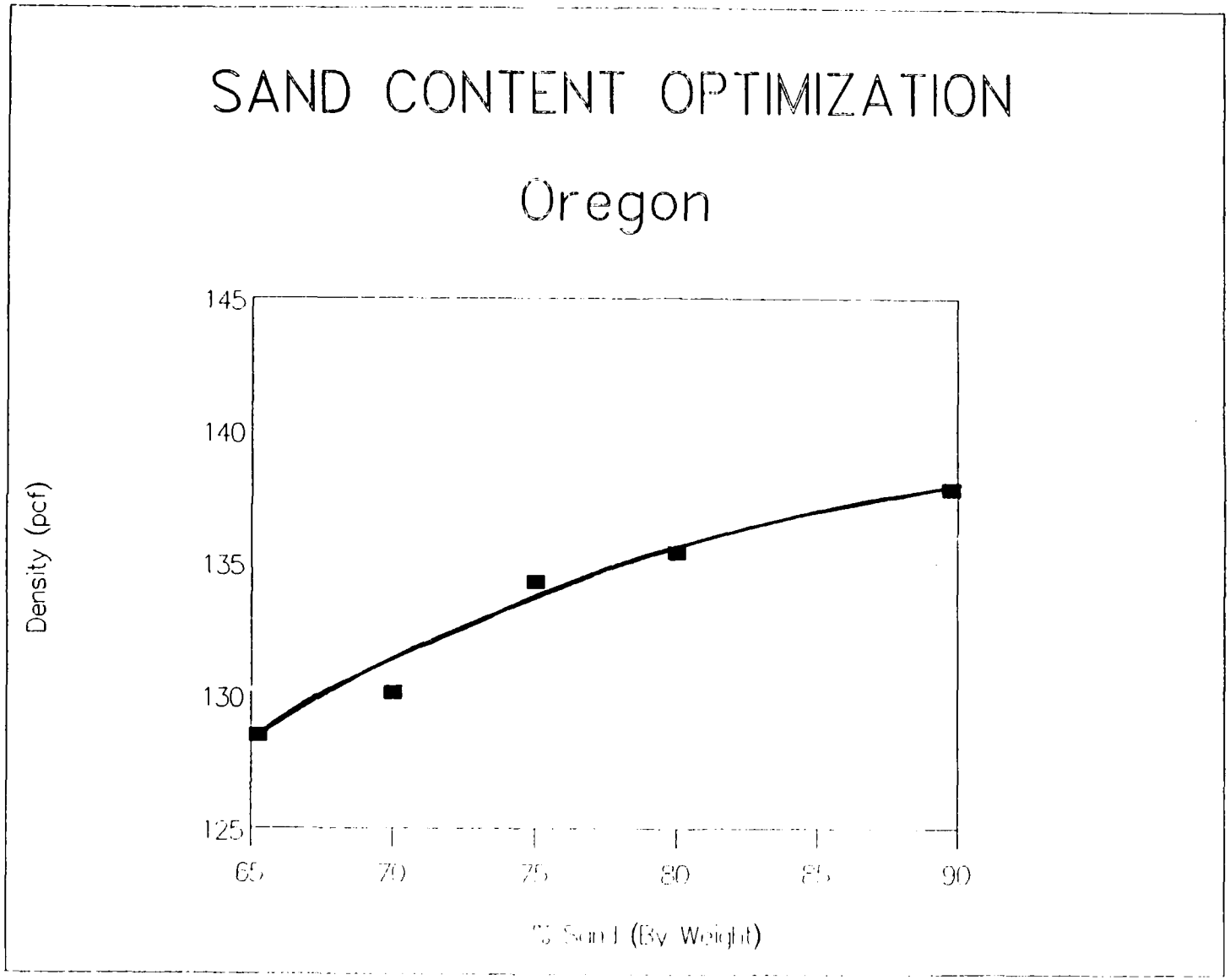

Figure 2.7 Sand Content Optimization, Oregon Source

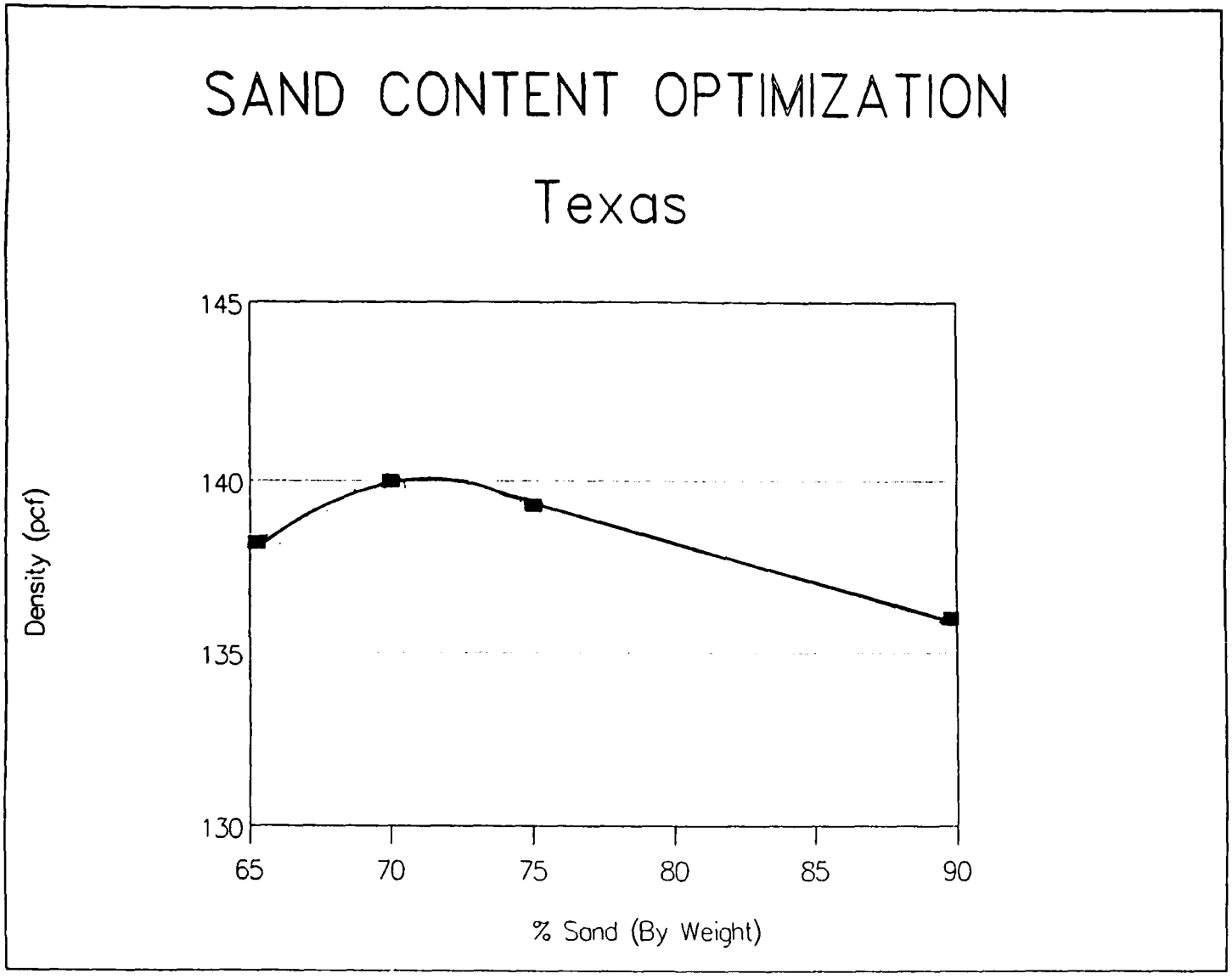

Figure 2.8 Sand Content Optimization, Texas Source

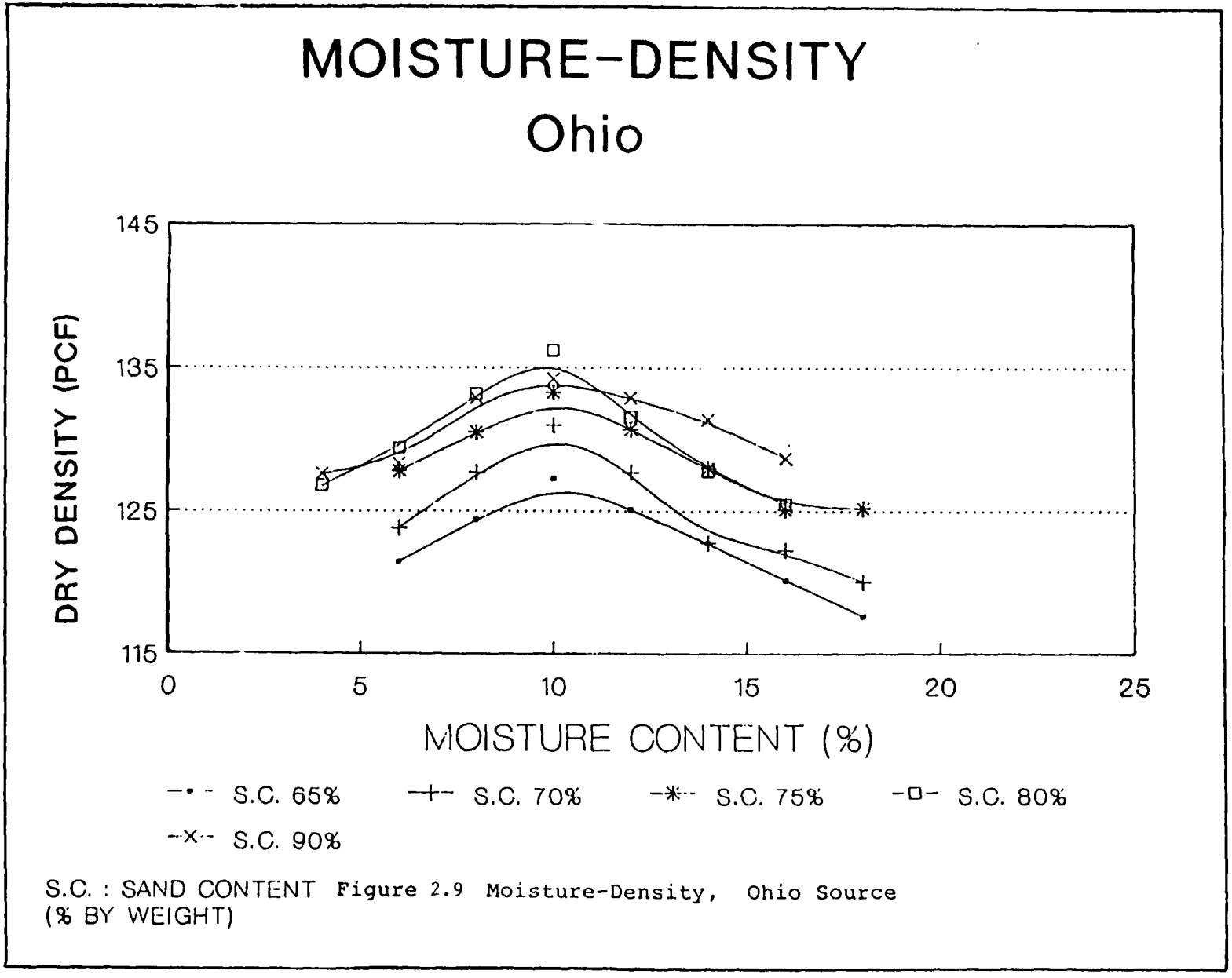

S.C. : SAND CONTENT (% BY WEIGHT)

Figure 2.9 Moisture-Density, Ohio Source

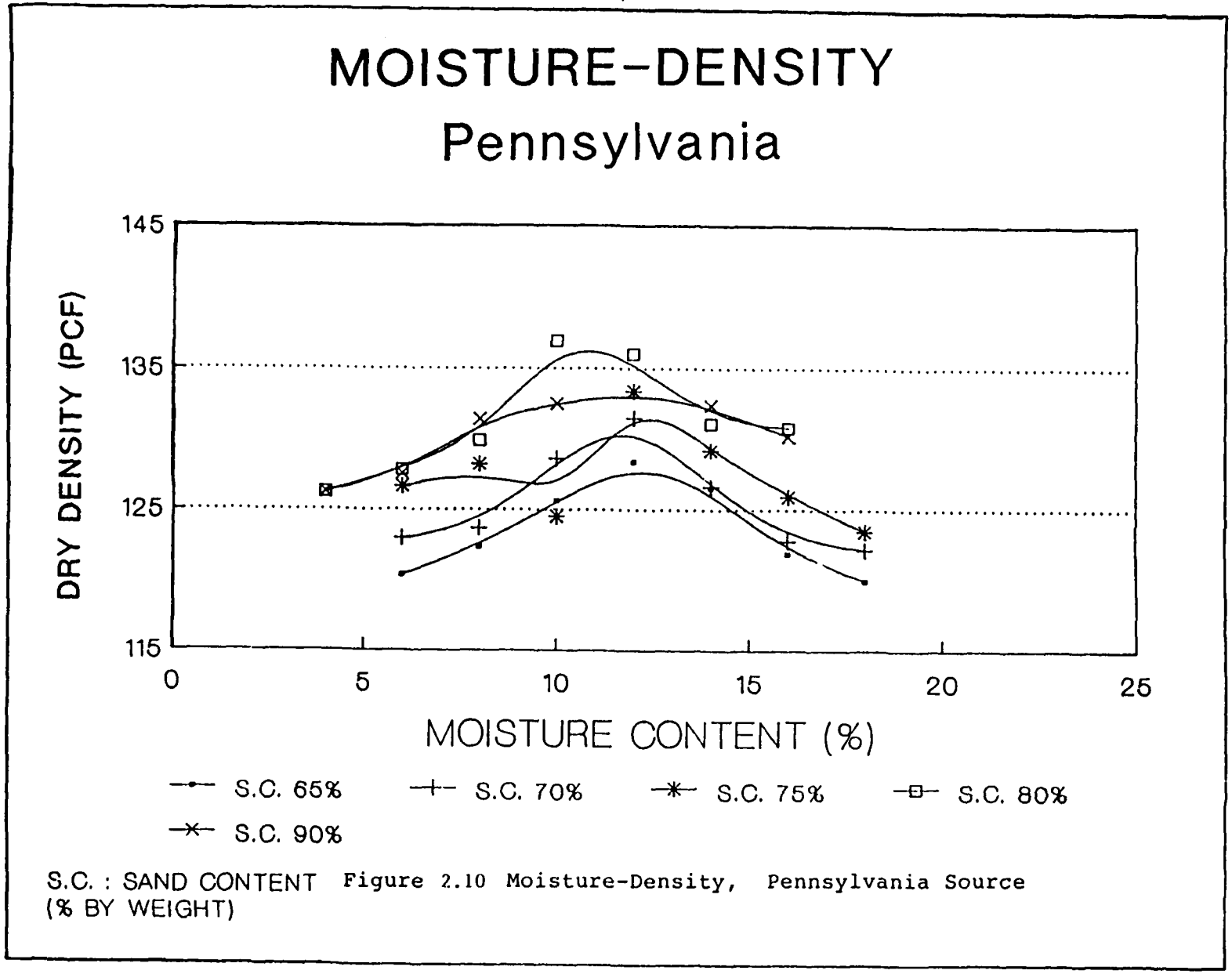

S.C. : SAND CONTENT (% BY WEIGHT)

Figure 2.10 Moisture-Density, Pennsylvania Source

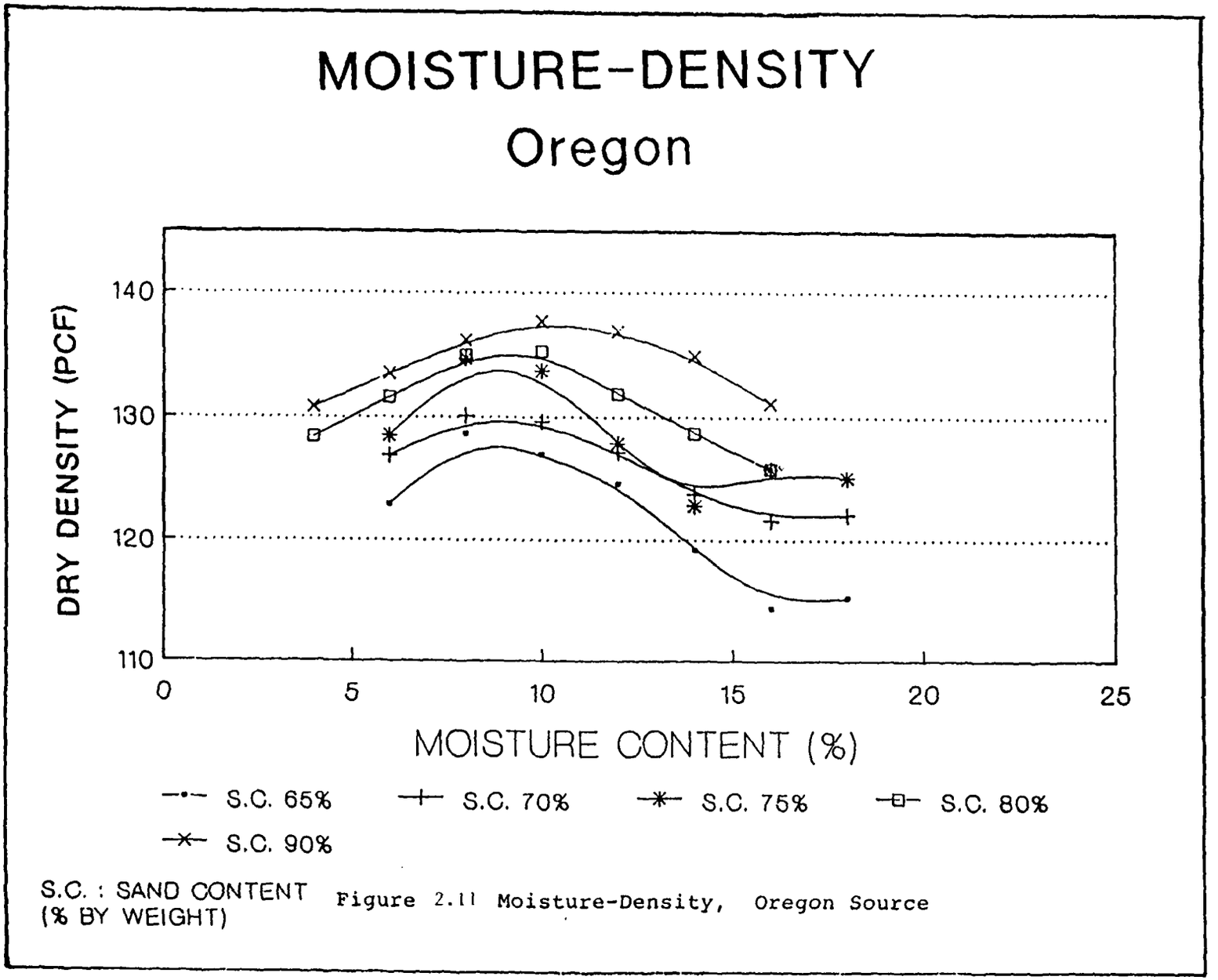

Figure 2.11 Moisture-Density, Oregon Source

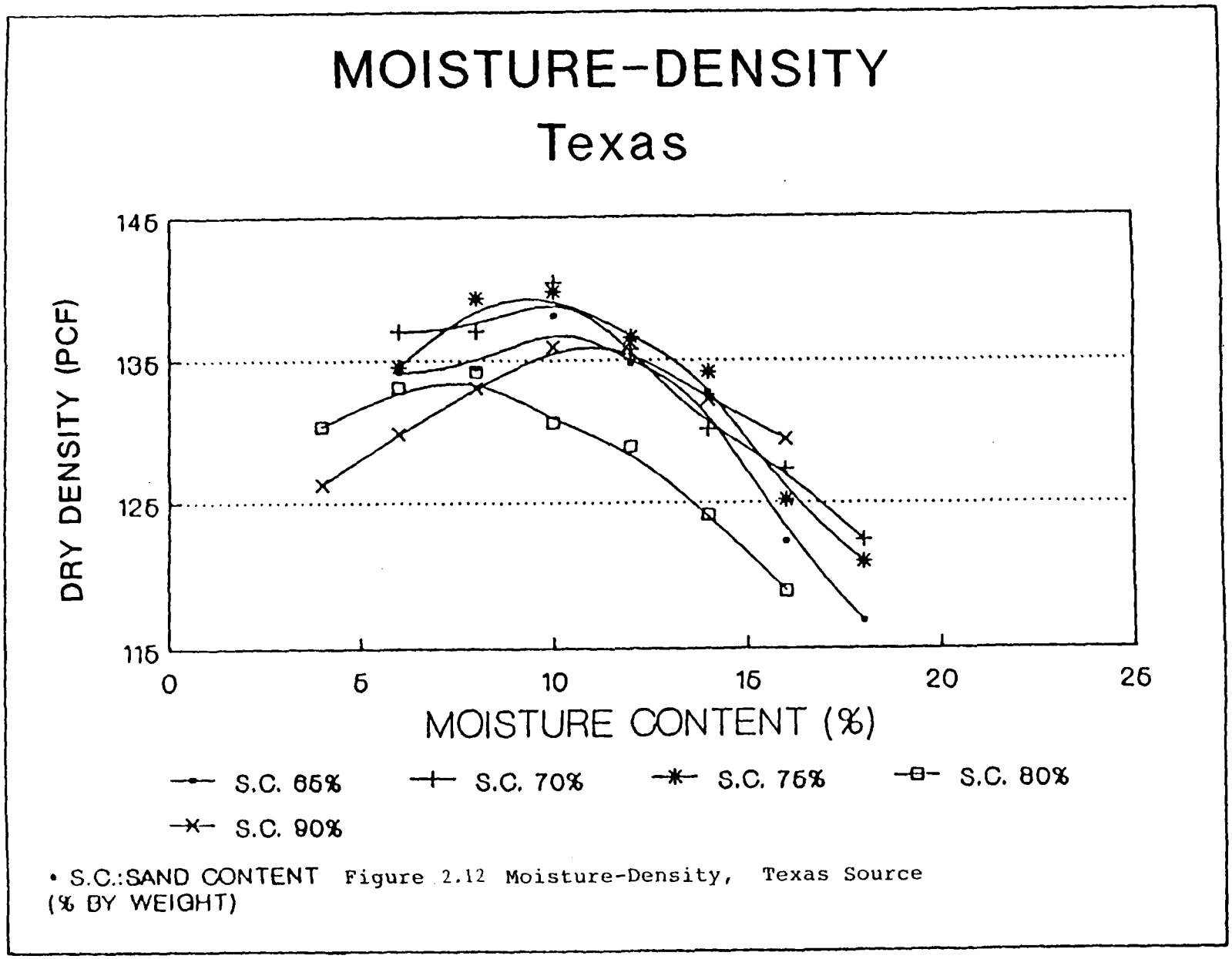

• S.C.:SAND CONTENT (% BY WEIGHT)

Figure 2.12 Moisture-Density, Texas Source

The results of this table and Figures 2.9 through 2.12 illustrate the sand content optimization for Ohio, Pennsylvania, Oregon, and Texas sources, respectively. These curves result in the following optimal sand contents:

	Sand Content (%)	Moisture Content (%)	Maximum Density (pcf)
Ohio	80	10	136
Pennsylvania	80	10.5	137
Oregon	80	9	135
Texas	73	10	140

Mix proportions for optimization of lime, cement, flyash ratio were designed as detailed below:

Design of experiment according to Table 2.2, "Mix Design Factorial" was conducted for four sources: Ohio, Pennsylvania, Oregon and Texas. Nine mix combinations for each source were proportioned as summarized below:

Mix proportions for cement, lime, and flyash optimization

Mix Combination (Lime: Flyash)	Cement	Lime	Flyash	Sand
2.5 : 11	.7	2	11.7	85.6
2.5 : 13.5	.65	1.95	14.0	83.4
2.5 : 15	.64	1.92	15.4	82.0
3.25 : 11	.86	2.59	11.7	84.9
3.25 : 13.5	0.84	2.52	14.0	82.7
3.25 : 15	0.83	2.48	15.3	81.4
4 : 11	1.05	3.15	11.6	84.2
4 : 13.5	1.03	3.07	13.8	82.0
4 : 15	1.01	3.03	15.2	80.8

Table 2.2 Factorial Mix Design

Material Source	Flyash Content, %	Lime Content, % 2.5	3.25	4
OHIO	11	x	x	x
	13.5	x	x	x
	15	x	x	x
OREGON	11	x	x	x
	13.5	x	x	x
	15	x	x	x
TEXAS	11	x	x	x
	13.5	x	x	x
	15	x	x	x
Lime/Cement Ratio		3 : 1		
Sand Content		Variable according to the above proportions.		

x 3 replicates

The water content that resulted from these mix combinations were the following:

Ohio source:	9.1 percent
Pennsylvania source:	9.5 percent
Oregon source:	8.25 percent
Texas source:	9.25 percent

Three replicates were prepared for each mix combination and tested for compressive strength. Samples were wrapped in plastic bags and cured at 73°F ± 3°F until the time of testing. A total of 27 samples were tested for each source.

2.6 OPTIMIZED MIX SELECTION

The selected mix proportions are tabulated below:

Source	Lime + Cement: Flyash Ratio	Lime: Cement Ratio	Maximum Dry Density (pcf)	Optimum Moisture Content (%)
Ohio	1:4	3:1	136	10
Oregon	1:4	3:1	135	9
Texas	1:3.85	3:1	140	10
Penn	1:3.33	4:1	137	10.5

The minimum compressive strength of the above four mixes was greater than 400 psi in all cases, which is in conformity with ASTM C 593 standards.

2.7 SAMPLE PREPARATION

Specimens for laboratory investigation using the optimized mixes were fabricated according to ASTM test procedure with appropriate modifications as necessary. Two types of cylindrical specimens were fabricated: 234 specimens, 2 inch in diameter and 4 inch in height and 156 specimens, 3 inch in diameter and 6 inch in height. The optimized mixes used for fabrication of the laboratory specimens are detailed below:

- Ohio Source:

Lime + Cement: Flyash	Ratio of	1:4
Lime: Cement	Ratio of	3:1
Material percentages:	Sand	80
	Flyash	16
	Lime	3
	Cement	1

- Oregon Source

Lime + Cement: Flyash	Ratio of	1:4
Lime: Cement	Ratio of	3:1
Material percentages:	Sand	80
	Flyash	16
	Lime	3
	Cement	1

- Texas Source

Lime + Cement: Flyash	Ratio of	1:3.85
Lime: Cement	Ratio of	3:1
Material percentages:	Sand	73
	Flyash	21.5
	Lime	4.1
	Cement	1.4

- o Pennsylvania Source

Lime + Cement: Flyash	Ratio of	1:3.33
Lime: Cement	Ratio of	4:1
Material percentages:	Sand	83
	Flyash	13
	Lime	3.2
	Cement	0.8

Sand was oven-dried before use in the mix. Proportioning of all ingredients in the mix was by weight, except water which was by volume. The quantity of water used in the mix for various sources is indicated below:

Source	Specimen Size (in.)	Water in CC. per Specimen
Ohio	2 x 4	50
	3 x 6	160
Oregon	2 x 4	45
	3 x 6	144
Texas	2 x 4	50
	3 x 6	160
Pennsylvania	2 x 4	52.5
	3 x 6	168

2.7.1 CYLINDRICAL SPECIMENS

Water in measured quantities was added to the solid components of the mix and mixed in a mechanical mixer until the mix was homogeneous. Specimens of size 2 in. x 4 in. and 3 in. x 6 in. were prepared by compacting the mixed material in the 2 inch and 3 inch molds respectively with collars attached. The compaction was performed in three 3 approximately equal layers to give a total compacted depth about 5 inches and 7 inches respectively for the two specimen sizes. Each layer was compacted with 7 uniformly distributed blows from the

5.5 lb. sleeve-type rammer dropping free from a height of 12 inches above the elevation of soil. During compaction, the mold rested on a dense, firm, uniform, and stable base. Following compaction, the extension collar was removed and the compacted soil was trimmed flush using a straightedge. The mold and moist mix were weighed and recorded. The mold with the moist mix was then wrapped with plastic and aluminum foil and oven-dried for 24 hours at 140 ^{o}F. The specimen was extruded from the mold after 24 hours of oven-drying, and weight of specimen determined, wrapped in plastic and aluminum foil, and kept in oven again at 140^{o}F to await test. The dry density and moisture contents of the mix were determined for comparison with the optimized mix design data established earlier.

Specimens of size 2 inch x 4 inch were used for unconfined compressive strength tests. Specimens of size 3 inch x 6 inch were saw-cut after removal from molds into three approximately equal sections of 3 inch x 2 inch, and used for modulus of resilience, indirect tensile strength, and fracture toughness tests. Separate sets of samples were prepared for the three pH levels of water.

To determine the effect of de-icing chemicals on the material properties of LCF mix, the specimens were dipped in urea and glycol and tested for the same properties as for the control specimens. In order to minimize the cost of the study, these tests were performed only on the Ohio source material. The specimens were dipped in glycol/urea for 24 hours before the tests.

2.7.2 BEAM SPECIMENS

In addition to cylindrical specimens, composite beam specimens were fabricated for fatigue and reflection cracking tests. The sizes and number of beam specimens fabricated are detailed below:

Ohio Source: LCF base thicknesses of 2 inch, 3 inch, and 4 inch.

Asphalt concrete overlay thicknesses of 1 inch, 1-1/2 inch, and 2 inch.

18 specimens to be tested at two stress levels.

Similar specimens were fabricated for the other three sources of materials.

The asphalt concrete mixtures used in the preparation of fatigue specimens were selected to meet the FAA specifications for asphalt concrete wearing course.

2.7.3 AGGREGATES

Crushed limestone aggregate from a local American Aggregate Company was utilized for the manufacture of asphalt concrete specimens. The aggregates used were #57 crushed limestone as the coarse aggregate and natural sand as the fine aggregate. The crushed aggregate generally showed sharp, angular, and gritty particles and, for the most part, contained at least one fractured face in the particles and were reasonably free from excessive dust or other deleterious coatings, weathered pieces, or excessive flaky and/or elongated pieces. Measured water absorption of particle size ranged between 2.9 percent and 3.2 percent. Aggregate gradation conformed to FAA specifications for asphalt concrete surface course. Gradation ranges of the #57 crushed aggregate and natural sand, based on frequent samplings, are shown in Table 2.3. Table 2.4 gives details about the combined gradation of #57 limestone aggregate and natural sand used in the development of the P-401 mix. Design of aggregate blends for this investigation is based on:

(i) Raw material aggregates and their individual gradings.
(ii) General conformance with FAA specifications for P-401 mix.

For mix design and investigation, five proportions of aggregate were used: 5.5, 6, 6.5, 7, and 7.5 percent by weight of total mix.

Table 2.3
Aggregate Gradation Limits

#57 Lime Stone		Natural Sand	
Sieve Size	% Passing	Sieve Size	% Passing
1/2"	100	3/8"	100
1"	95-100	#4	95-100
1/2"	25-60	#8	70-100
#4	0-10	#16	45-80
#8	0-5	#30	25-60
		#50	5-30
		#100	1-10
		#200	0-4

Table 2.4

Combine Aggregate Gradation of P-401 Asphaltic Concrete

Sieve Size	Percent Passing	FAA Gradation Limits
1/2"	100	100
3/8"	91	79-93
#4	70	59-73
#8	58	46-60
#16	45	34-48
#30	30	24-38
#50	17	15-27
#100	9	8-18
#200	3	3-6

Note: 1 in. = 25.4mm

2.7.4 SPECIMEN CONSTRUCTION

The optimal asphalt content for the selected aggregate gradation was determined using Marshall design procedures and 75 blows/face compaction efforts. Optimal asphalt content was determined as the average of asphalt content for optimum stability, density, and 4 percent air voids. Figure 2.13 shows the Marshall mix design properties for this mix.

Specimens were constructed in two stages. First asphalt concrete beams 3 inch wide, 24 inch long and three thicknesses namely 1 inch, 1-1/2 inch, and 2 inch were fabricated. This included an asphalt concrete hot mix which was prepared in the laboratory and placed in a steel beam mold according to the job-mix formula referred to above. The temperature of the mix was about 280^{o}F. A wire comb was passed through the loose hot mix back and forth for even distribution of the mixture in the mold. The mixture in the mold was then pressed under steadily increasing load until the asphaltic mixture was compacted to a desired thickness rather than specific load to ensure that desired density would be achieved. The mold was then dismantled and the specimen was placed on a stiff support, such as a piece of wood or steel, to await the second stage of specimen preparation. All precautions were taken to prevent damage to the beam samples before the next stage of specimen preparation. The compacted specimens were allowed to cool at room temperature for 24 hours.

The second stage of specimen preparation consisted of joining the LCF mix with the asphalt concrete beam. The asphalt concrete beam was treated with a prime coat of MC-70 cutback asphalt at the rate of 0.25 gallon per square yard (1.1 liter per square meter) and allowed to cure. The beam was then placed in the steel mold and LCF mix of predetermined quantity was placed over the asphalt concrete beam. A wire comb was passed through the loose mix back and forth for even distribution of the LCF material over the asphalt beam. The mixture in the mold was compressed uniformly with increasing load until the LCF mixture was compacted to the desired thickness to ensure that desired density would be achieved. The maximum load was then maintained constant for 2 to 3

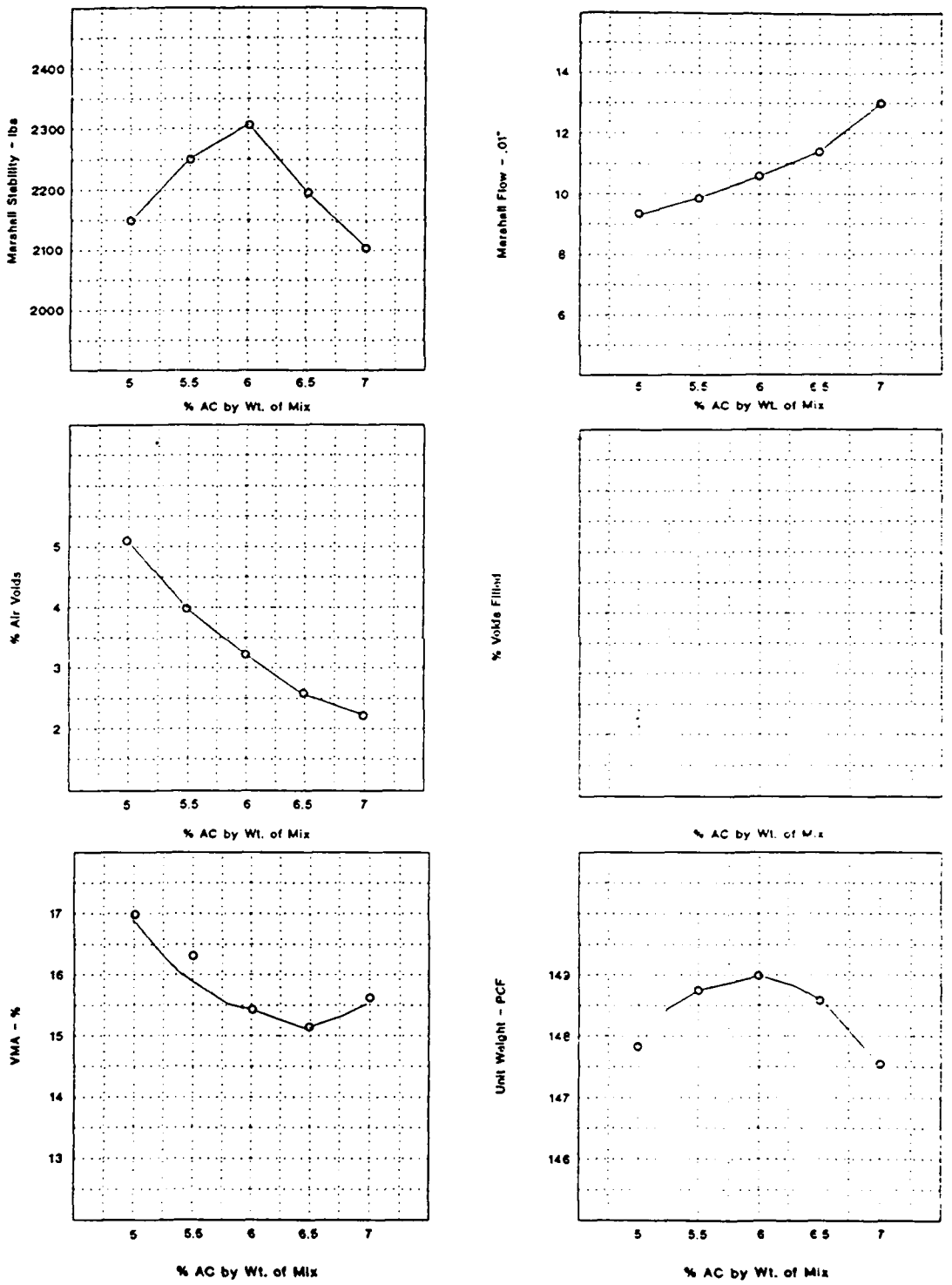

Figure 2.13 - Marshall mix design data for P-401

minutes until the pressure was stabilized. This procedure enabled the same optimal density of the LCF, as was determined by mix optimization to be obtained. The mold was then dismantled and the specimen placed on a stiff support, such as wood or steel plate. The specimen was wrapped with plastic and aluminum foil and cured at room temperature of 73 ^{o}F $\pm$ 3 ^{o}F for 60 days.

2.8 LABORATORY TESTS

The specimens prepared according to the procedures delineated in section 2.1 were tested to establish the following properties:

- Modulus of resilience,
- Indirect tensile strength,
- Fracture toughness,
- Unconfined compression, and
- Fatigue.

A full factorial design format for the laboratory tests for mixture characterization is presented in Tables 2.5 and 2.6. The procedure for conducting each type of laboratory test is described in the following subsections.

2.8.1 MODULUS OF RESILIENCE, M_r

The concept of diametrical (resilience) modulus has been previously applied to asphaltic mixtures. For short-duration dynamic loads, the value for Young's Modulus (E) is similar to the value for Resilience Modulus (M_r), a material property useful in pavement analysis. The test required to determine M_r involves applying a dynamic load of known duration and magnitude (below the indirect tensile strength of the sample) across the vertical diameter of the cored specimen. The elastic deformation across the horizontal diameter of the specimen is measured with displacement transducers. After recording the

Table 2.5 Full factorial design of experiment for LCF mixtures.

Material Source	Ohio			Oregon			Texas			Pennsylvania		
pH Value	5	7	9	5	7	9	5	7	9	5	7	9
Curing Time (days)												
1	3	3	3	3	3	3	3	3	3	3	3	3
3	3	3	3	3	3	3	3	3	3	3	3	3
7	3	3	3	3	3	3	3	3	3	3	3	3
14	3	3	3	3	3	3	3	3	3	3	3	3
28	3	3	3	3	3	3	3	3	3	3	3	3

Note:

1. Specimen size for unconfined compression test was 2 in. x 4 in., and for modulus of resilience, indirect tensile strength and fracture toughness was 3 in. x 2 in.

2. All specimens were cured at 140°F for aging period indicated in the table.

Table 2.6 Factorial design of experiment of LCF mixtures.

Curing Time (days) / De-icing Chemical / pH Value	Glycol			Urea		
	5	7	9	5	7	9
3	3	3	3	3	3	3
14	3	3	3	3	3	3
28	3	3	3	3	3	3

Note:

1. Specimen size for unconfined compression test was 2 in. x 4 in., and for modulus of resilience, indirect tensile strength and fracture toughness was 3 in. x 2 in.
2. Three specimens were tested for each variable.
3. All specimens were cured at 140°F and dipped in Glycol/Urea for 24 hours before test.

magnitude of the dynamic load and deformation, the Modulus of Resilience (M_r) is calculated using the equation:

$$M_r = \frac{P(u + 0.2734)}{d\ t} \qquad (2.1)$$

where:

P = Magnitude of dynamic load;
u = Poisson's ratio
t = Specimen thickness
d = Total deformation

2.8.2 INDIRECT TENSILE STRENGTH, s_y

The ultimate strength of an asphaltic mixture under an indirect tensile stress field is obtained after diametrically applying a vertical load, at a rate of load piston increase of 0.065 inch/minute until the maximum load (yield strength) that the specimen is able to withstand, is reached. The indirect tensile strength (s_y) is then calculated using the equation:

$$s_y = \frac{2P}{3.14Dt} \qquad (2.2)$$

where:

P = Maximum load, (lb.)
D = Specimen diameter, (in.)
t = Specimen thickness, (in.)

2.8.3 FRACTURE TOUGHNESS, K_{1c}

The Ohio State University procedure was used to determine the fracture toughness (K_{1c}) of cored specimens. The method consists of cutting a right-angled wedge into the core specimen and initiating a crack (0.25 in. long) at the top of the notch. The specimen is set on a base with the wedge pointing upwards, and a vertical load is applied to it through a three-piece set up

consisting of two plates (placed against the sides of the wedge) and a semicircular rod placed between the two plates to transmit the load to the sides of the wedges.

The results of the tests (conducted at room temperature) allowed the calculation of the fracture toughness, K_{1c} through the equation:

$$K_{1c} = F(s)\ F(g)\ C^{1/2}\ \frac{P}{t\ R} \qquad (2.3)$$

where:

$$F(s) = 6.530078e^{4.30577\ (\ C\ /\ R\ )^{2.475}} \qquad (2.4)$$

F(s) = Stress factor

$$F(g) = 3.950373e^{-3.07103\ (C\ /\ R\ )^{0.25}} \qquad (2.5)$$

F = Geometry factor
C = Crack length (inches)
P = Maximum vertically applied load (lbs)
t = Thickness of test specimen
R = Radius of test specimen

The fracture toughness test provides pavement engineers with an additional parameter for evaluating cracking potential (a controlling asphalt pavement design criterion).

2.8.4 UNCONFINED COMPRESSIVE STRENGTH, q_u

This test was performed according to ASTM D 4219 for the determination of the compressive strength of LCF mixes. This test method consists of applying a compressive axial load to molded LCF specimens (2 inch x 4 inch) at a rate of 15 psi per second until failure occurred.

2.8.5 FATIGUE TESTS

Fatigue tests of LCF beams with asphalt concrete overlay are designed to study the reflection cracking of LCF through the asphalt overlay. The fatigue experiments were conducted using a beam on an elastic foundation with geometry as shown in Figure 2.14. The selection of this experimental set-up was based on a two-dimensional modeling of a pavement structure in which beams represent the pavement and subgrade. The dimensions of the beam and foundation, as well as the stiffness of foundation, are selected with consideration to simulating the stress and strain at the bottom of a pavement structure subjected to traffic loading.

The test set-up is the same as previously used by Resource International Inc., and researchers at The Ohio State University to study the fatigue properties of asphaltic mixtures. The fatigue tests were performed using a dynamic load function of Haversine shape. An MTS electro-hydraulic testing system was used to generate the load factor. To ensure complete recovery of the sample before the next load cycle, a rest period of 0.4 second was allowed between each load application.

The duration of load application in all tests was kept constant at 0.1 second. All tests were performed at room temperature (73 ^{o}F $\pm$ 3 ^{o}F) and at two stress levels for each type of specimen.

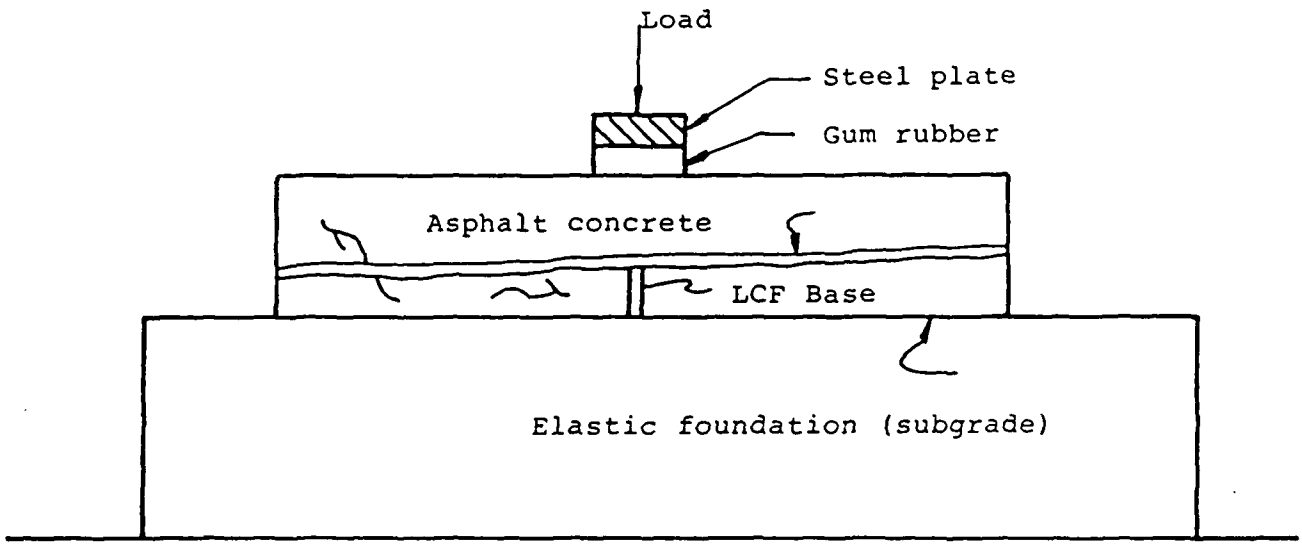

Figure 2.14 Fatigue Test Set-Up

CHAPTER 3 - LABORATORY TEST RESULTS

3.1 GENERAL RESULTS

The performance investigation of lime + cement + flyash + sand mixtures included the comparison of the performance of materials obtained from four sources and two experimental designs. The first design utilized three factors; source (Ohio, Oregon, Pennsylvania, and Texas); water pH level (5, 7 and 9); and curing time (1,3,7,14 and 28 days at a constant curing temperature of 140°F). There were three independent replicates for each combination of factors and the response variables of interest were:

- Unconfined compressive strength, q_u,
- Modulus of resilience, M_r,
- Indirect tensile strength, $\acute{U}_y$, and
- Fracture toughness, K_{1C}.

The second design also used three factors but was confined to the Ohio source material only. These factors were pH level (5,7,9), curing time (3,14, and 28 days at constant curing temperature of 140°F) and treatment (control, Urea and Glycol). Again, there were three independent replicates for each combination of factors and the response variables of interest were the same as for the first design. Also the control data from the first design was used in the second design for the purpose of comparison of the properties of the Ohio source LCF mixture when tested after soaking in Urea and Glycol, the de-icing materials, for a period of 24 hours prior to laboratory tests. The primary hypothesis of the second design was to determine whether or not the treatment with de-icing chemicals had any effect on the response variables while the secondary hypothesis was to determine whether or not the pH of mixing water had an effect on the responses.

Discussions in this chapter center around test results of experimental designs and the identification of any noticeable and consistent behavioral trends of

the test data. Summary of all test results in tabular and graphical format for each source are presented in
Tables 3.1 through 3.5 and Figures 3.1 through 3.16.

However, before discussions concerning the material response characteristics of the four LCF mixtures are presented, a few remarks concerning the conduct of the laboratory tests are in order. As stated in section 4.1 all mixtures were subjected to curing times of 1, 3, 7, 14, and 28 days at a temperature of 140 ^{o}F prior to testing. After all tests were completed, data acquired, and analyses underway it became apparent that the material characteristic parameters were responding in an unpredictable manner. This is evidenced by the fact that almost without exception the values for the response variables decreased significantly at 28 days cure time and in some instances this occurred after 14 days cure time. Normally, one would expect the strength of a concrete mixture to increase with curing time. However, the effect of maturity, in the form of curing specimens at higher than normal temperatures over a period of time, is to achieve strength characteristics within a shorter time period than if the specimens were cured at normal temperatures. It is also true that subjecting specimens to high temperatures could result in a loss in strength characteristics after a long period of time if special care is not taken to provide the proper conditioning environment. It is suspected that each of the specimens tested in this study experienced a loss in each of its response variables after some period of curing time (probably after 7 days) due to a lack of proper moisture level present during the curing process.

In an effort to accommodate this situation the following procedure was employed. Bergstrom[30] has established the effect of temperature and age, or maturity, on the strength characteristics of concrete. The maturity, M, is defined as the product of curing time in hours by the curing temperature in

Table 3.1 Summary of laboratory test results of Urea and Glycol dipped samples. (Ohio source)

pH value	Tests Preformed	De-icing Chemical / Curing Time (days)	UREA			GLYCOL		
			3	14	28	3	14	28
5		Qu (psi)	718	790	859	748	684	737
		MRx10^6 (psi)	0.59	0.71	0.68	0.53	0.78	0.81
		σ_y (psi)	110	120	150	110	110	140
		K_{1c} (psi $\sqrt{in}$)	140	310	510	200	270	520
7		Qu (psi)	727	822	1003	769	849	902
		MRx10^6 (psi)	0.53	0.78	0.74	0.54	0.88	0.77
		σ_y (psi)	130	120	140	140	150	140
		K_{1c} (psi $\sqrt{in}$)	130	310	480	210	310	450
9		Qu (psi)	732	960	976	626	939	836
		MRx10^6 (psi)	0.53	0.84	0.89	0.55	0.74	0.70
		σ_y (psi)	120	120	170	130	110	150
		K_{1c} (psi $\sqrt{in}$)	130	230	450	150	330	600

Table 3.2 Summary of laboratory test results. Ohio source.

pH value	Tests preformed	Curing Time (days) 1	3	7	14	28
5	Qu (psi)	400	810	990	1,100	1175*
	MRx10^6 (psi)	0.61	1.00	1.04	1.10*	1.13*
	σ_y (psi)	40	120	145*	170	190*
	K_{1c} (psi $\sqrt{in}$)	40	210	360	330	530
7	Qu (psi)	280	810	1,080	1,130	1275*
	MRx106 (psi)	0.62	0.74*	0.79*	0.87	0.88*
	σ_y (psi)	80	100	110	180	183*
	K_{1c} (psi $\sqrt{in}$)	50	130	280	340	420
9	Qu (psi)	220	720	940	1,190	1395*
	MRx10^6 (psi)	0.71	0.75*	0.79	0.81	0.84
	σ_y (psi)	50	140	150*	170	185*
	K_{1c} (psi $\sqrt{in}$)	30	110	340	390	410

Note: 1. Test results are average of three tests.
2. For individual test data please refer to Appendix "B".

Table 3.3 Summary of laboratory test results.
Pennsylvania source.

pH value	Tests Preformed	Curing Time (days) 1	3	7	14	28
5	Qu (psi)	100	290	670	950	1450*
	MRx10^6 (psi)	0.41	1.11	1.01	1.14*	1.12*
	σ_y (psi)	20*	50	70	150	185*
	K_{1c} (psi $\sqrt{in}$)	25	70*	140*	210*	285*
7	Qu (psi)	130	320	680	850	1445*
	MRx106 (psi)	0.38	1.21	1.13	1.34	1.44*
	σ_y (psi)	20	40	101*	175	266*
	K_{1c} (psi $\sqrt{in}$)	50*	115*	185*	240*	285*
9	Qu (psi)	150	240	590	970	1315*
	MRx10^6 (psi)	0.34	0.86	1.06	1.28	1.41*
	σ_y (psi)	20	40	90*	140	190*
	K_{1c} (psi $\sqrt{in}$)	45*	105*	175*	240*	290*

Note: 1. Test results are average of three tests.
2. For individual test data please refer to Appendix "B".
* Predicted value

Table 3.4 Summary of laboratory test results.
Oregon source.

pH value	Tests preformed	Curing Time (days) 1	3	7	14	28
5	Qu (psi)	310	720	1,310	1,110	1270*
	MRx10^6 (psi)	0.64	0.70*	0.75*	0.75	0.78
	σ_y (psi)	40	130	170*	220	255*
	K_{1c} (psi $\sqrt{in}$)	50	80	208*	370	450
7	Qu (psi)	260	770	970	1,350	1555*
	MRx106 (psi)	0.59	0.71*	0.78*	0.80	0.83
	σ_y (psi)	60	140	150	220	235*
	K_{1c} (psi $\sqrt{in}$)	50	210	280*	370	510
9	Qu (psi)	400	770	1,230	1,310	1460*
	MRx10^6 (psi)	0.59	0.61*	0.69*	0.68	0.75
	σ_y (psi)	90	130	165*	180	190*
	K_{1c} (psi $\sqrt{in}$)	50	150	270*	460	470

Note: 1. Test results are average of three tests.
2. For individual test data please refer to Appendix "B".
* Predicted value

Table 3.5 Summary of laboratory test results. Texas source.

pH Value	Tests Preformed	Curing Time (days) 1	3	7	14	28
5	Qu (psi)	730	1,620	1,870	2145*	2290*
	MRx10^6 (psi)	0.74	0.72*	0.80*	0.79	0.88
	σ_y (psi)	170	230	250*	260	270
	K_{1c} (psi $\sqrt{in}$)	120	140	400*	655*	970
7	Qu (psi)	550	1,590	1,660	1,940	2085*
	MRx106 (psi)	0.56	0.67*	0.86*	0.87	1.07
	σ_y (psi)	60*	130	230	295	355*
	K_{1c} (psi $\sqrt{in}$)	140	190	440*	640*	830
9	Qu (psi)	650	1,870	1,710	2,040	2,380
	MRx10^6 (psi)	0.72	0.66*	0.77	0.79	0.92
	σ_y (psi)	165*	190	215*	220	230
	K_{1c} (psi $\sqrt{in}$)	150	160	410*	600*	790

Note: 1. Test results are average of three tests.
2. For individual test data please refer to Appendix "B".
* Predicted value

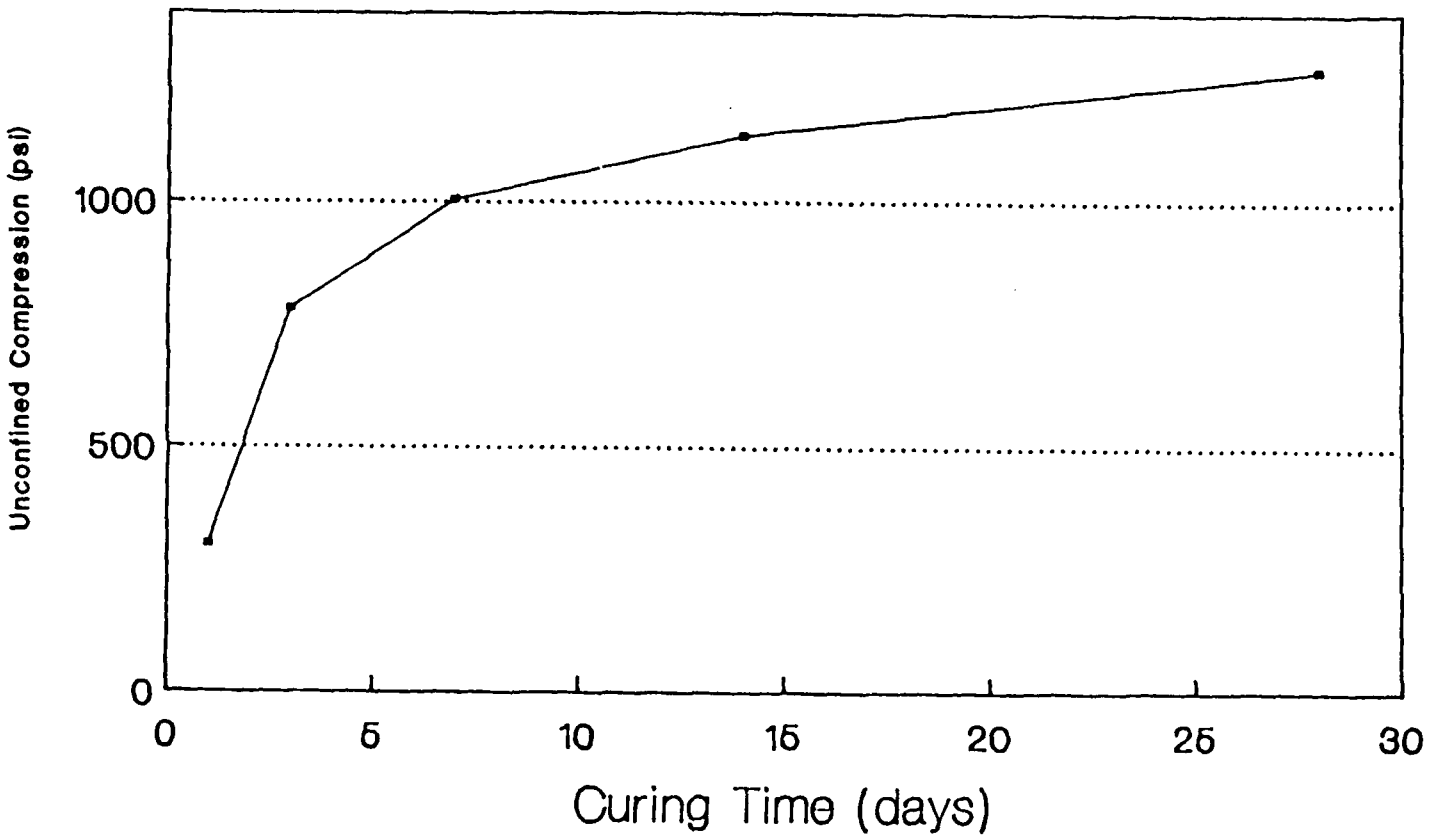

Figure 3.1 Unconfined Compressive Strength Vs. Time

Ohio Source

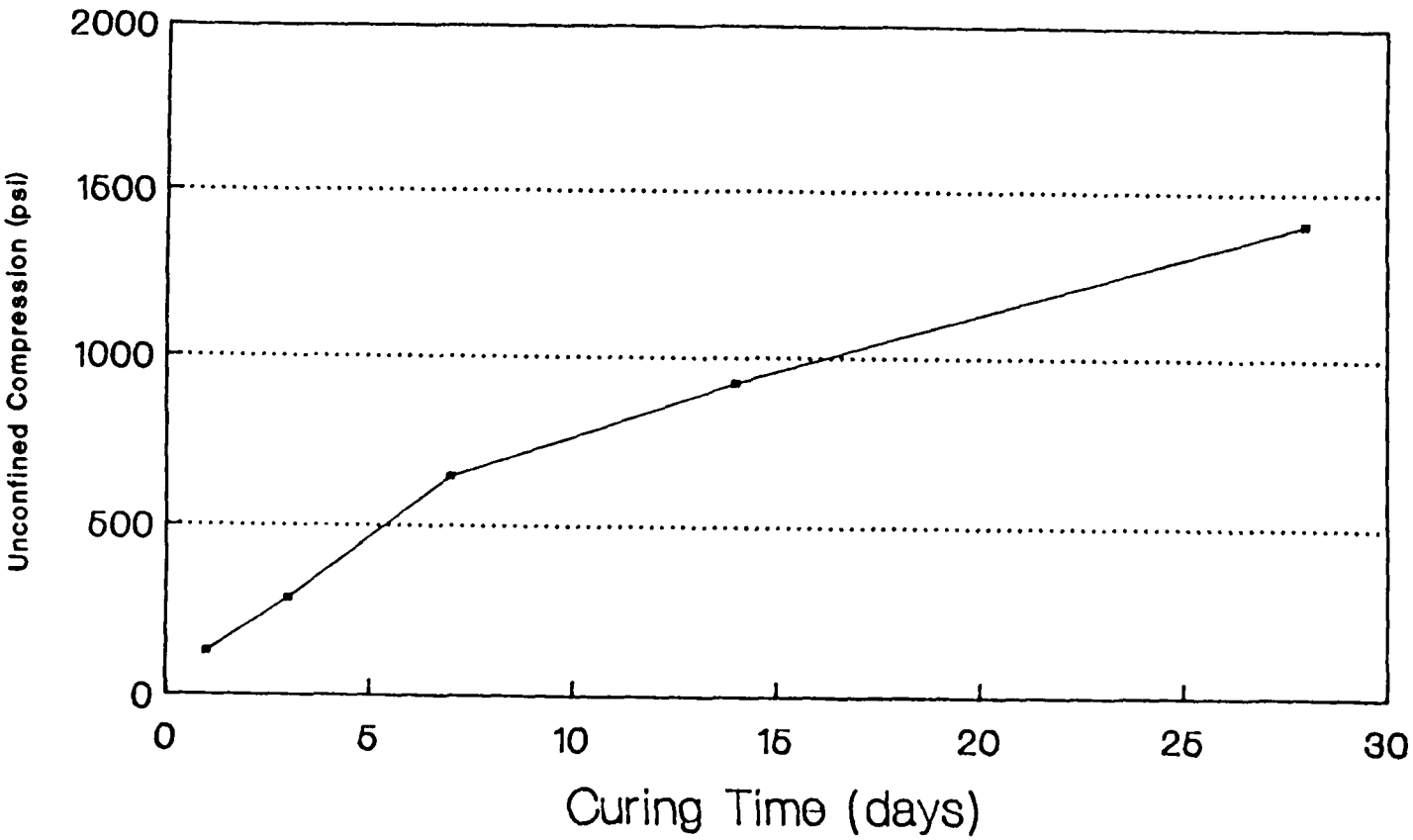

Figure 3.2 Unconfined Compressive Strength Vs. Time

Pennsylvania Source

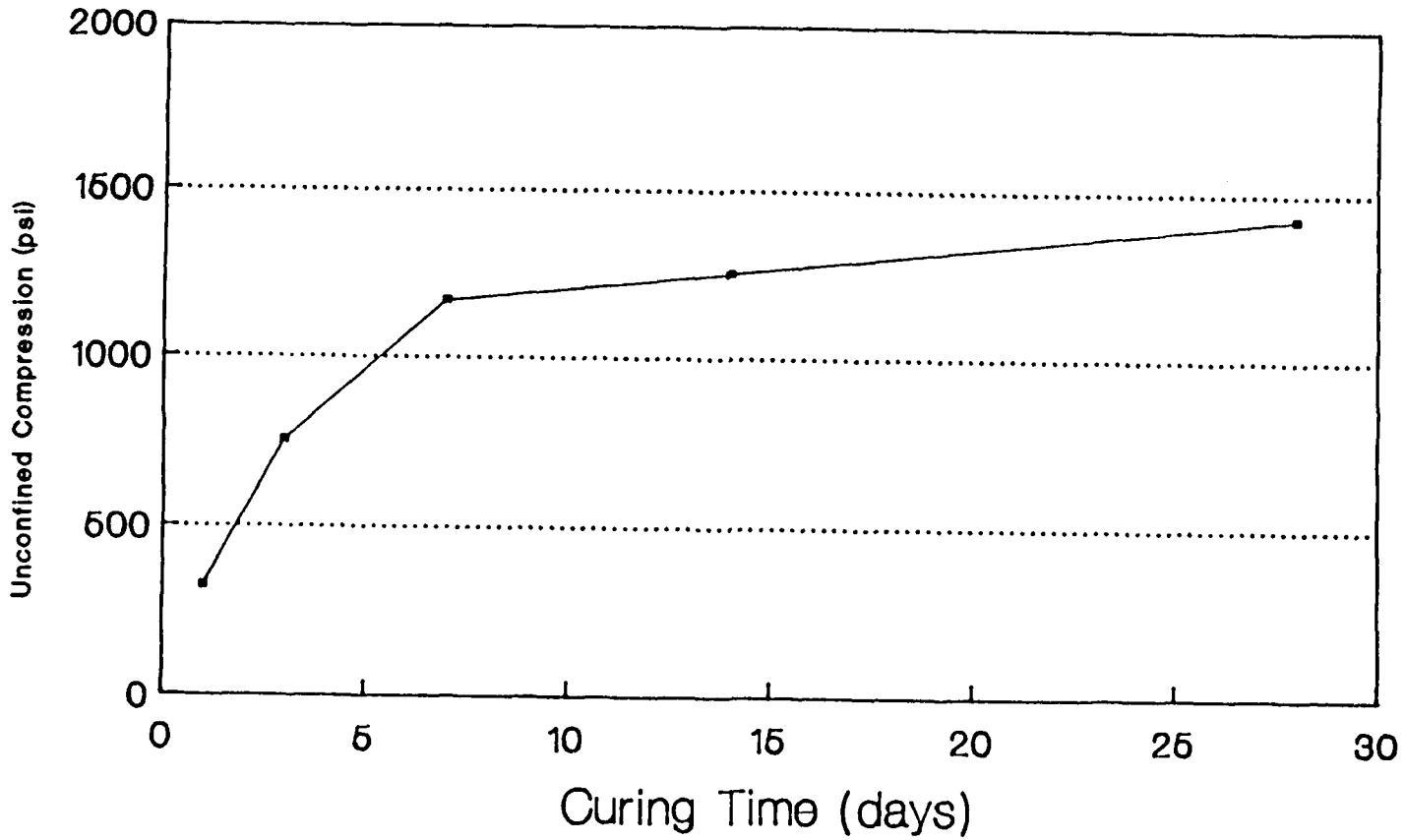

Figure 3.3 Unconfined Compressive Strength Vs. Time

Oregon Source

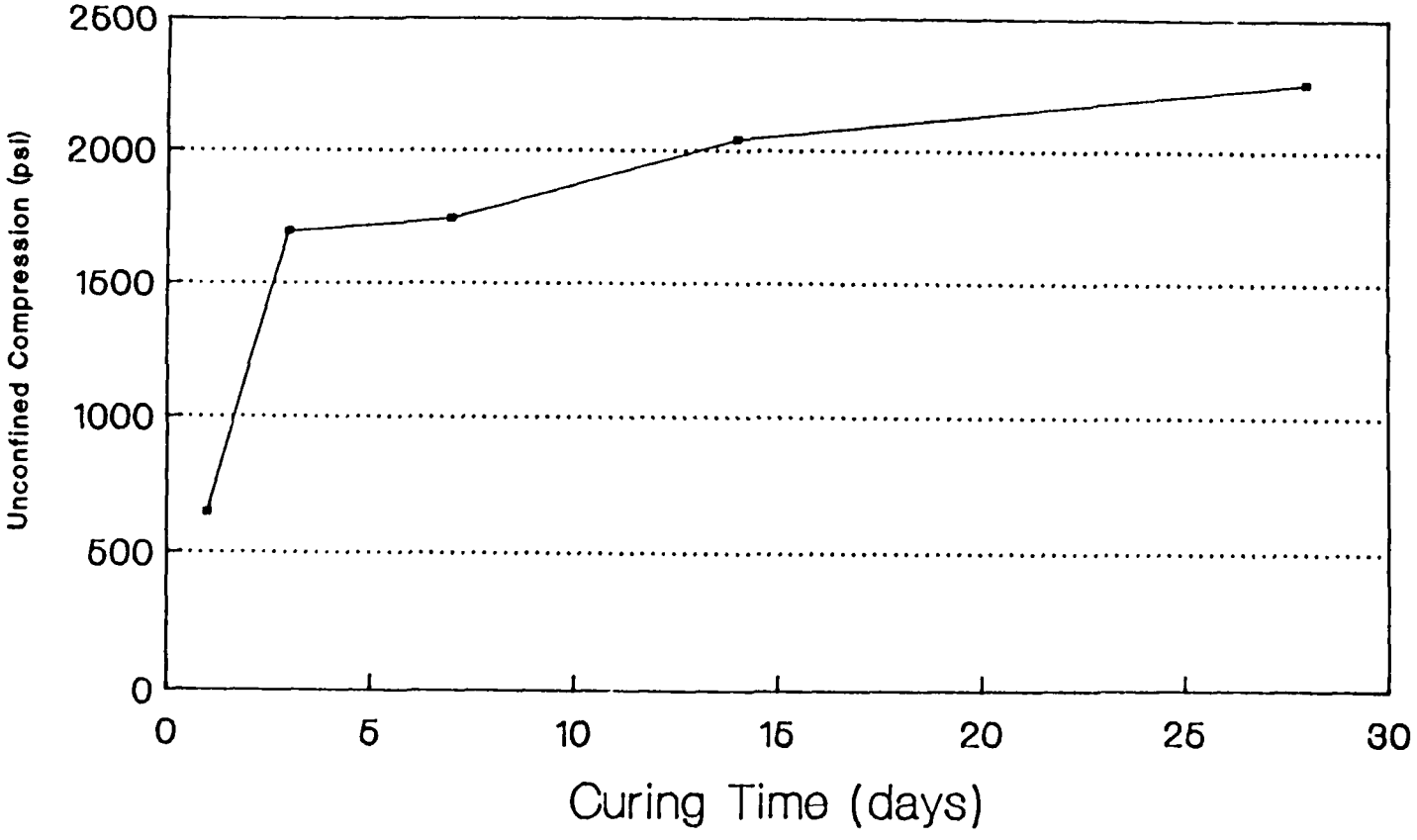

Figure 3.4 Unconfined Compression Strength Vs. Time

Texas Source

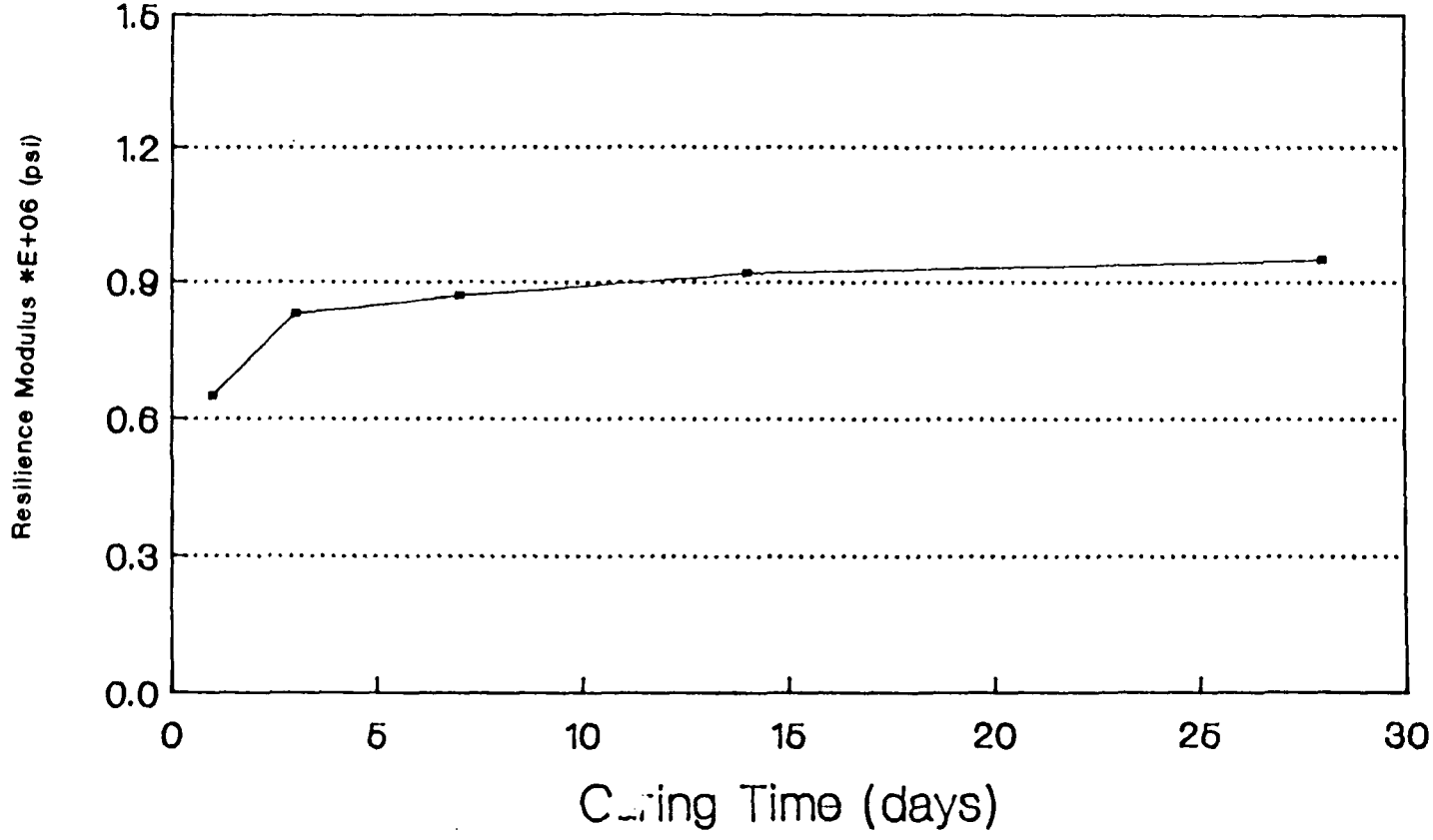

Figure 3.5 Resilient Modulus Vs. Time

Ohio Source

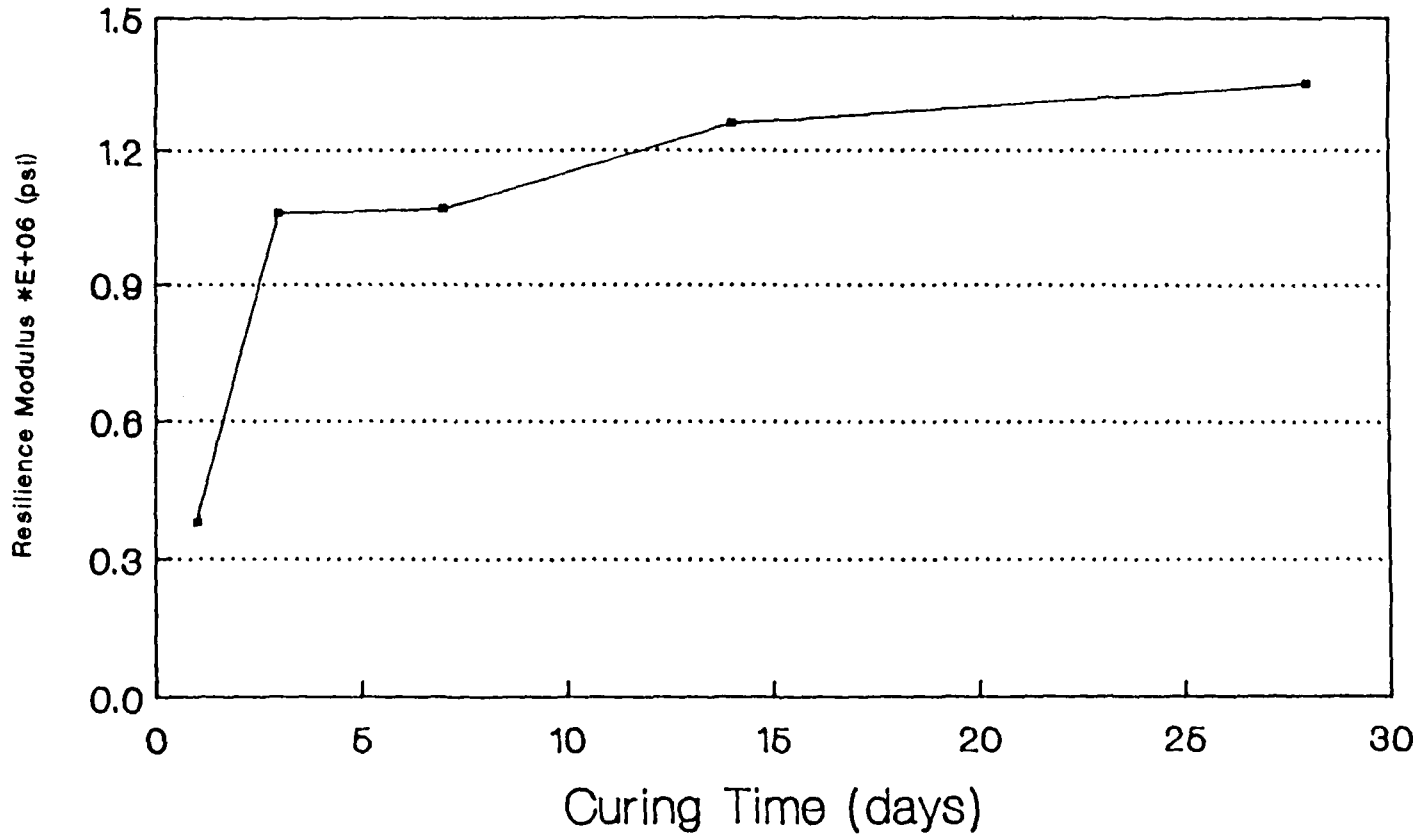

Figure 3.6 Resilient Modulus Vs. Time

Pennsylvania Source

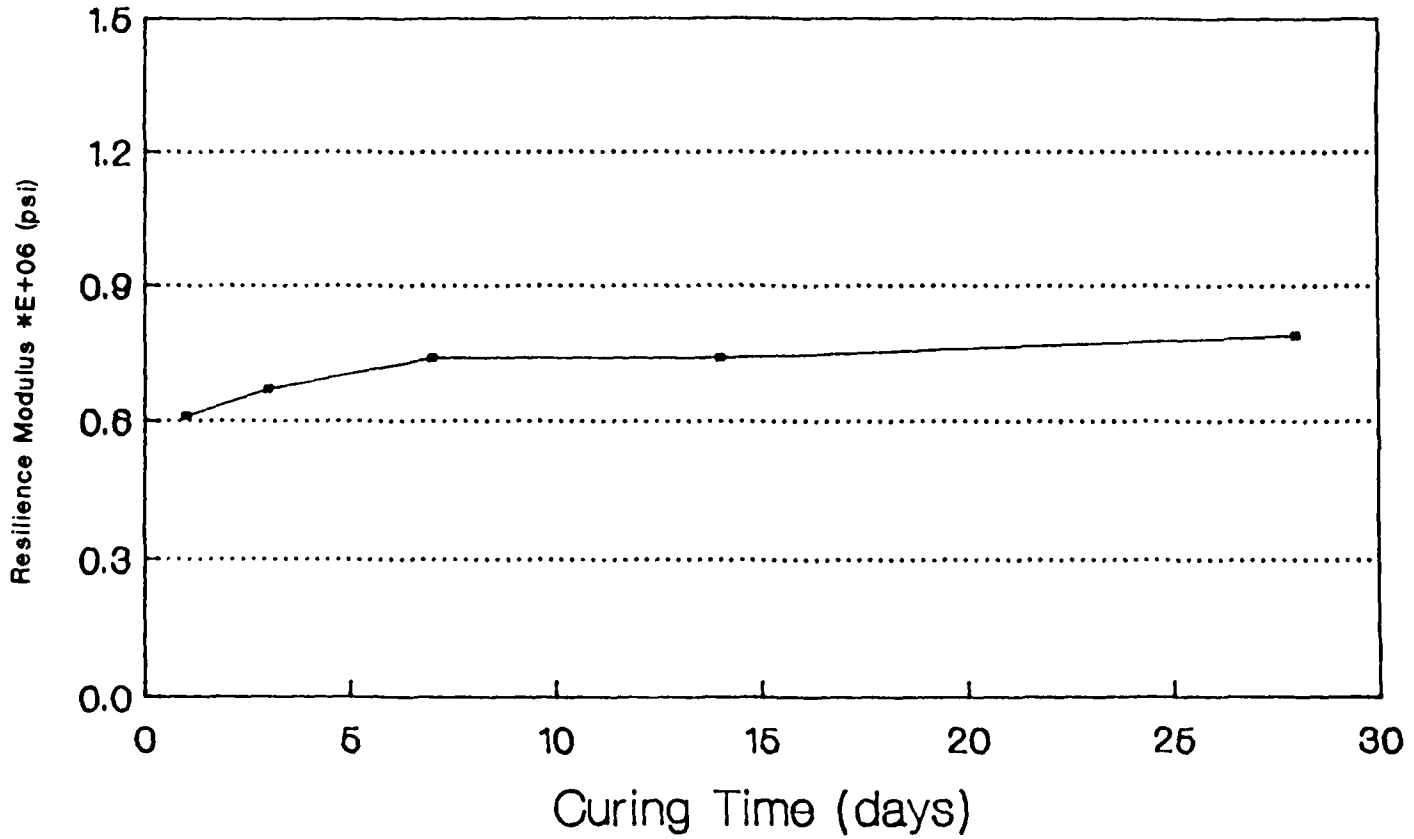

Figure 3 . 7 Resilient Modulus Vs. Time

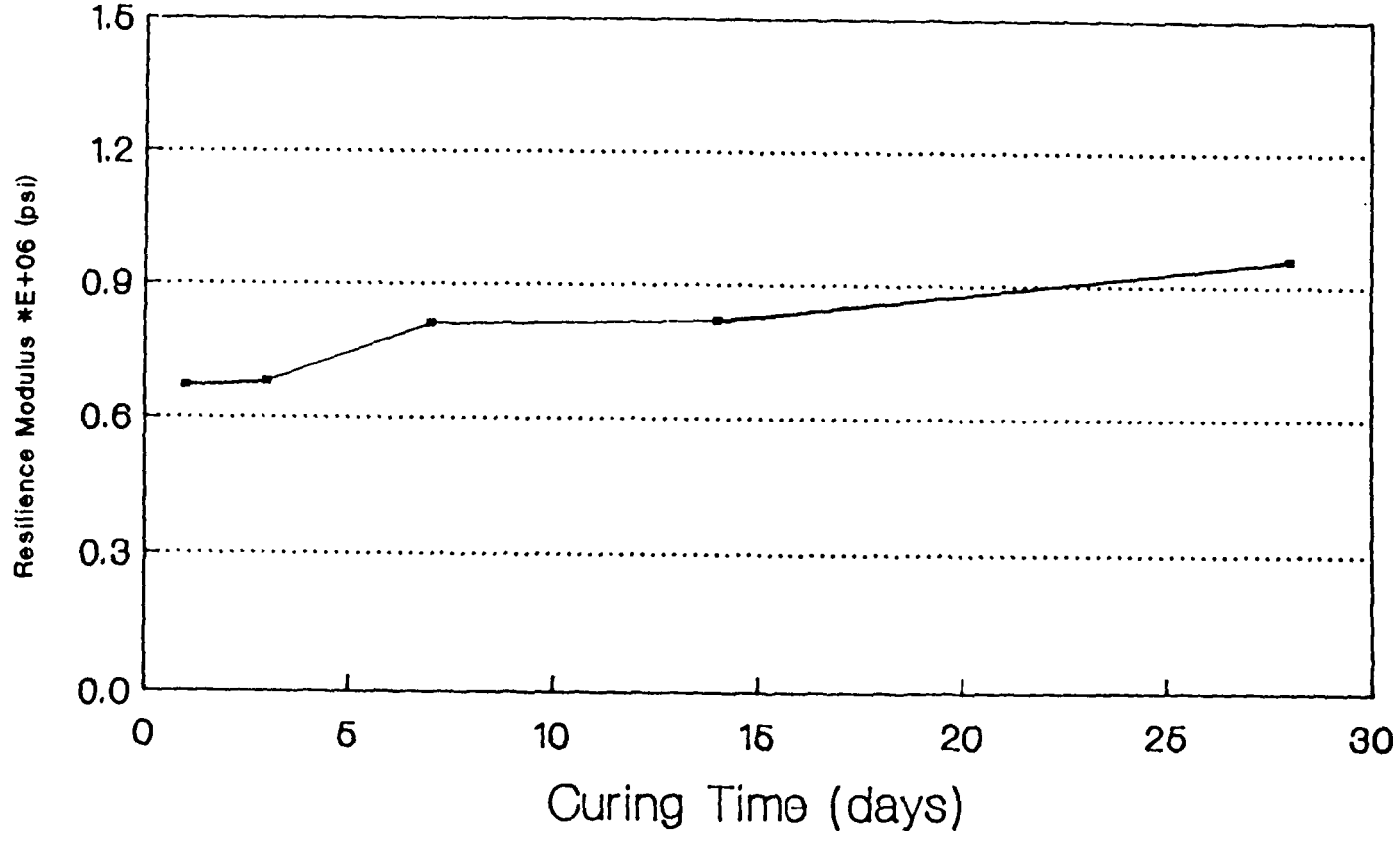

Figure 3.8 Resilient Modulus Vs. Time

Texas Source

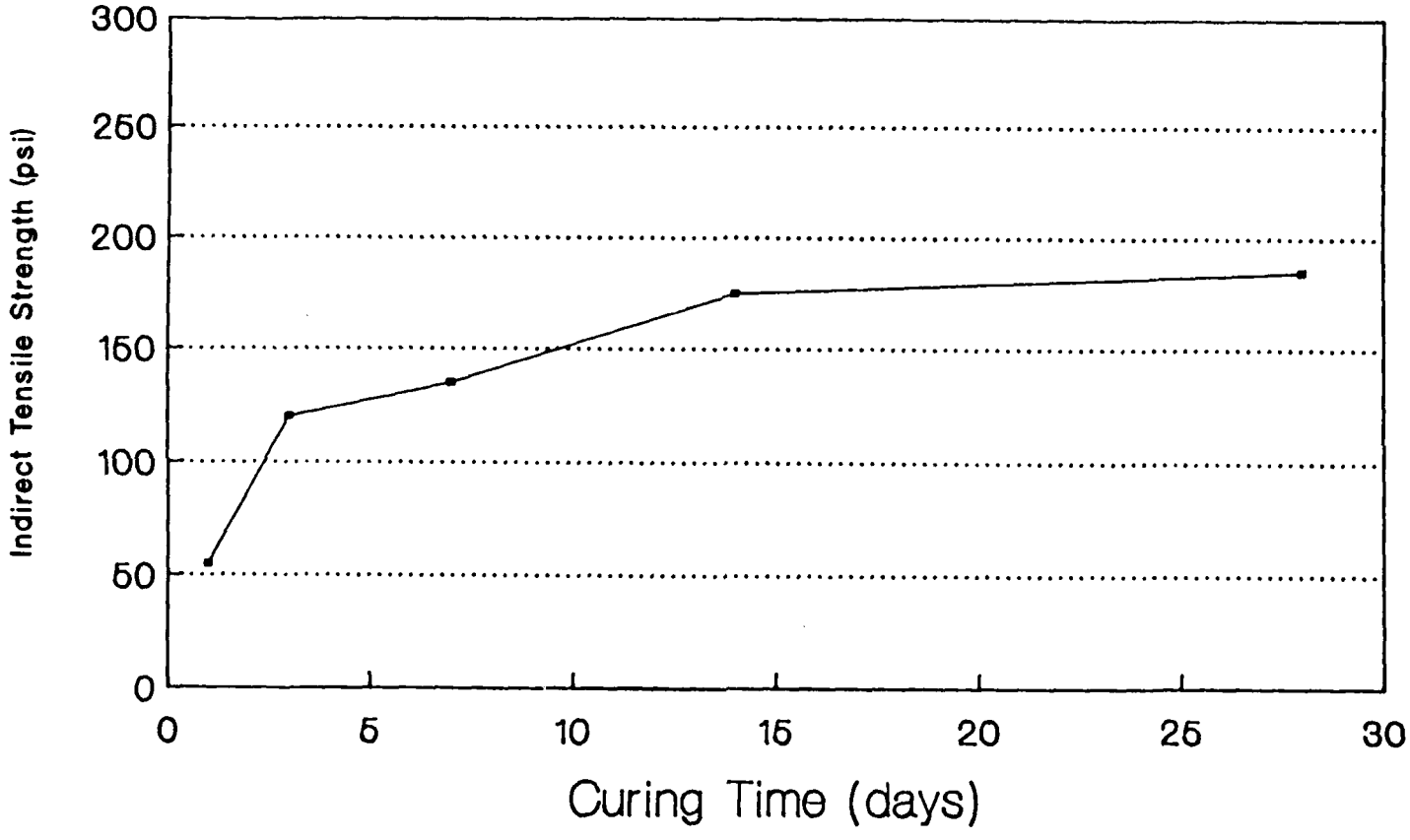

Figure 3.9 Indirect Tensile Strength Vs. Time

Ohio Source

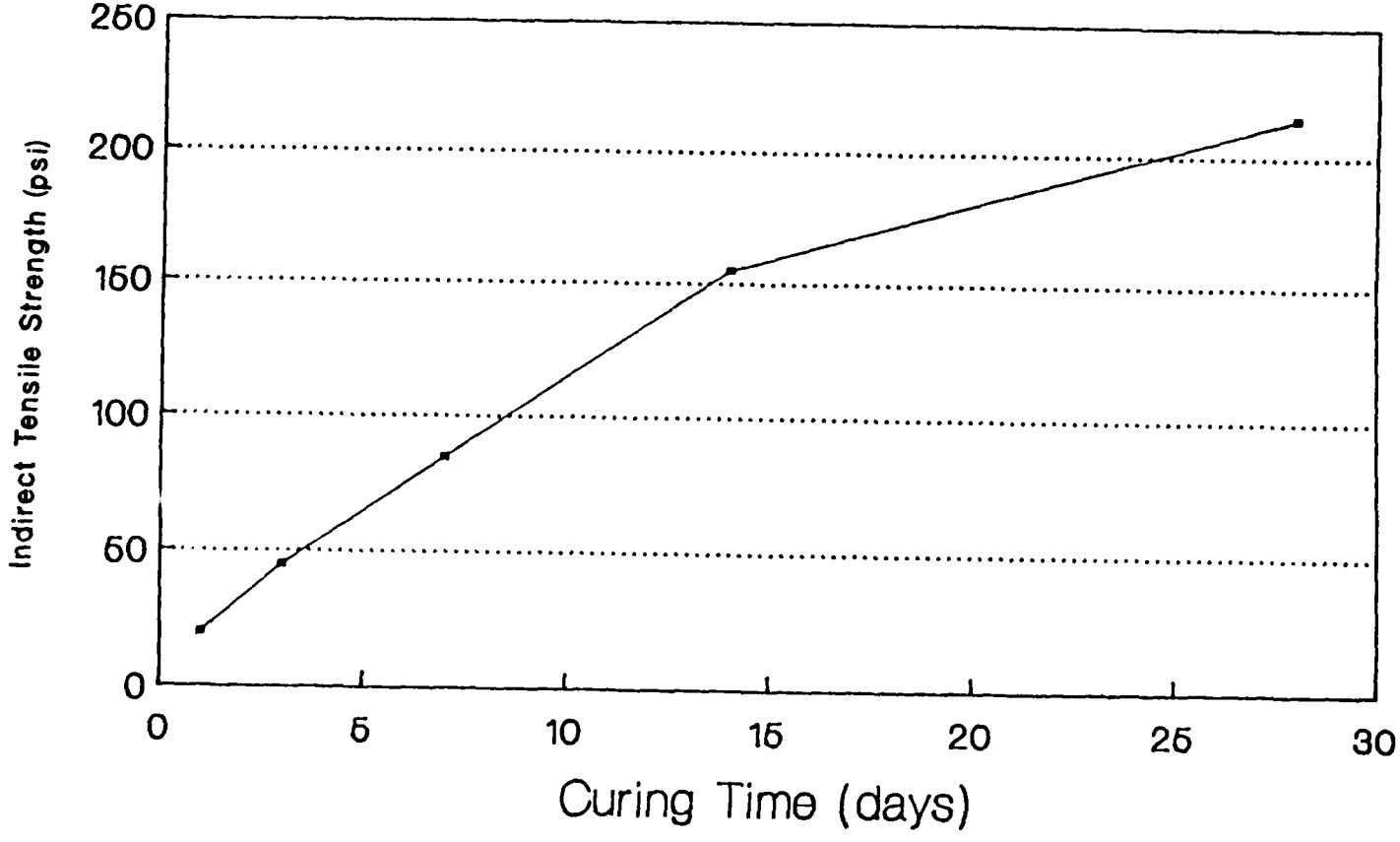

Figure 3.10 Indirect Tensile Strength Vs. Time

Pennsylvania Source

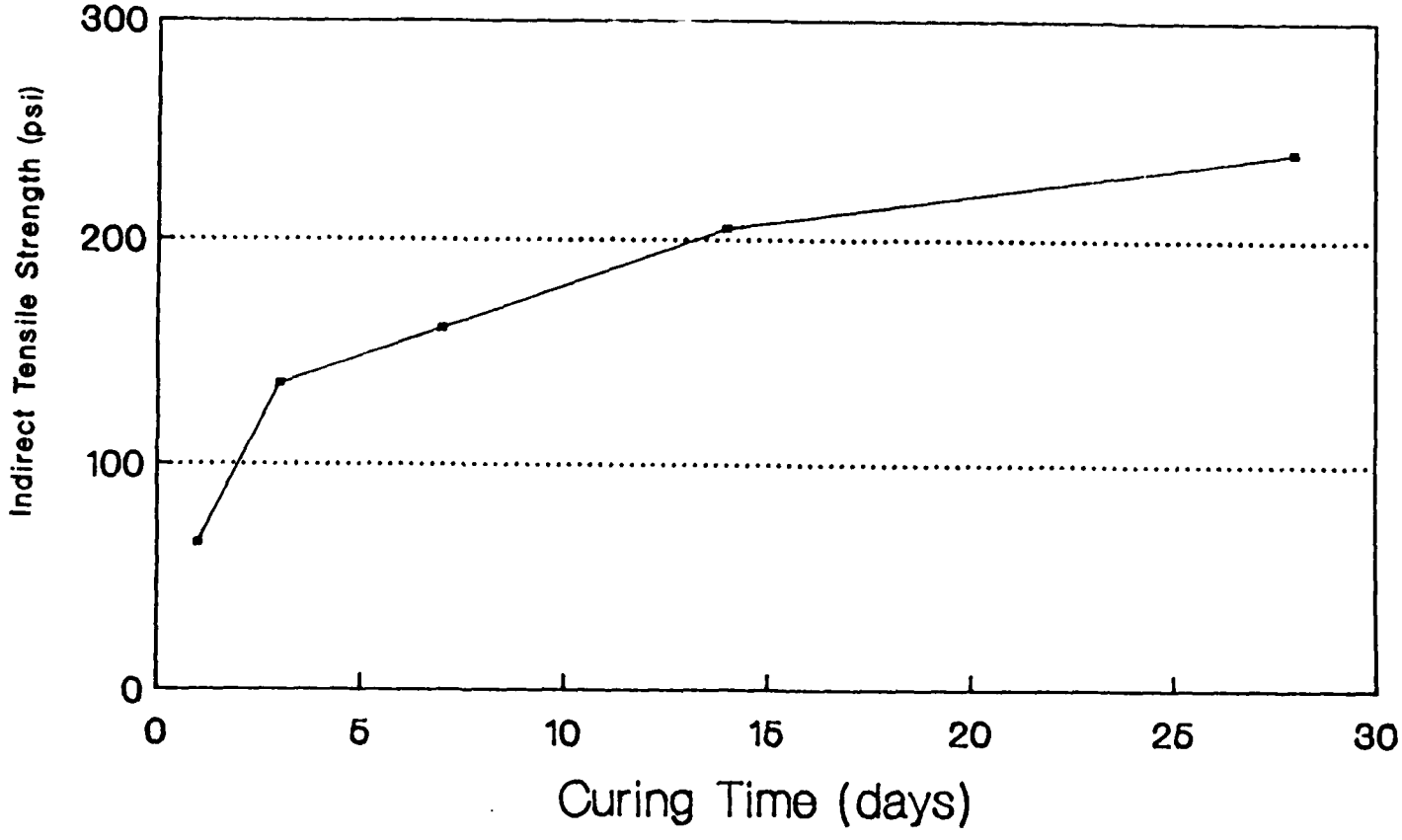

Figure 3.11 Indirect Tensile Strength Vs. Time

Oregon Source

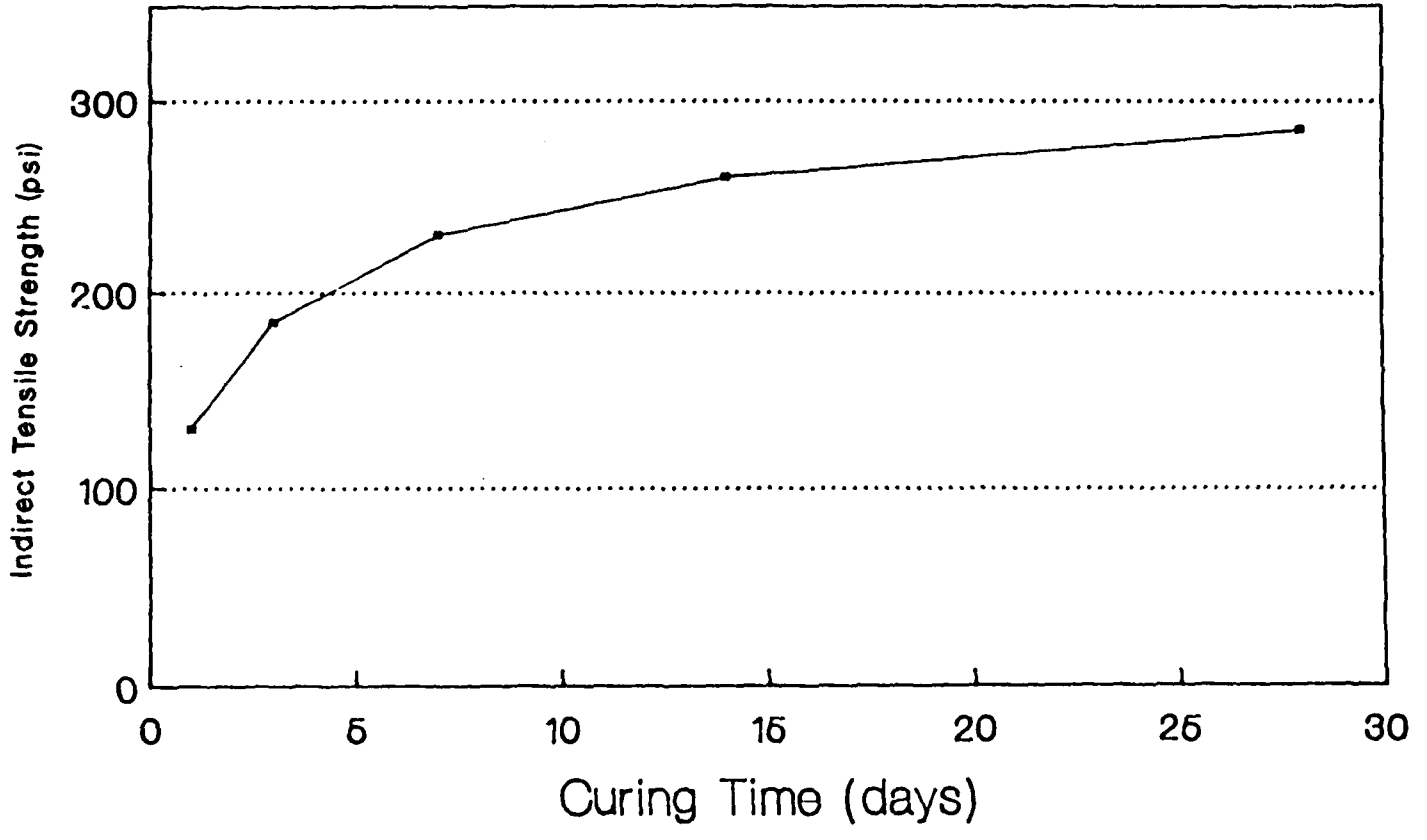

Figure 3.12 Indirect Tensile Strength Vs. Time

Texas Source

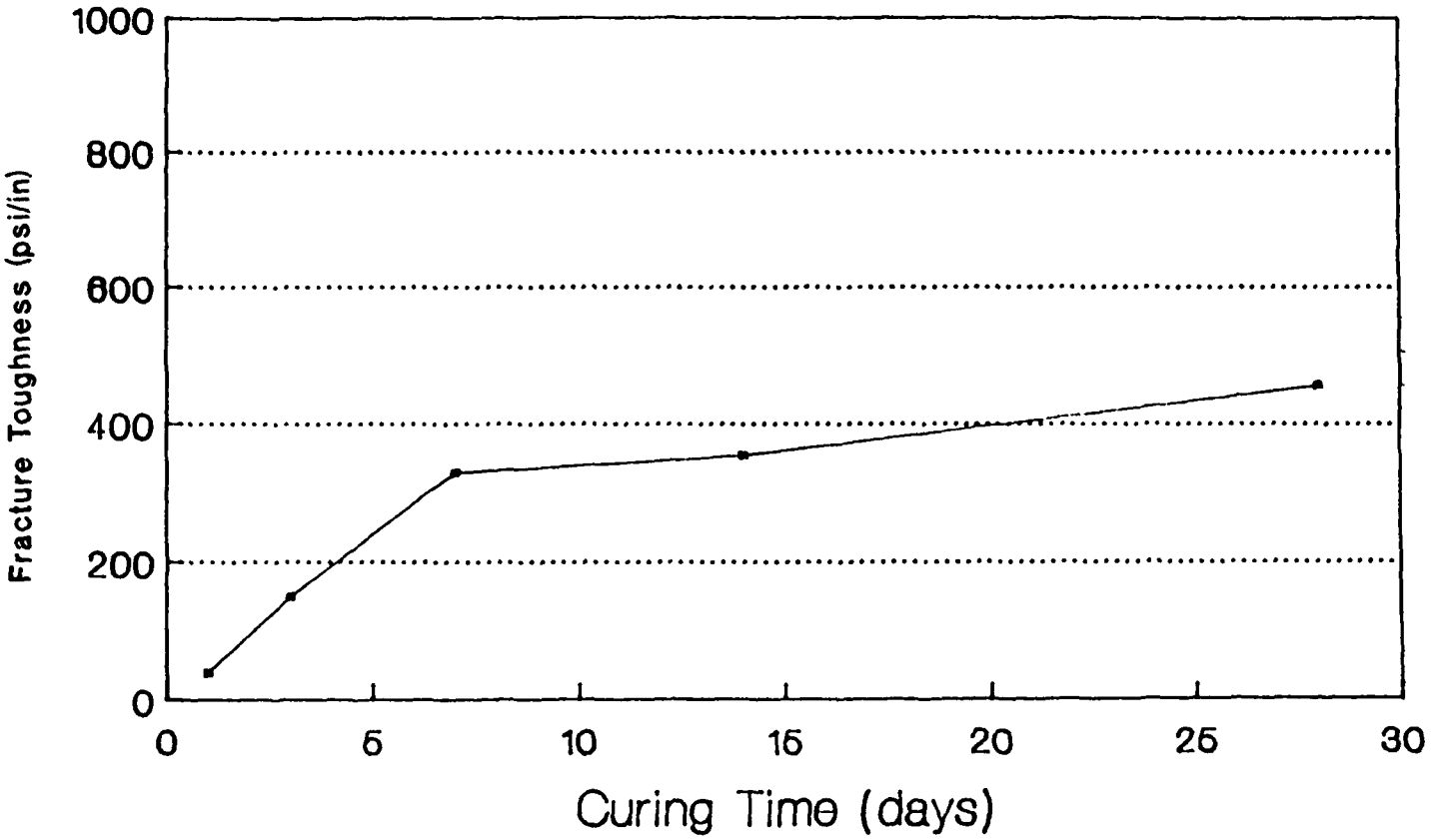

Figure 3.13 Fracture Toughness Vs. Time

Ohio Source

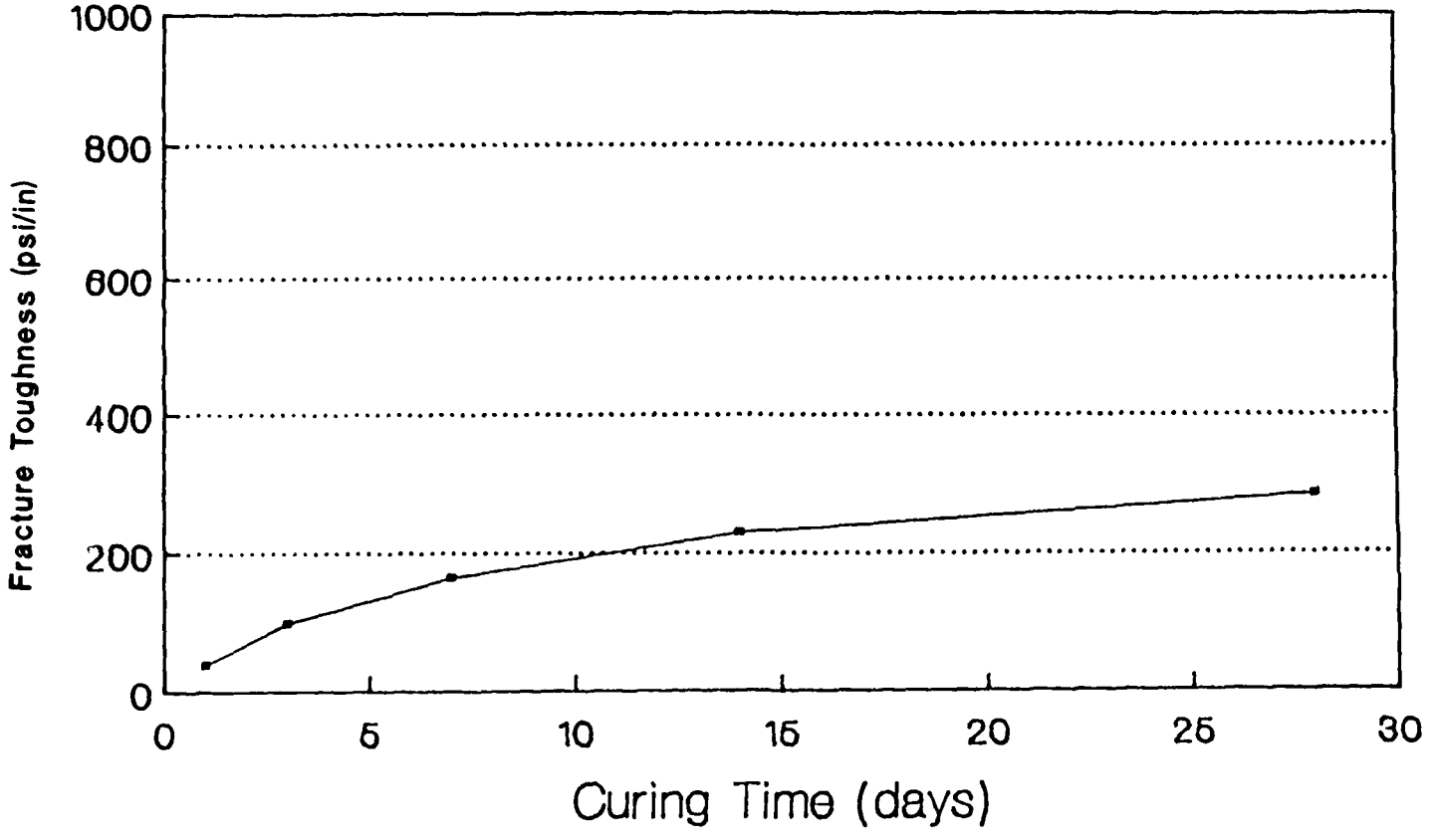

Figure 3.14 Fracture Toughness Vs. Time

Pennsylvania Source

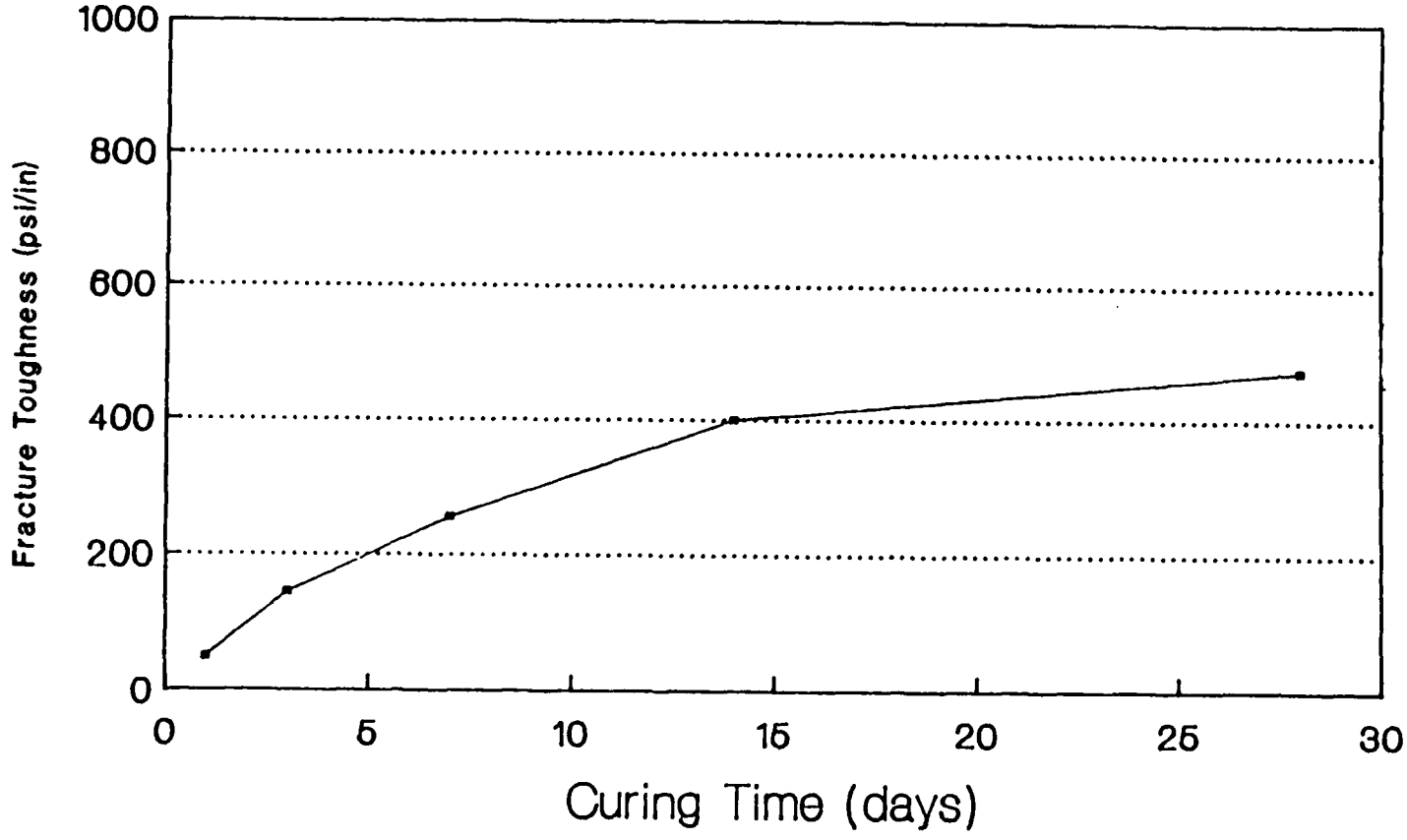

Figure 3.15 Fracture Toughness Vs. Time

Oregon Source

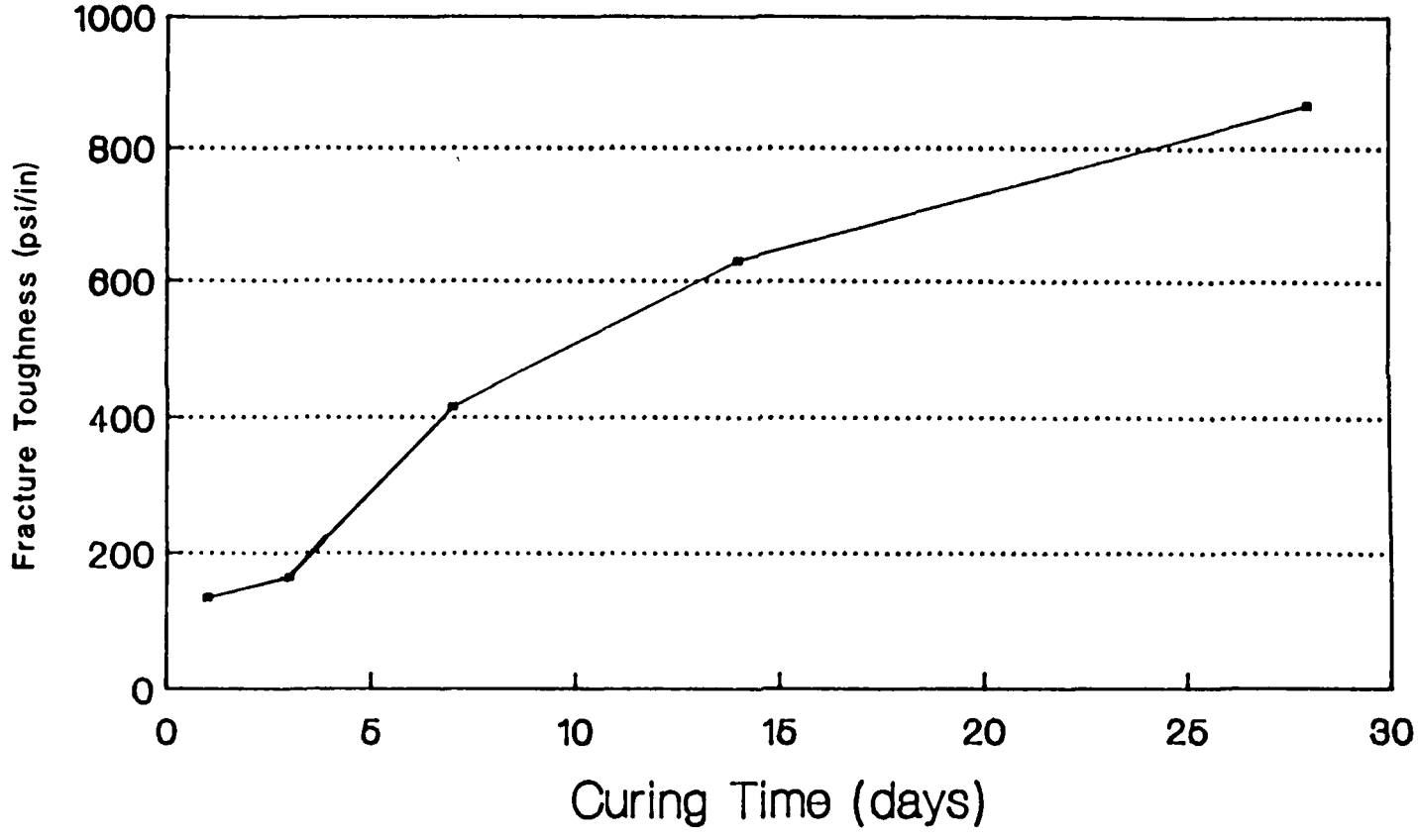

Figure 3.16 Fracture Toughness Vs. Time

Texas Source

degrees above $-10^{o}C$. The value of a strength characteristic, say q, as a function of M is given by

$$q = m M + c \qquad (3.1)$$

where m and c are constants and are determined empirically.

Since laboratory samples were available for curing times of 1, 3, 7, 14, and 28 days it was felt that the samples subjected to the lowest curing time (1,3, and 7 days) were, obviously, less affected by the process. Although this is logical, it is also borne out by the fact that all response variables decreased significantly after 28 days curing and in some instances after 14 days, as mentioned above. Therefore the test data for all response variables for 1, 3, and 7 days were subjected to the maturity function described above and each of the response variable values were then predicted at the 14- and 28- day periods. This procedure is felt to provide a conservative estimate for the LCF mixture strength characteristics as a function of cure time.

3.2 UNCONFINED COMPRESSIVE STRENGTH

Test results indicated that unconfined compressive strength for all sources has a fairly uniform rate of strength gain. The Texas source (Table 3.5 and Figure 3.4) has the largest value of strength, 2250 psi, after the 28 day curing period followed by the Pennsylvania, Oregon, and Ohio sources. These last three sources have approximately the same level of compressive strength, 1,400 psi, after 28 days
(see Tables 3.2, 3.3, and 3.4 and Figures 3.1, 3.2, and 3.3).

3.3 MODULUS OF RESILIENCE

Test results for modulus of resilience are presented in Figures 3.5 through 3.9 and Tables 3.2 through 3.5. These results indicate that the Pennsylvania source has the largest value for M_r, slightly greater than 1.4×10^6 psi, at the 28- day period. The Texas and Ohio sources have about equal values of M_r, 1.0×10^6 psi, followed by the Oregon source whose M_r value is about 0.8×10^6 psi

after 28 days curing time.

3.4 INDIRECT TENSILE STRENGTH

Test results for Indirect Tensile Strength are graphically presented in Figures 3.9 through 3.12 and listed in Tables 3.2 through 3.5. These data indicate that the Texas source achieves the highest level for $\acute{U}_y$, about 290 psi, after the 28- day cure period. The Oregon source achieves about 250 psi, followed by the Pennsylvania source at 220 psi and lastly the Ohio source at 180 psi for $\acute{U}_y$ after the 28 day period.

3.5 FRACTURE TOUGHNESS

Test results for fracture toughness are graphically presented in Figures 3.13 through 3.16. These data reveal that the Texas LCF source specimens achieve the highest value for K_{1C}, about 875 psi $in^{1/2}$ (Figure 3.16), followed by the Oregon and Ohio sources at the 450 psi $in^{1/2}$ level (Figures 3.13 and 3.15), and last the Pennsylvania source at the 300 psi $in^{1/2}$ level (Figure 3.14) after the 28 day cure period.

3.6 EFFECT OF DE-ICING CHEMICALS

As explained in section 2.8 two treatments (Urea and Glycol) were employed to determine what effect de-icing chemicals have on the material response characteristics of the LCF mixtures. A summary of the original laboratory test results for the treated samples is presented in Table 3.1

Comparison of response parameters q_u, M_r and $\acute{U}_y$ for samples treated with de-icing chemicals with the results for untreated samples indicates that there is a loss of strength in the treated samples. However, the de-icing chemicals appear to have no impact on the measured value of the fracture toughness, K_{1C}.

There is also no significant difference between Urea and Glycol treatments for each of the response parameters measured. That is, the Ohio source LCF mixture response parameters, q_u, M_r, $\acute{U}_y$ and K_{1C}, have (practically) the same

values whether treated with Urea or Glycol.

3.7 EFFECT OF WATER PH LEVEL

The water pH level was varied to determine what effect this factor has on the material response characteristics of the Ohio LCF mixture. The results of these tests, including predicted values where appropriate, are presented in Tables 3.1 through 3.5.

These results were also subjected to the same analyses procedure mentioned in subsection 3.6 for the same purpose, i.e., is there a statistically significant difference in the response characteristic of the Ohio LCF mixture due to water pH level.

The outcome of this analysis indicated that the water pH level did not have a significant effect on the material response characteristics over the range of pH levels and sample ages tested.

Since the results of the foregoing analyses indicated that LCF mixture material response characteristics do not depend on water pH level, the graphical presentations of the laboratory results, Figures 3.1 through 3.16, for the four LCF sources are presented as average values for the variable over the three water pH levels.

3.8 FATIGUE

3.8.1 FATIGUE TEST RESULTS

Before the start of the fatigue tests, it was expected that the test results would resemble a standard fatigue pattern. That is, the expected pattern was expected to follow a standard S-N curve, approaching the fatigue limit asymptotically.

However, it became apparent during the tests that the LCF beam specimens were not responding in a manner typical of accepted beam fatigue behavior. The

results are shown in Table 3.6. They appear to indicate that there was almost no low- cycle fatigue behavior for the LCF beams.

The only reliable information obtained for the low- cycle behavior was the static strength of the specimens.

At load levels lower than the load corresponding to the value for flexural strength, the fatigue life of the specimen appears to be independent of the load level. The slope is zero for the line representing the relation between applied dynamic load the number of cycles to failure. The transition from low to high cycle fatigue is so abrupt that it has not been discernable in testing of the specimens. The abrupt failure is assumed to be a result a very short time between the initiation of cracks of the specimen under load, and the spread of the cracks to a great enough extent to cause failure.

3.8.2 SUGGESTIONS FOR ADDITIONAL FATIGUE TESTS

Other more elaborate techniques to monitor crack initiation and growth are available but were beyond the scope and cost of this study. Stress coating, trip gages, and acoustic signature techniques have been used for this purpose in the past and in current fracture related research

Table 3.6. Fatigue and Flexural
Test Results for LCF Specimens

LCF SPECIMEN SOURCE	THICKNESS INCHES (A/C+LCF)	LOAD, LB FLEXURE	LOAD, LB FATIGUE	EQUIV THICKNESS INCHES	NORM. LOAD, PSI FLEXURE	NORM. LOAD, PSI FATIGUE
Ohio	1 + 2	213		2.7	29	
Ohio	1.5 + 2	251		3.1	27	
Penn	1 + 4	505		4.7	23	
Penn	1 + 3		233	3.7		17
Penn	1 + 4		370	4.7		17

studies and could be employed in a more complete investigation of fatigue fracture of LCF pavement materials.

In addition, there is evidence that pavements that support moving traffic, such as runways, are subjected to stress reversal. That is, as the aircraft load moves past a point on the pavement, that point is alternately subjected to tension and compression. A fatigue test could be designed that would subject the samples to stress reversal and would be more representative of the stresses to which the pavement might be subjected when exposed to moving traffic.

CHAPTER 4 - DESIGN AND CONDUCT OF FIELD TESTS

4.1 OBJECTIVE

The objective of the field test activities was to study the long-term changes in the behavior of LCF pavements that may occur as a result of pozzolanic activity and environmental forces. In order to accomplish this objective core samples were obtained from four airports. They were analyzed for the effects of pavement age on modulus of resilience and unconfined compressive strength.

4.2 PREVIOUS RESEARCH

The curing of LFA is controlled by three factors: time, moisture, and temperature. Each directly impacts the pozzolanic reaction and must be controlled to ensure proper setting and compressive strength.

MacMurdo and Barenberg[12] conducted extensive tests on the effects of time and temperature on LFA pavements. The results are shown in Figure 4.1. As can be seen from the figure, the effect of temperature on the compressive strength is not linear.

It is important to consider the effects of temperature on curing when planning LFA placement. Adequate curing must be obtained prior to the beginning of cyclic freeze-thaw to assure satisfactory field performance.[13] Curing conditions should be specified with the purpose of producing at least the minimum LFA mixture strength.

LFA mixtures cured for 7 days at 100°C (under ASTM C593 conditions) have exhibited strengths ranging from 500 psi to 1000 psi. After 1 to 2 years these values may exceed 1500 psi and ultimately maybe in excess of 3000 psi.[7] Though ultimate strengths are fairly high, many engineers feel that the slow rate of strength development is undesirable and is a function of the slow chemical reaction between lime and flyash. To compensate for low early

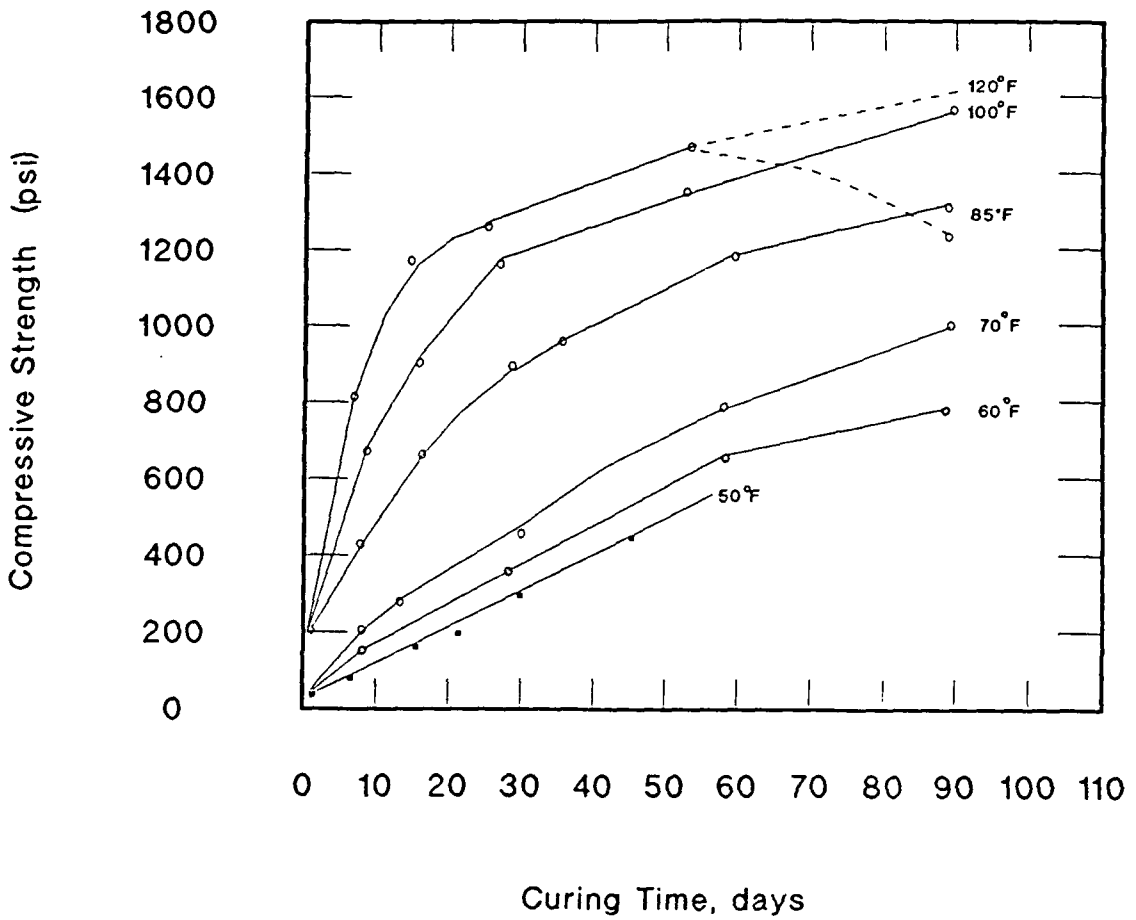

Figure 4.1 Effects of Curing Time and Temperature on the Strength Development of a Lime-Flyash-Aggregate Mixture [12]

strengths, admixtures are used to accelerate early strength gains. Portland cement has proven effective in this requirement.

Under proper curing conditions, chemical reactions in LFA mixtures will continue as long as sufficient lime and flyash are present.[14]
Figure 4.2 shows compressive strength growth with age of a LFA mixture in the Chicago area.

4.3 APPROACH

To accomplish the field test activities two tasks were undertaken; core extraction and core testing. A summary of these tasks is presented in the following paragraphs.

4.3.1 EXTRACTION OF CORES

Test cores were taken from LFA pavements at Portland Airport, and LCF pavements at New York and New Jersey Airports. At each airport, test cores were taken from two taxiway areas with three points per area on the selected pavements, 500 feet from one end and in the middle. At each point the test cores were extracted from the keel section and the left and right pavement edges.

In 1986 project representatives visited the offices of the Port Authority of New York and New Jersey and met with the airport planning, design, and maintenance engineering staffs. At that time, the goals and objectives of the LCF study effort were presented and support was requested in extracting sample pavement cores at JFK and Newark Airports. Each of the Port Authority organizations agreed to support the study. All extractions and refilling of pavements were to be done by Port Authority engineers.

Later in 1986 project personnel visited Portland International Airport to arrange and coordinate the extraction of LCF cores from the site runway. It was agreed at the meeting that seven (7) full depth cores would be extracted from Runway 10R.

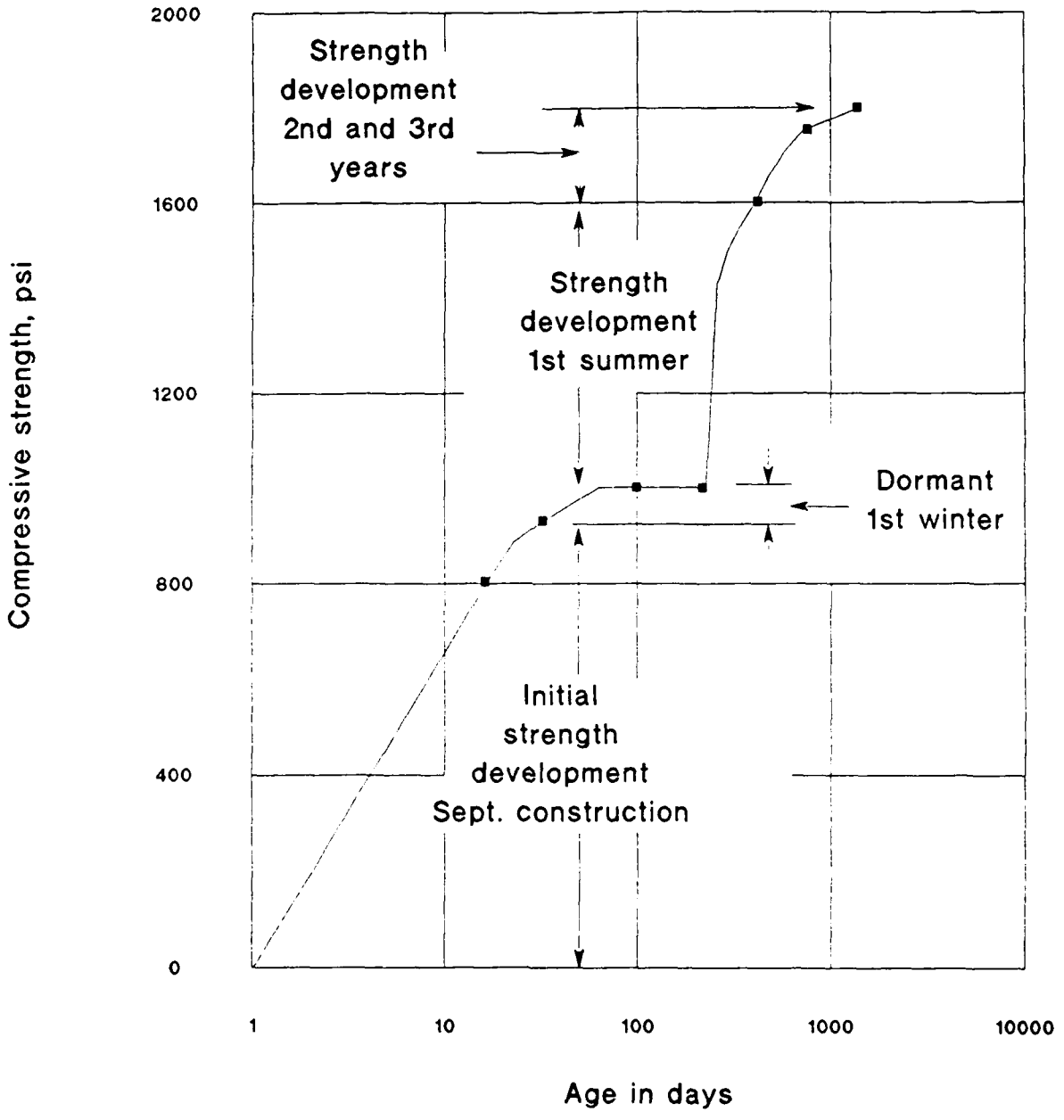

Figure 4.2

Compressive Strength Development of Lime-Flyash-Stabilized Mixture in Chicago Area [16]

Courtesy: Alberg and Barenberg, "Pozzolanic Pavements," Bulletin 473, Eng. Experiment Station, University of Illinois (1965)

The coring process at Portland Airport was completed in 3 hours. The coring was done by Concrete Coring of Vancouver, Washington. Seven cores were extracted from the locations given in Table 4.1. Core locations were chosen in order to assure collection of samples from areas with heavy, moderate, and light volumes of traffic.

None of the cores was damaged by the extraction process. The only breaks occurring in the full depth cores were the natural separations occurring between lifts.

Cores 1-6 were marked, wrapped, sealed, boxed, and shipped to Tuskegee University to be tested. Core 7 was sent to Northwest Testing Laboratories, Inc. of Portland, Oregon, to be tested as a reference sample. This reference helped validate the testing done at Tuskegee University and also provided verification that no damage occurred to the cores during their transport.

In April of that year project personnel visited the New York World Trade Center to meet with representatives from the Port Authority of New York and New Jersey to finalize the plans for core removal at Newark and JFK Airports. At the meeting, it was agreed that cores would be extracted at JFK Airport later that month. Similarly, core extractions would begin at Newark Airport the next day after completion of the JFK extractions.

Eleven cores were extracted at JFK and labeled No.'s 8 through 18. Cores #8-#14 and #18 were boxed and shipped to Tuskegee University. Cores #15, #16, and #17 were sent to the Port Authority's materials lab for testing. Figures 4.3 and 4.4 show the location of each core extraction with respect to the taxiway from which they were extracted. Shown in Figure 4.5 is an overall layout of the airport.

JFK Airport had experienced slippage of the wearing course over the LCF base course on some of the taxiways. These areas were described by the representatives as looking like waves in the pavement. At this point it was determined that coring at these locations may give some insight into why this

Table 4.1

Portland Extraction Matrix

Core Number	Location	Lift Designations
1	500 ft. from end of runway; 70 ft. left of centerline	A, B
2	500 ft. from end of runway; 10 ft. left of centerline	A, B, C
3	500 ft. from end of runway; 10 ft. right of centerline	A, B, C
4	1,200 ft. from end of runway; 70 ft. left of centerline	A, B
5	1,200 ft. from end of runway; 10 ft. left of centerline	A, B, C
6	1,200 ft. from end of runway; 10 ft. right of centerline	A, B, C
7	1,400 ft. from end of runway; 10 ft. left of centerline	A, B, C

Figure 4.3

JFK Core Locations, April 21, 1986

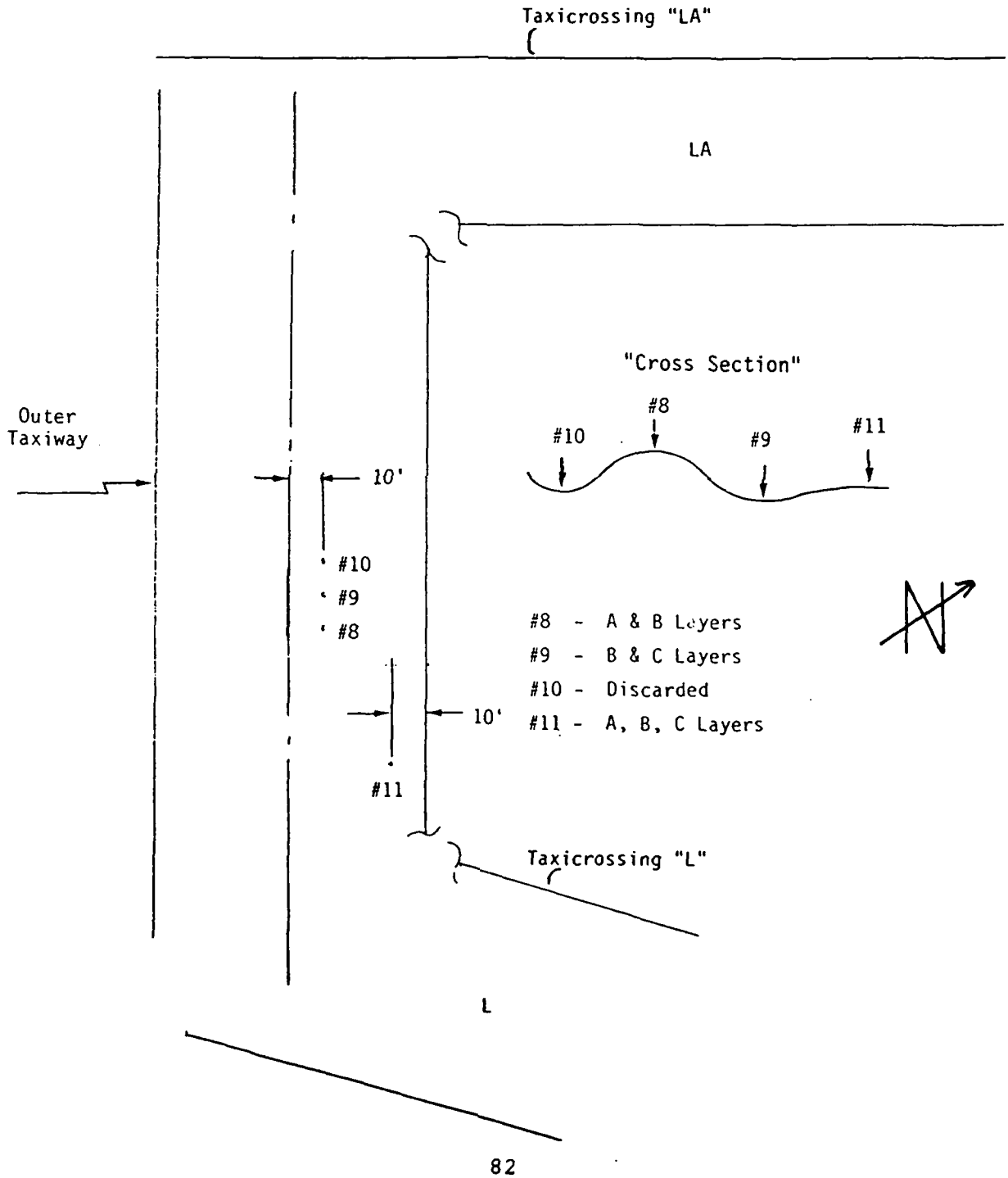

Figure 4.4

JFK Core Locations, April 22, 1986

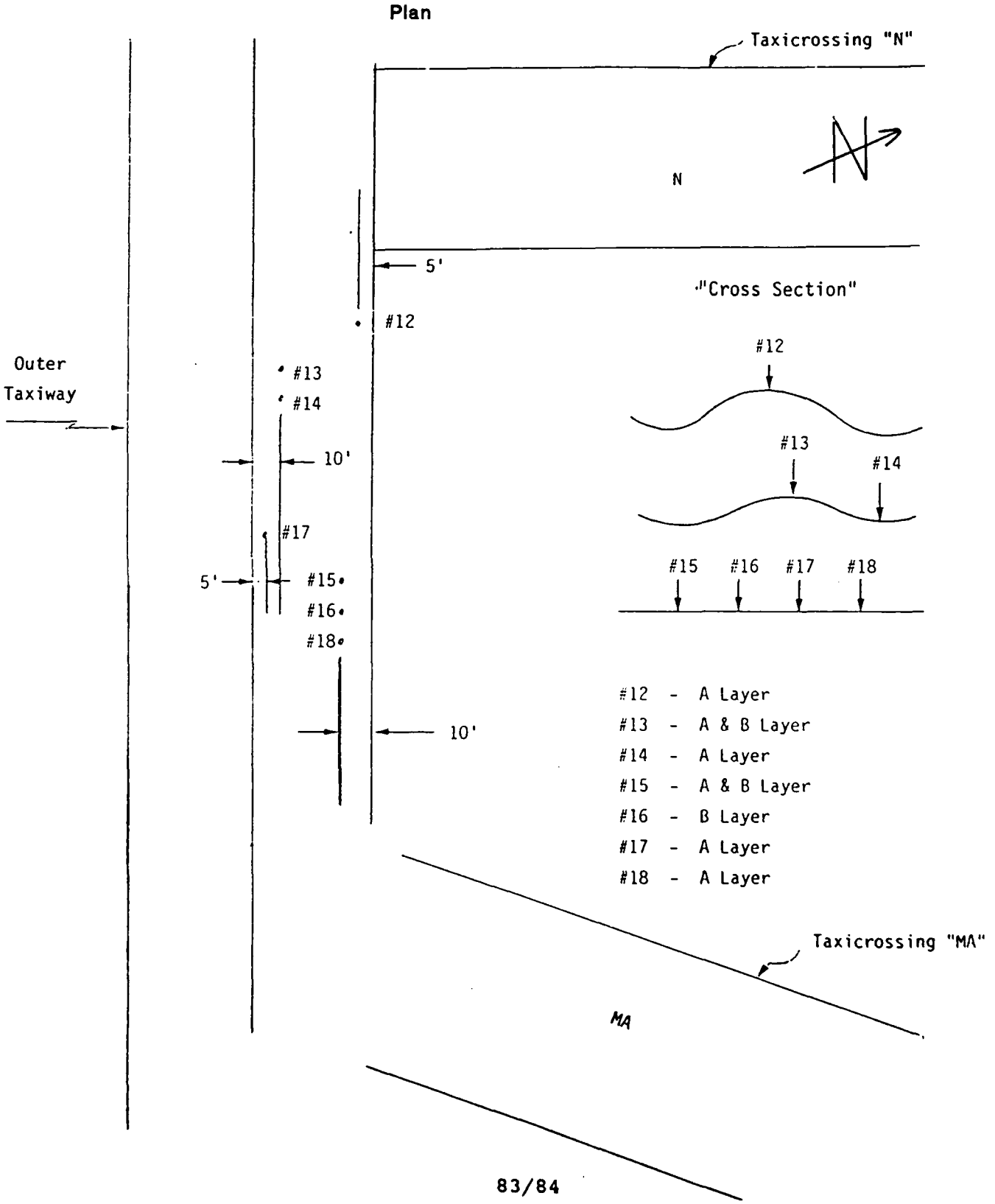

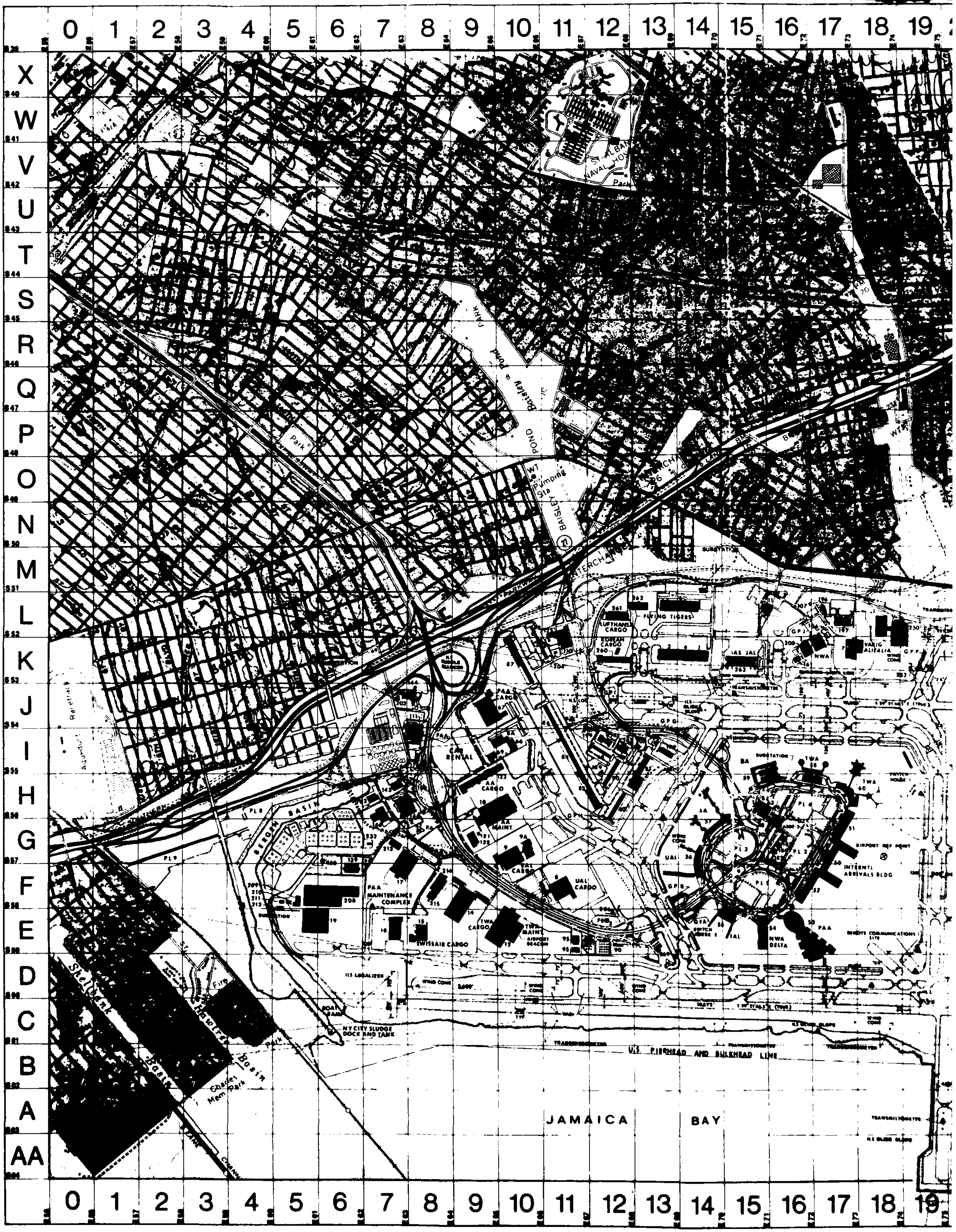
0 1 2 3 4 5 6 7 8 9 10 11 12 13 14 15 16 17 18 19
X W V U T S R Q P O N M L K J I H G F E D C B A AA
Park
Baisley Pond
POND
WT Pumping Sta
BAISLEY
INTERCHANGE
SUBSTATION
FLYING TIGERS
LUFTHANSA CARGO
KOREAN CARGO
VARIG
NWA
PAA CARGO
CAR RENTAL
AA CARGO
AA MAINT.
BERGEN BASIN
TWA
UAL
UAL CARGO
PAA MAINTENANCE COMPLEX
SWISSAIR CARGO
TWA CARGO
INTERNTL ARRIVALS BLDG
NWA DELTA
PAA
NY CITY SLUDGE DOCK AND TANK
U.S. PIERHEAD AND BULKHEAD LINE
Hawtree Basin
Charles Mem Park
Fire
JAMAICA BAY

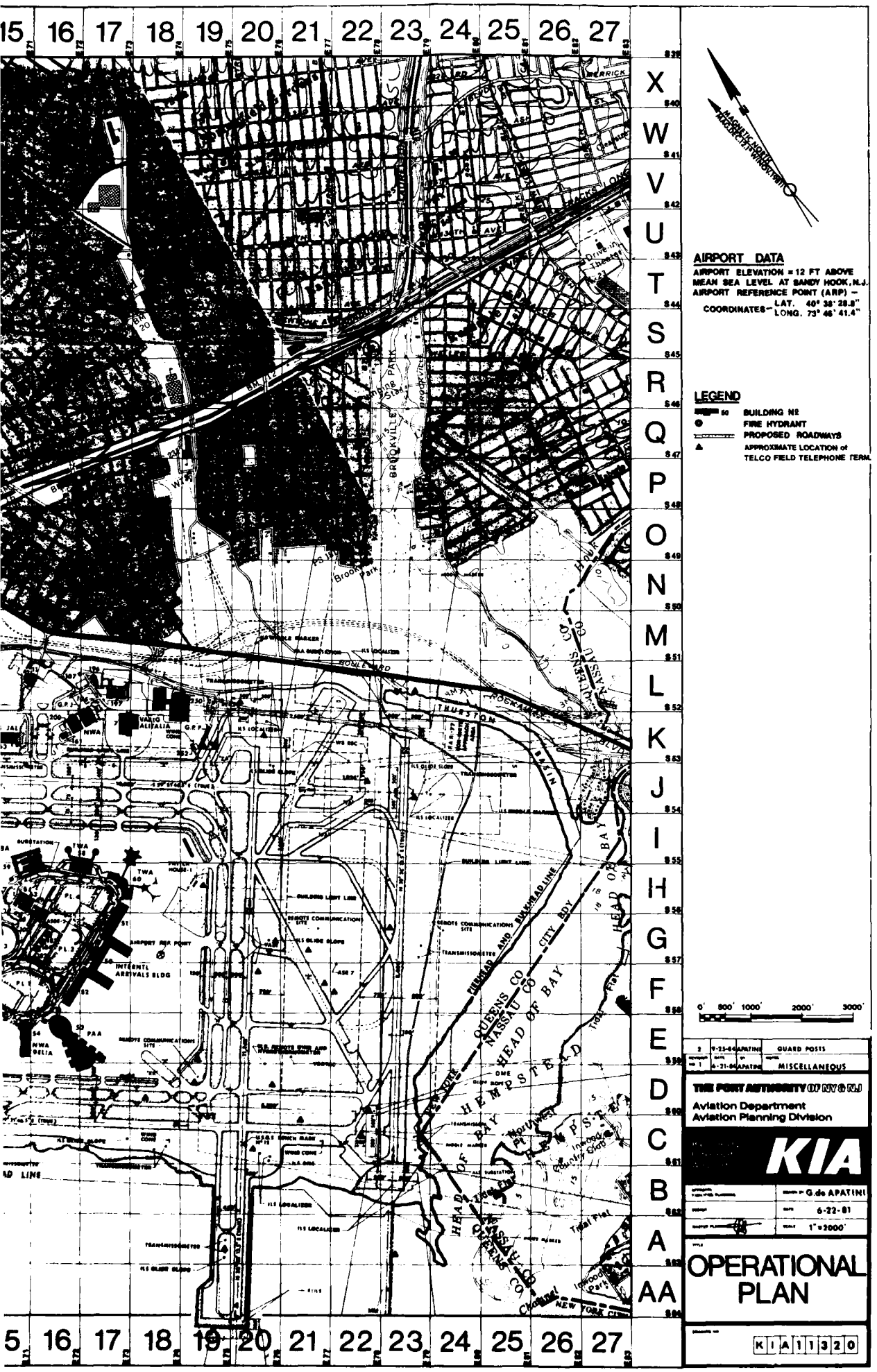

85/86 Figure 4.5

problem occurred and if it was LCF related. Cores were taken from the tops and valleys of the waves, and at areas where no waving occurred (this is shown in the "cross section" in Figure 4.3).

Extraction of three completed layers (A, B, and C) from each site was rare. Most cores experienced at least one layer that was cracked; fractured or damaged. These conditions were experienced in all the areas where cores were extracted, not just in the areas where waving had occurred. It should be noted that the cracking and fracturing that occurred in the cores pointed to the possibility of fatigue of the LCF base course.

In some cases the bottom layer ("C") was not found. One possible explanation for this is the length (approximately 14") of the coring bit used. Initially the core extraction method used involved extending the core bit through the entire depth of the pavement (to cut the core layers) and then trying to retrieve each layer. This method may have forced the "C" layer into the subgrade, causing it not to be retrievable. This procedure was changed at Newark Airport, where coring was only to the depth of the bottom of the "C" layer. Results for acquiring all three layers improved. It should be mentioned that the core extraction at Portland Airport used a 36-inch bit and no problems were encountered recovering any layers.

Nine cores were extracted at Newark International Airport from the locations shown in Figures 4.6, 4.7, and 4.8. Figure 4.9 is an overall layout of the airport. The cores were labeled Nos. 19 through 28. Cores #19 through #23 and cores #25, #27 and #28 were sent to Tuskegee University to be tested. Cores #24 and #26 were given to the Port Authority for testing. The results from these tests were used to validate testing at Tuskegee.

Figure 4.6

Newark Core Locations, April 23, 1986

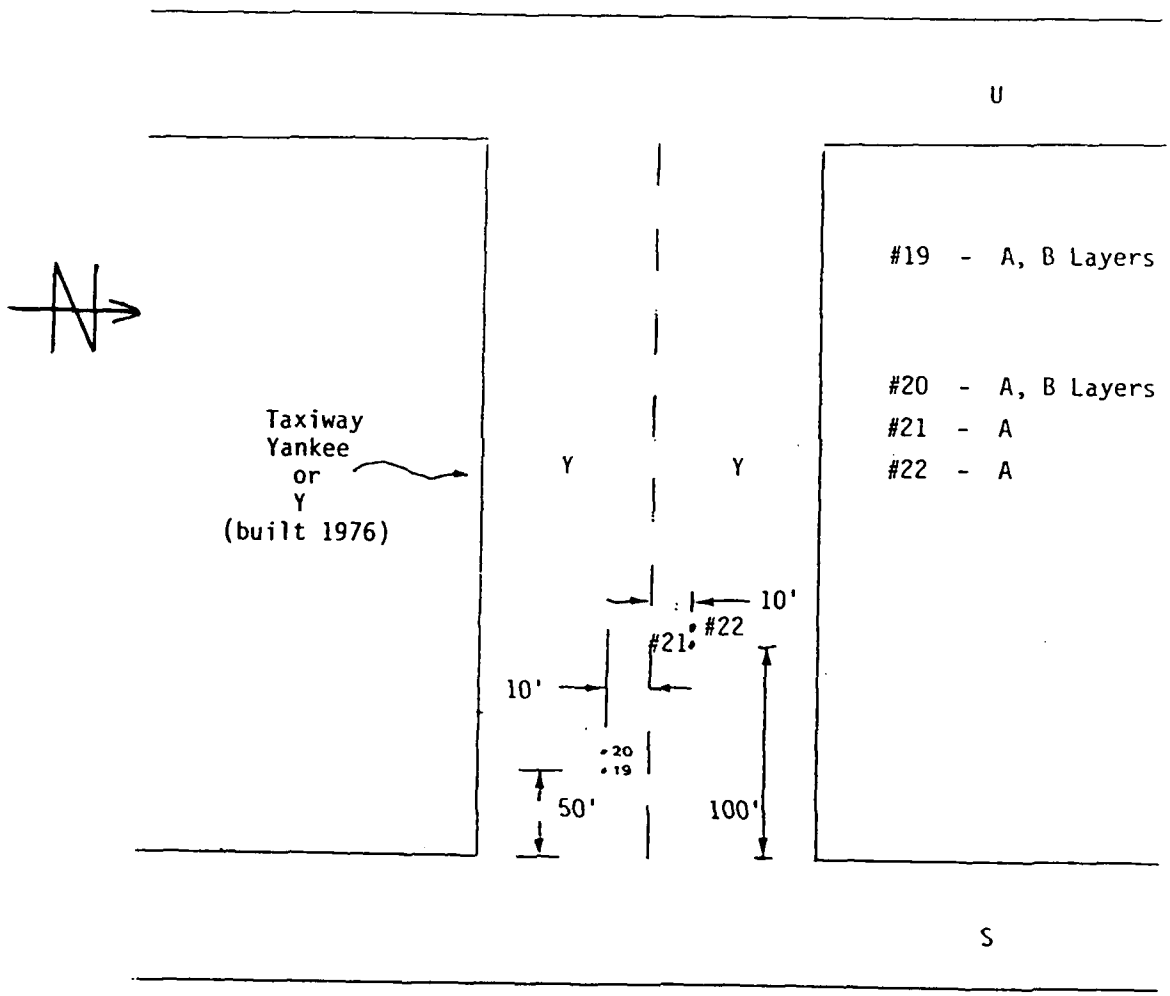

Figure 4.7

Newark Core Locations, April 24, 1986

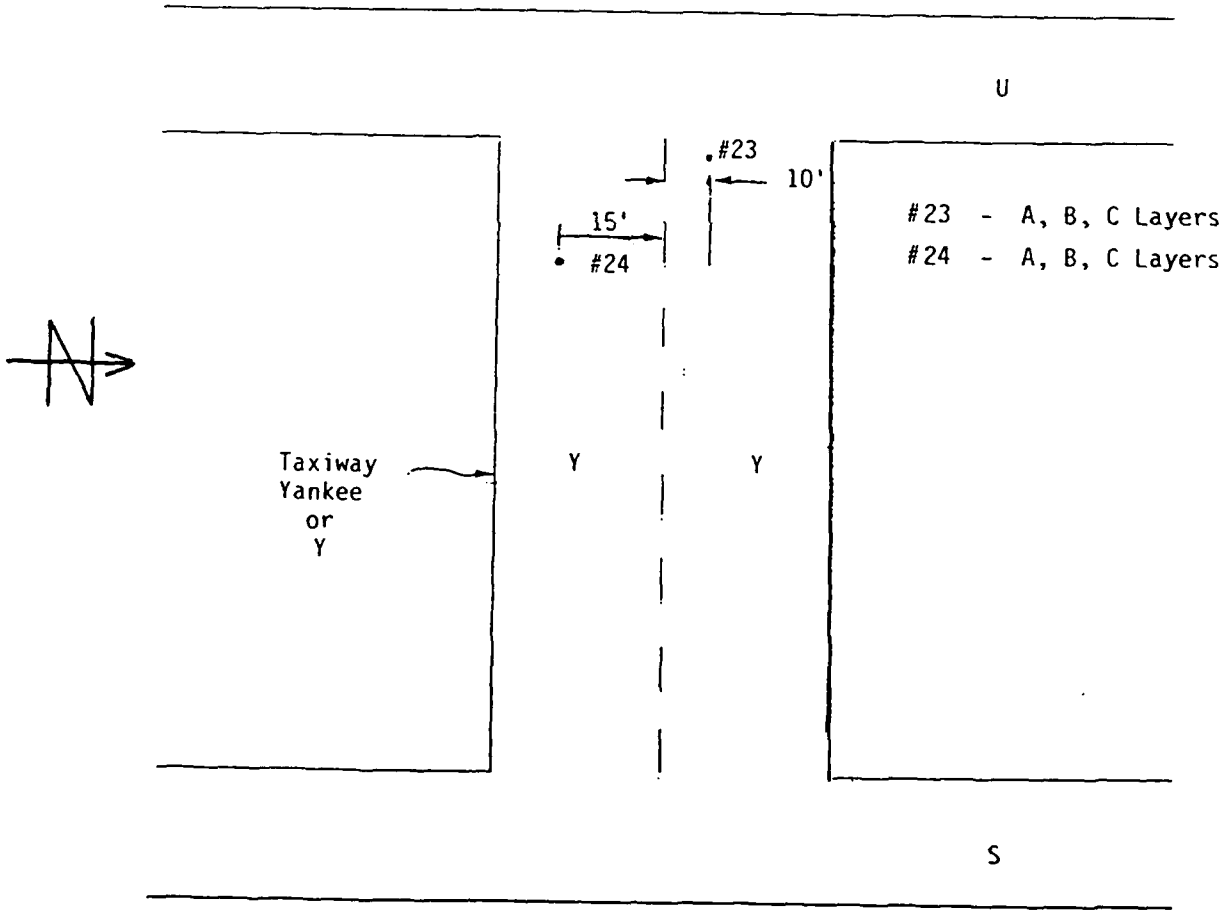

Figure 4.8

Newark Core Locations, April 24, 1980

#25 - A, B, C
#26 - A, B
#27 - A, B

These cores were extracted from the apron of Terminal "C"

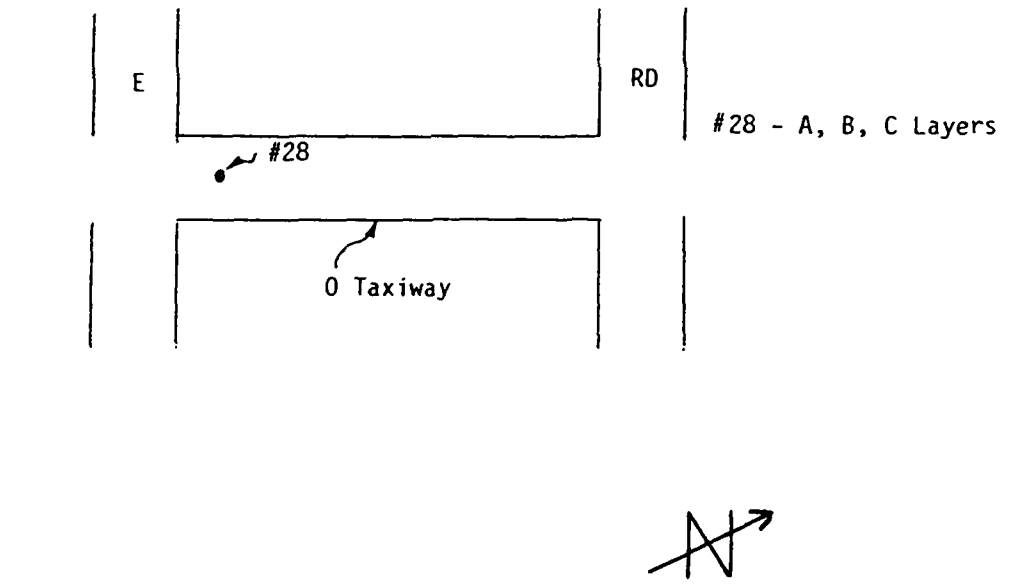

NEWARK INTERNATIONAL AIRPORT OPERATIO

LOC.	BLDG. NO.	
E 14	1	PASSENGER TERMINAL A
F 12	2	PASSENGER TERMINAL B
E 10	3	PASSENGER TERMINAL C
J 3	5	MEDICAL CLINIC
D 14	7	LOT D TOLL BOOTH (NOT IN SERVICE)
G 8	10	P.A. ADMIN. & POLICE BLDG.
J 4	11	P.A. MAINT. GARAGE
E 5	12	BUTLER AVIATION HANGAR
C 6	14	U.A.L. HANGAR
E 4	22	BUTLER AVIATION
C 13	23	HERTZ RENTAL CAR ADMIN. BLDG.
C 13	24	HERTZ RENTAL CAR MAINT. BLDG.
C 13	25	NATIONAL RENTAL CAR ADMIN. BLDG.
C 13	26	NATIONAL RENTAL CAR MAINT. BLDG.
C 13	27	AVIS RENTAL CAR ADMIN. BLDG.
C 13	28	AVIS RENTAL CAR MAINT. BLDG.
C 13	42	P.A. UTILITY BLDG.
H 3	44	ELECTRICAL BLDG.
G 7	45	SWITCH HOUSE NO. 2
F 13	46	CENTRAL HEATING & REFRIG. PLANT
J 3	49	P.A. HEATING PLANT
H 3	51	P.A. MAINT.
E 5	52	BUTLER AVIATION
J 3	53	P.A. MAINT.
E 5	54	BUTLER AVIATION
F 4	55	BREWSTER HANGAR
F 4	57	PUMP HOUSE
H 3	75	GETTY SERVICE STATION
J 3	77	P.A. MAINT. STORAGE
J 4	81	P.A. SAND & SALT STORAGE BLDG.
J 4	82	P.A. STORAGE BLDG.
J 4	83	P.A. MAINT. GARAGE
J 3	84	P.A. LANDSCAPING STORAGE BLDG.
H 4	88	NORTH PASSENGER TERMINAL
C 6	89	GUARD POST (INACTIVE)
E 6	90	GUARD POST J
J 4	91	GUARD POST H
J 7	94	SWITCH HOUSE NO. 1
C 6	95	FLAGSHIP INT'L INC. (A.A.L)
F 19	96	GUARD POST F
D 10	97	GUARD POST D
D 14	98	GUARD POST E
D 10	99	GUARD POST C 4
J 3	102	P.A. MAINT. STORAGE
H 3	103	TOLL BOOTH LOT 1
H 3	104	PEDESTRIAN WALKWAY
D 11	105	CENTRAL TOLL BLDG.
D 11	106	HTG. & REFRIG. PLANT for TOLL BLD.
D 14	107	LOT D
I 3	108	LOT. 3
D 14	109	LOT. D
J 3	110	LOT. 3
J 9	111	LOT. 4
I 3	113	LOT 3
E 4	114	LOT 4
F 19	116	ALLIE
E 19	117	FUEL
G 8	119	CONT
A 6	140	CUMI
F 5	150	AMR C
D 5	151	AMR C
E 6	152	AMR C
F 5	153	AMR C

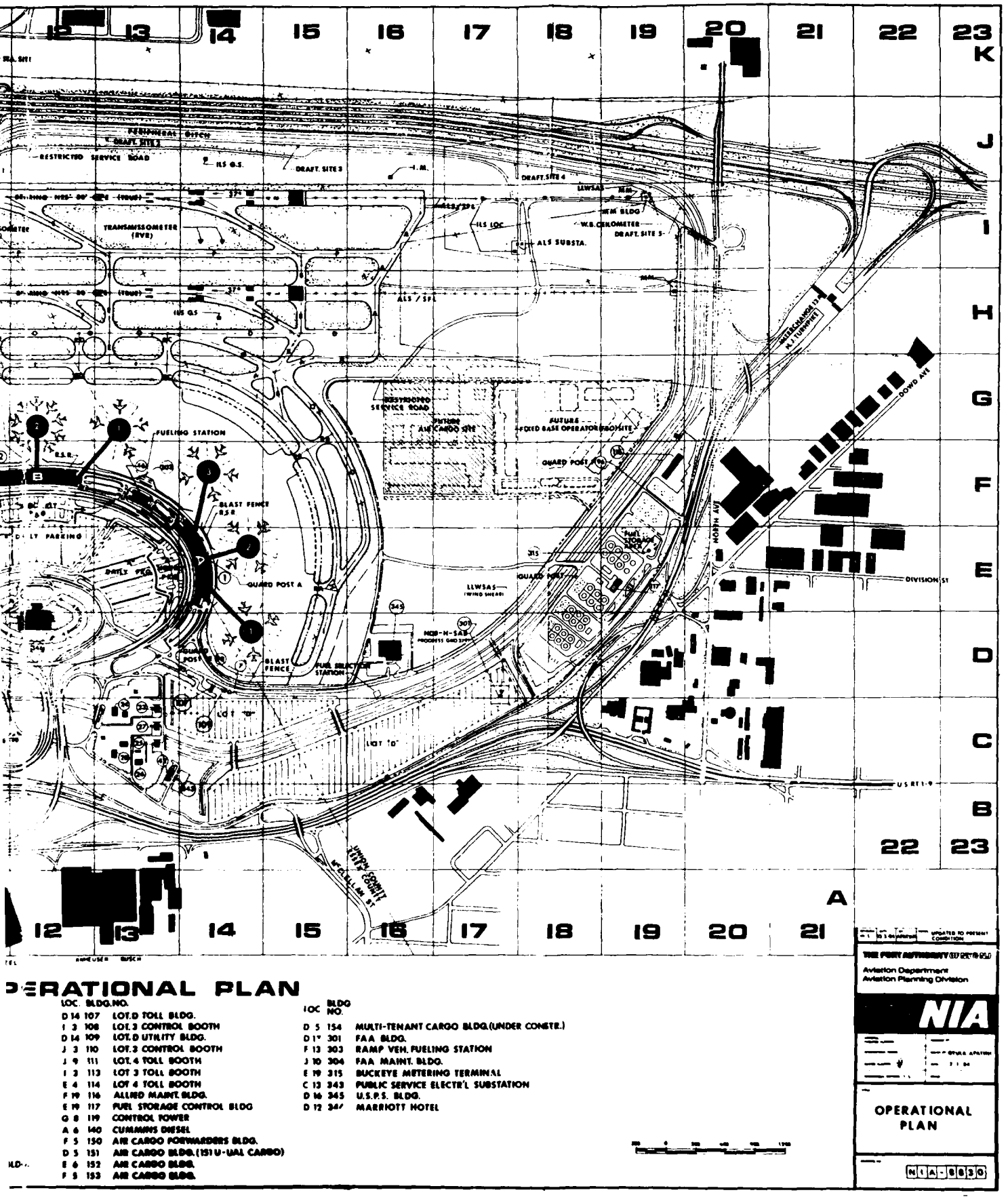

OPERATIONAL PLAN

LOC.	BLDG.NO.	
D 14	107	LOT. D TOLL BLDG.
I 3	108	LOT. 3 CONTROL BOOTH
D 14	109	LOT. D UTILITY BLDG.
J 3	110	LOT. 3 CONTROL BOOTH
J 9	111	LOT. 4 TOLL BOOTH
I 3	113	LOT 3 TOLL BOOTH
E 4	114	LOT 4 TOLL BOOTH
F 19	116	ALLIED MAINT. BLDG.
E 19	117	FUEL STORAGE CONTROL BLDG
Q 8	119	CONTROL TOWER
A 6	140	CUMMINS DIESEL
F 5	150	AIR CARGO FORWARDERS BLDG.
D 5	151	AIR CARGO BLDG. (151 U-UAL CARGO)
E 6	152	AIR CARGO BLDG.
F 5	153	AIR CARGO BLDG.

LOC	BLDG NO.	
D 5	154	MULTI-TENANT CARGO BLDG. (UNDER CONSTR.)
D 17	301	FAA BLDG.
F 13	303	RAMP VEH. FUELING STATION
J 10	304	FAA MAINT. BLDG.
E 19	315	BUCKEYE METERING TERMINAL
C 13	343	PUBLIC SERVICE ELECTR'L SUBSTATION
D 16	345	U.S.P.S. BLDG.
D 12	347	MARRIOTT HOTEL

UPDATED TO PRESENT CONDITION

THE PORT AUTHORITY OF NY & NJ

Aviation Department
Aviation Planning Division

NIA

OPERATIONAL PLAN

NIA-0830

Figure 4.9

In selecting sites for the coring of Newark Airport, use was made of previous coring data to help in the selection of 3 different coring areas which corresponded to different ages of LCF material (1 year - 13 years). Cores were extracted from two sites having historical coring data (taxiway Yankee and terminal area "C") and also from one area that had no previous data.

Problems occurred during core extraction. These problems were caused by the weather. The temperature was approximately 30°F and caused the coring bits to contract after being raised out of the ground. Much difficulty was encountered in removing the cores from the bits without damage. After four (4) unsuccessful attempts at retrieving a full depth core the operation was terminated until the following day when the temperature was much higher and core extraction was completed without incident.

4.3.2 TESTING OF EXTRACTED CORES

The cores were tested in the Stress Analysis and Materials Research Laboratory at Tuskegee University. The tests were conducted in accordance with ASTM standards D4123-82 and C39-84 for resilience modulus and unconfirmed compressive strength, respectively.

4.4 TEST PROCEDURE FOR INDIRECT TENSION TEST FOR RESILIENCE MODULUS OF ELASTICITY

Indirect tension tests for determining resilience modulus of elasticity were conducted in accordance with ASTM designation D4123-82. Test cores were placed in lime saturated water at 73.4 degrees F plus or minus 3.0 degrees F for at least 40 hours. The tests were done in accordance with ASTM designation C 42 section 6.3. The test specimens were then placed in a controlled temperature cabinet at 77 degrees plus or minus 2 degrees F for at least 24 hours prior to testing.

The repeated load indirect tension test for determining resilience modulus of

concrete cores was conducted by applying compressive loads in a haversine wave form. The load was applied vertically in the vertical diametral plane of a cylindrical specimen of concrete. The resulting Poisson's ratio and resilience moduli were calculated using values for measured deformation.

4.5 APPARATUS

4.5.1 TESTING MACHINE

The test machine used was MTS Model 810 which has a function generator Model 410 capable of producing the desired wave form.

4.5.2 DEFORMATION MEASUREMENTS

The values of the vertical and the horizontal deformations were measured using the X-Y recorder and Linear Variable Differential Transducer (LVDT). The LVDT was fixed at the mid height of the specimen.

4.5.3 LOADING STRIP

A pair of metal loading strips with a concave surface having a radius of curvature equal to the nominal radius of the test specimens was made to apply load to the specimen. The dimensions of the loading strip were designed in accordance with ASTM designation D4123.

4.5.4 CAPPING EQUIPMENTS

The capping plates which were used to cap the core ends were made in accordance with ASTM designation C617.

Compression Platen MTS Model 643.41B grip was used to test concrete cores.

4.6 TEST PROCEDURE FOR RESILIENCE MODULUS TEST

The test specimens were placed in a controlled temperature cabinet and heated to the test temperature. The specimens were kept in controlled temperature at least for 24 hours prior to testing. The diameter and length of the cores were measured before testing.

The specimens were placed in the loading apparatus. They were positioned so that the loading strips were parallel and centered on the vertical diametral plane.

The specimens were preconditioned by applying a repeated haversine waveform load to the specimen without impact for a minimum period sufficient to obtain uniform deformation readout. The minimum load was determined so that the resilient deformation was stable. Each test specimen was tested at three loading frequencies: 0.5HZ, 1.0HZ, and 2.5HZ.

The horizontal and vertical deformations were monitored during the test. If the total cumulative vertical deformation was found greater than 0.001 inch during the test then the applied loads were reduced.

The resilience modulus tests were completed within 4 minutes from the time the specimens were removed from the temperature-controlled cabinet.

4.7 TEST PROCEDURE FOR UNCONFINED COMPRESSION TEST

The diameter and length of the specimens were measured after taking them out from the saturated lime solution.

The end surface of the specimen was capped with a sulphur mortar capping compound in accordance with ASTM designation.

The specimens were placed in the lower platen of the grip MTS Model 643.41B. The rate of loading was set such that the moving head travelled at a rate approximately 0.05 in/min. Load was applied continuously and without shock.

The load was applied until the specimens failed. The maximum load carried by the specimen during the test was recorded with the help of an X-Y recorder.

CHAPTER 5 - FIELD TEST RESULTS

5.1 GENERAL RESULTS

Because of the results of previous research, it was expected that the field test results would confirm that LCF pavements exhibit increasing strength as they age. This was only partially confirmed.

Figures 5.1 and 5.2 and Tables 5.1 through 5.4 represent the results of tests of modulus of resilience and unconfined compressive strength for core samples taken from the runway pavements that were tested.

The samples taken from Newark Airport had ages of 3, 10, and 16 years at the time of testing. The compressive strength test results for Newark showed the greatest strength for the ten year old samples. The resilience modulus for the Newark samples was greatest at 16 years.

For both compressive strength and resilience modulus, the samples from Portland Airport showed the highest test results. The test results for JFK were low for compressive strength and resilience modulus.

These results may have been influenced by exposure to differing environmental conditions (e.g. temperature, chemicals), mix design or other factors. Analysis of these factors was beyond the scope of the project. However, it would appear that further information could be gained by testing samples from the same pavements several times as they age.

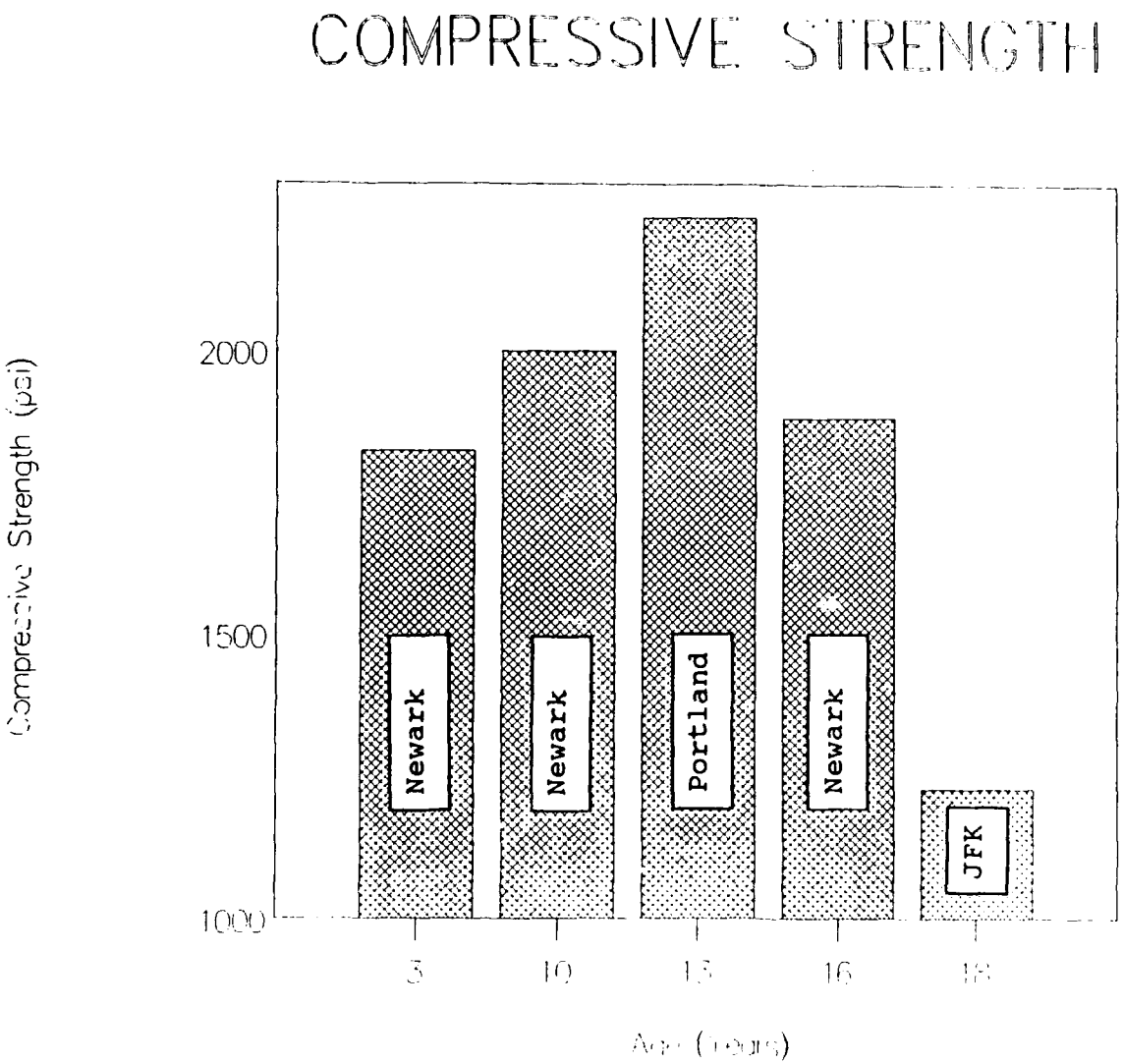

Figure 5.1 - Compressive Test Results

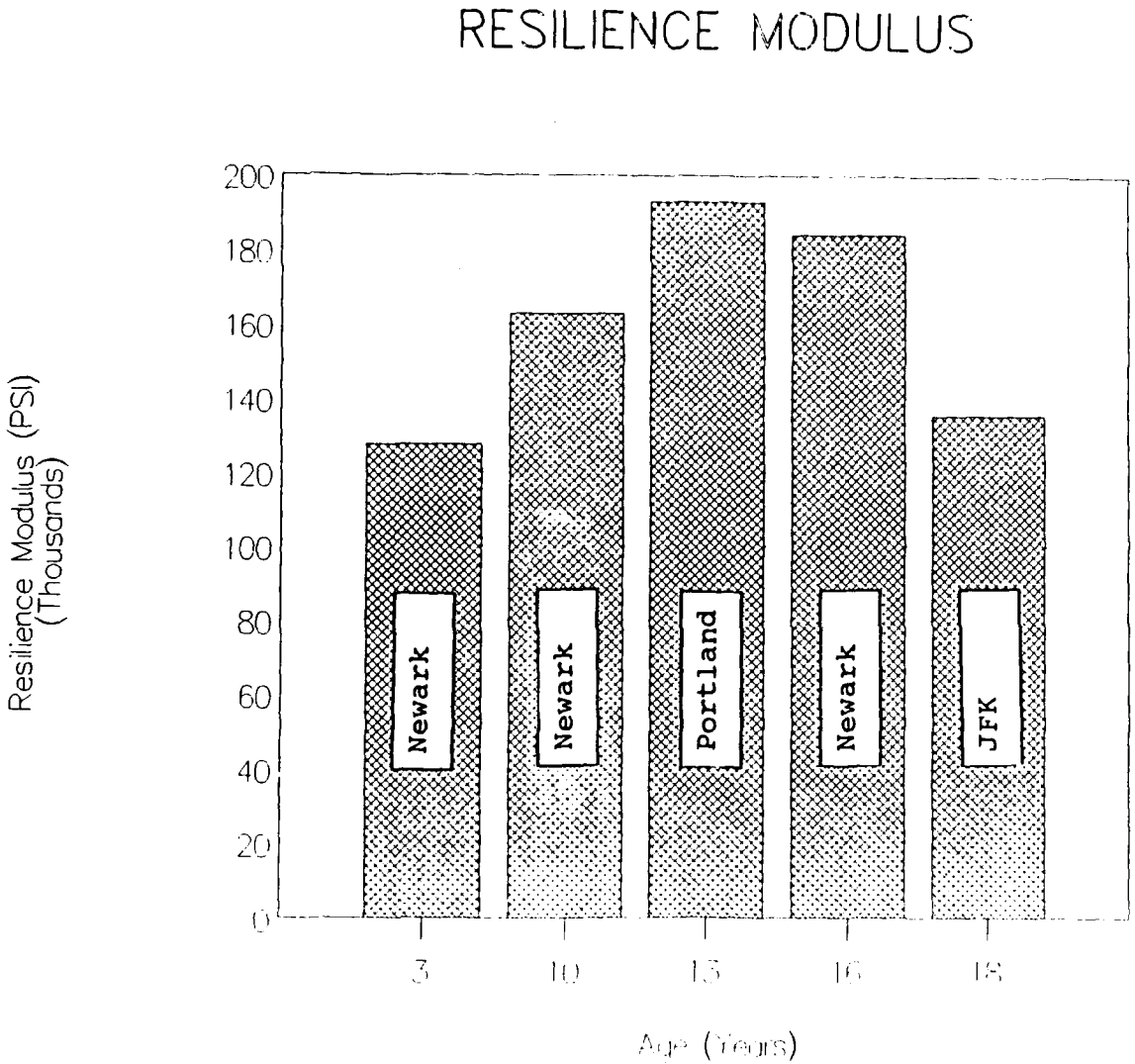

Figure 5.2 - Resilience Modulus Test Results

Table 5.1

COMPRESSION TEST RESULTS

SAMPLE	SOURCE	LAB	AGE yrs	DIAMETER in	LENGTH in	STRENGTH psi
1A	Portland	Tuskegee	13	2.6	5.3	2754
1B	Portland	Tuskegee	13	2.6	5.2	1705
2A	Portland	Tuskegee	13	2.6	5.2	2594
2B	Portland	Tuskegee	13	2.6	5.3	3337
2C	Portland	Tuskegee	13	2.6	4.1	3182
3A	Portland	Tuskegee	13	2.6	5.3	1324
3B	Portland	Tuskegee	13	2.6	5.3	3024
3C	Portland	Tuskegee	13	2.6	5.3	2502
4A	Portland	Tuskegee	13	2.6	5.3	2429
4B	Portland	Tuskegee	13	2.6	5.3	1360
5A	Portland	Tuskegee	13	2.6	5.3	1117
5B	Portland	Tuskegee	13	2.6	4.3	2026
5B	Portland	Tuskegee	13	2.6	4.3	1429
5C	Portland	Tuskegee	13	2.6	5.5	3050
6A	Portland	Tuskegee	13	2.6	5.2	1930
6B	Portland	Tuskegee	13	2.6	5.3	1800
6C	Portland	Tuskegee	13	2.6	5.4	2412
8A	JFK	Tuskegee	18	2.6	5.4	2682
8B	JFK	Tuskegee	18	2.6	5.3	703
9B	JFK	Tuskegee	18	2.6	5.3	1290
9C	JFK	Tuskegee	18	2.6	3.6	536
11A	JFK	Tuskegee	18	2.6	5.2	750
11B	JFK	Tuskegee	18	2.6	3.1	585
11C	JFK	Tuskegee	18	2.6	5.2	864
12A	JFK	Tuskegee	18	2.6	4.9	1381
13A	JFK	Tuskegee	18	2.6	5.3	1410
13B	JFK	Tuskegee	18	2.6	5.4	1498
14A	JFK	Tuskegee	18	2.6	5.3	1510
18A	JFK	Tuskegee	18	2.6	5.4	1516
19A	Newark	Tuskegee	10	2.6	5.4	2051
20A	Newark	Tuskegee	10	2.6	5.4	2317
20B	Newark	Tuskegee	10	2.6	5.1	1340
21A	Newark	Tuskegee	10	2.6	5.4	2515
22A	Newark	Tuskegee	10	2.6	3.4	2330
22A	Newark	Tuskegee	10			2345
23A	Newark	Tuskegee	10	2.6	5.4	2025
23B	Newark	Tuskegee	10	2.6	5.3	1340
23C	Newark	Tuskegee	10	2.6	4.3	1731
25A	Newark	Tuskegee	3	2.6	5.3	2943
25B	Newark	Tuskegee	3	2.6	5.2	1704
25C	Newark	Tuskegee	3	2.6	5.4	1201
27A	Newark	Tuskegee	3	2.6	5.4	1390
27B	Newark	Tuskegee	3	2.6	5.2	1880
28A	Newark	Tuskegee	16	2.6	5.4	2151
28B	Newark	Tuskegee	16	2.6	5.2	1518
28C	Newark	Tuskegee	16	2.6	3.4	1976

Table 5.2

COMPRESSION TEST (FIELD)
RESULTS VS. AGE OF PAVEMENT

AGE (yrs)	STRENGTH AVG (psi)	STRENGTH MIN (psi)
3	1823.6	1201
10	1999.3	1340
13	2233.8	1117
16	1881.7	1518
18	1227.1	536

Table 5.3

RESILIENCE MODULUS TEST RESULTS

SOURCE	LAB	AGE yrs	DIAMETER in	LENGTH in	RESILIENT MODULUS psi
Portland	Tuskegee	13	2.6	5.3	112,391
Portland	Tuskegee	13	2.6	5.2	74,712
Portland	Tuskegee	13	2.6	5.2	118,746
Portland	Tuskegee	13	2.6	5.3	155,464
Portland	Tuskegee	13	2.6	4.1	155,178
Portland	Tuskegee	13	2.6	5.3	130,454
Portland	Tuskegee	13	2.6	5.3	83,698
Portland	Tuskegee	13	2.6	5.3	225,153
Portland	Tuskegee	13	2.6	5.3	575,755
Portland	Tuskegee	13	2.6	5.3	140,692
Portland	Tuskegee	13	2.6	5.3	114,134
Portland	Tuskegee	13	2.6	4.3	509,279
Portland	Tuskegee	13	2.6	5.5	97,542
Portland	Tuskegee	13	2.6	5.2	410,779
Portland	Tuskegee	13	2.6	5.3	75,721
Portland	Tuskegee	13	2.6	5.4	106,370
JFK	Tuskegee	18	2.6	5.4	169,870
JFK	Tuskegee	18	2.6	5.3	274,330
JFK	Tuskegee	18	2.6	5.3	98,486
JFK	Tuskegee	18	2.6	3.6	177,709
JFK	Tuskegee	18	2.6	5.2	181,144
JFK	Tuskegee	18	2.6	3.1	149,100
JFK	Tuskegee	18	2.6	5.2	79,887
JFK	Tuskegee	18	2.6	4.9	110,926
JFK	Tuskegee	18	2.6	5.3	125,664
JFK	Tuskegee	18	2.6	5.4	88,212
JFK	Tuskegee	18	2.6	5.3	84,675
JFK	Tuskegee	18	2.6	5.4	83,688
Newark	Tuskegee	10	2.6	5.4	98,303
Newark	Tuskegee	10	2.6	5.4	156,047
Newark	Tuskegee	10	2.6	5.1	234,380
Newark	Tuskegee	10	2.6	5.4	138,261
Newark	Tuskegee	10	2.6	3.4	278,042
Newark	Tuskegee	10	2.6	5.4	119,813
Newark	Tuskegee	10	2.6	5.3	78,463
Newark	Tuskegee	10	2.6	4.3	199,045
Newark	Tuskegee	3	2.6	5.3	104,159
Newark	Tuskegee	3	2.6	5.2	135,840
Newark	Tuskegee	3	2.6	5.4	105,141
Newark	Tuskegee	3	2.6	5.4	161,160
Newark	Tuskegee	3	2.6	5.2	131,045
Newark	Tuskegee	16	2.6	5.4	158,386
Newark	Tuskegee	16	2.6	5.2	135,582
Newark	Tuskegee	16	2.6	3.4	258,105

Table 5.4

RESILIENCE MODULUS
VS. AGE OF PAVEMENT

AGE yrs	COMPRESSIVE STRENGTH AVG psi	MIN psi
3	127,469	104,159
10	162,794	78,463
13	192,879	74,712
16	184,024	135,582
18	135,308	79,887

5.2 FIELD TEST PROCEDURES

Resilience modulus of elasticity was calculated by using horizontal and vertical deformation at frequencies of 0.5, 1.0, 2.5 Hz. The value of resilience modulus was calculated and the average of these was taken. The calculated resilience 3 modulus was calculated and the average of these was taken.

The compressive strength of the specimen was calculated by dividing the maximum load carried by the specimen during the test by the average cross-sectional area of the specimen. Sample calculations are shown in the following sections.

5.3 Sample Calculation for Resilience Modulus for Core 2A

The total modulus of resilience E_{Rt} was calculated as follows:

$$E_{Rt} = P (g + 0.27)/t\, d_{Ht}$$

where

$g = 3.59\ d_{Ht}/d_{Vt} - 0.27$

g = Total resilient poisson's ratio

d_{Ht} = Total recoverable horizontal deformation

d_{Vt} = Total recoverable vertical deformation

P = Repeated load

t = Thickness of specimen

Result:

Frequency (Hz)	.5	1.0	2.5
d_{Ht} (in)	0.000125	0.000115	0.0000675
d_{Vt} (in)	0.00056	0.00052	0.00045
P (lbs)	87	87	87
t (in)	2.65	2.65	2.65
g	0.5314	0.524	0.2685
E_{Rt} (psi)	210,465	226,654	261,911

Average Resilience Modulus = 210,465 + 226,654 + 261,911 = 233,010 psi

5.4 Sample Calculation for Unconfined Compression Test for Core 2C

D	=	2.63 in	=	Diameter of core
L/D	=	1.57	=	Ratio of length to diameter
cf	=	0.96	=	Correction factor for L/D
P	=	18,000	=	Load at sample failure
A	=	5.43 in.	=	Area
P/A	=	3315	=	Compressive Strength

Corrected Compressive Strength = 3315 x cf = 3315 x 0.96 = 3182.0 psi

CHAPTER 6 - SUGGESTED LCF PAVEMENT DESIGN GUIDELINES

6.0 APPROACH

The design approach for LCF pavements must consider the fact that LCF pavements exhibit the characteristics of a flexible pavement just after construction and become rigid pavements as they mature. Engineers of the Port Authority of New York and New Jersey developed a design method which incorporated the dual characteristics of LCF pavements. The analysis presented in this report for the design of LCF pavements is similar to that of the Port Authority[26] with the following exceptions.

- LCF strength characteristics that resulted from the tests are available for preliminary design and planning.

- Equations for calculation of the maximum tensile and compressive stresses imposed by an aircraft load on a pavement slab are expanded to take into account the location of the load relative to the edges of the pavement.

The basic concept involves looking separately at specific design characteristics of rigid and flexible pavements. The final design is derived by taking the greater thickness determined by the separate analyses.

The objectives of the approach are several: minimize the likelihood of pavement failure over a long service life (20 years), minimize aircraft and pavement vibration, minimize the need for pavement maintenance that may disrupt traffic flow, and maximize economy in the use of material, equipment, and manpower resources.

In order to attain these objectives, the approach attempts to accomplish the following:

Aircraft and pavement vibration are minimized in order to promote passenger comfort and to extend the life of the pavement. The design approach minimizes compaction and horizontal displacement of the subgrade and maintains substantial separation between the natural wavelength of vibration of the aircraft and the wavelengths of any significant pavement surface deviations.

The need for pavement maintenance is minimized by keeping low the likelihood of pavement rupture caused by either fatigue or inability to withstand instantaneous loads. The design approach considers the effects of pavement flexure during many aircraft operations and the ability of the pavement to withstand compression and tensile loads.

Economy is achieved through minimizing the quantity of paving materials while designing to meet performance objectives, and minimizing manpower and equipment costs required for maintenance and repair.

The steps of the recommended design approach are as follows:

1. Determine the pavement thickness based on control of aircraft and pavement vibration response
2. Determine the pavement thickness based on elastic mass analysis
3. Determine pavement thickness based on stress, strain, and strength relationships:

- Tension
- Compression

4. Determine the pavement thickness based on fracture toughness
5. Select the maximum thickness determined in steps 1 through 4, above
6. Add a margin of safety

6.1 PAVEMENT DESIGN BASED ON CONTROL OF AIRCRAFT AND PAVEMENT VIBRATION RESPONSE

Port of New York Authority design methods are recommended to be adopted for control of aircraft and pavement vibration response. These methods assume the following conditions for vibration response to be held within a range of acceptable passenger comfort.

Vibration response of an aircraft in motion along a pavement is a function of the pavement roughness, aircraft velocity, and the natural frequency of the aircraft. It is conveniently modeled as the acceleration of the aircraft in a direction normal to the pavement.

The simplest model of aircraft/pavement interaction occurs with the aircraft moving across a smooth pavement. Aircraft vibrations caused by its motion and the rotation of its machinery become driving function for the vibration of the pavement. The pavement vibrates in response to excitation by the aircraft.

In normal use, the pavement is not smooth but develops surface deviations over time due to the stresses of use. The second model of vibration response has pavement roughness as a forcing function and aircraft vibration as a response. In the third level, the aircraft and pavement are responding to each other.

The allowable surface deviation (*) from a smooth plane as a pavement approaches the limit of its planned service life is related to the velocity and natural frequency of the aircraft and to the length of the deviation by

$$* = K L^{1/2} \qquad (6.1)$$

in which

$$K = .63\ DI \frac{f}{v} \qquad (6.2)$$

and

DI = tolerance for mean vehicle response
f = natural frequency of the aircraft
v = aircraft velocity
L = wavelength of the surface deviation

In this expression L is assumed to be that significant wavelength that, at the aircraft velocity, causes aircraft vibrations at the natural frequency of the aircraft.

The normal tolerance, DI, for vehicle response is the acceptable level of aircraft vibration during landing, taxiing, and takeoff, considering safety and comfort of passengers, and impact on pilots. It is assumed to be .12 g for pavements in concentrated traffic areas and .30 g for pavements in infrequent traffic areas.

The values of the constant K for typical conditions of aircraft operation are shown in the following table.

Condition	Velocity fps	Wavelength ft	Value of K DI = .12 g	Value of K DI = .3 g
Ground movement	10 - 15	3 - 7	.0100	.025
Taxiing	50 - 120	14 - 35	.0036	.009
Takeoff	170 - 340	50 - 70	.0026	.007

The maximum deformation that is expected to occur in a pavement after N traffic operations is defined by

$$D_N = D_1 + D_0 \log N \qquad (6.3)$$

in which

D_N = total transverse permanent deformation after N traffic operations

D_1 = a constant

D_0 = The rate of progressive transverse deformation

Values for the parameters D_1 and D_0 may be determined by testing.

6.2 PAVEMENT DESIGN BASED ON ELASTIC MASS ANALYSIS

The objective of elastic mass design methods is to determine the pavement thickness required to distribute the expected aircraft loads to the subgrade. The properties of the subgrade immediately below the pavement are the major factors in determining the ability of a flexible pavement to rebound from a deformation. Evidence of this was found in Newark tests[25] where more than 85 percent of the pavement's elastic deflection was transformed into deformation of the subgrade.

The thickness required of an LCF pavement in its elastic state is, therefore, determined from the elastic properties of the pavement and the subgrade.

In applying the Boussinesq theory for estimation of the stress-strain relationship in an elastic mass,[25] the following equations apply.

For distribution of the stress:

$$s_z = p \left[1 - (z / R)^3 \right] \qquad (6.4)$$

Where

s_z = Normal stress at depth z below the surface of elastic mass

p = Load intensity

R = $(a^2 + z^2)^{1/2}$

a = Radius of load area

For deformation W_z of the mass at depth z:

$$W_z = R \frac{p}{E} [2 - (z / R)^2 - z / R] \qquad (6.5)$$

Where

E = Young's modulus

z, p, R and a are defined above, and Poisson's ratio is assumed to be 0.

The modulus of resilience is defined as:

$$M_r = p (u + 0.2734) / s t \qquad (6.6)$$

In which

u = Poisson's ratio

t = specimen thickness

For short duration dynamic loads, such as imposed by a moving aircraft, Young's modulus is similar to the modulus of resilience. Substituting M for E_r in estimating the elastic mass deformation gives:

$$W_z = \frac{R p [2 - (z / R)^2 - z / R]}{M_r} \qquad (6.7)$$

If s_z and W_z in the above relationships are taken as the tolerance of the subgrade for stress and deformation, then z plus a margin of safety becomes the thickness of the pavement at those levels of stress and deformation.

6.3 PAVEMENT DESIGN BASED ON STRESS, STRAIN AND STRENGTH RELATIONSHIPS

As an LCF pavement ages, it exhibits the load response behavior of a slab. As a result, analysis of LCF pavement design must include consideration of the pavement as an elastic slab. The pavement should be designed to have a thickness that will enable it to withstand the stresses imposed by aircraft loads.

An elastic slab supported by an elastic medium, when subjected to a normal force, is deformed in one of the following three ways.[26]

If the action of the force is remote from any edge, then the slab is deformed to form a concave "dish" around the force location. The maximum stress, s_M, in the dish formed in a thin plate is expressed by:

$$s_M = \frac{3 (L + u) p}{6.28 t^2} (\log \frac{L}{a} + 0.61159) \qquad (6.8)$$

and the maximum deflection y_M of the pavement is:

$$y_M = \frac{p}{8 k L^2} \qquad (6.9)$$

where

u = Poisson's ratio
p = Single wheel load
a = Radius of tire contact area
t = Pavement thickness
E = Young's modulus
k = Subgrade modulus

and

$$L = [E t^3 / (12 k (1 - u^2))]^{1/4} \qquad (6.10)$$

A thick plate is one for which (a < 1.7 t). For a thick plate, the radius of tire contact area a is replaced by a so-called equivalent radius b, where

$$b = (1.6\ a^2 + t^2)^{1/2} - 0.675\ t \qquad (6.11)$$

If the force acts adjacent to an edge of a thin pavement but remote from a corner, then the maximum stress is located under the area of the load and is expressed by:

$$s_M = \frac{0.863\ (1 + u)\ p}{t^2} [\ \log \frac{L}{a} + 0.207\ ] \qquad (6.12)$$

The maximum pavement displacement is:

$$y_M = \frac{1}{6^{1/2}} (1 + 0.4\ u) \frac{p}{k\ L^2} \qquad (6.13)$$

and the equivalent radius b replaces the radius a for a thick pavement.

If the force acts in a corner of a thin pavement, so that the circle of its area is adjacent to two edges, then

$$s_M = \frac{3\ p}{t^2} [\ 1 - (a_1 / L)^{0.6}\ ] \qquad (6.14)$$

$$y_M = \frac{p}{k\ L^2} (1.1 - 0.88\ a_1 / L) \qquad (6.15)$$

where a_1 is the distance from the corner to the center of the area of the load, s occurs at a distance 2 L (a_1)$^{1/2}$ from the corner, y occurs at the corner, and the equivalent radius b replaces the radius a for a thick pavement.

6.3.1 PAVEMENT DESIGN BASED ON INDIRECT TENSILE STRENGTH

A flexible pavement subjected to an aircraft load experiences some tensile stresses. The stresses appear in deformed areas formed around the location of a tire.

The indirect tensile strength represents the yield strength load of the materials used in the testing program when they are under tensile load. The pavement slab design must have sufficient strength to withstand the expected tensile stresses.

The design procedure has two objectives:

- Set the pavement thickness to a value that will ensure that the maximum stress in the pavement is less than the indirect tensile strength by an adequate margin of safety, and
- Set the pavement thickness to a value that will ensure that the maximum pavement stress is less than s_y.

According to the first objective:

$$t < \frac{p}{3.16\, a\, s_y} + M \qquad (6.16)$$

where

s_y = Tensile strength defined in equation 2.2
p = Single tire load
a = Radius of tire area on pavement
M = Margin of safety

According to the second objective:

$$s_M < s_y \qquad (6.17)$$

where s_M is the maximum stress in equations 6.8, 6.12 and 6.14.

6.3.2 PAVEMENT DESIGN BASED ON COMPRESSIVE STRENGTH

A flexible pavement subjected to an aircraft load experiences compression forces. The forces appear under the aircraft tires and in concave regions of curvature where a depression ("dish") is formed around the location of a tire.

The compressive strength represents the yield strength load of the materials used in the testing program when they are under compressive load. The pavement slab design must have sufficient strength to withstand the expected compression stresses.

The design procedure is to set the pavement thickness to a value that will ensure that the maximum stress in the pavement is less than the compressive strength by an adequate margin of safety. For this situation to occur, the following relationship must hold:

$$s < q_u \qquad (6.18)$$

where s is the maximum value from equations 6.8, 6.12 and 6.14, and q_u is the compressive strength.

6.4 PAVEMENT DESIGN BASED ON FRACTURE TOUGHNESS

Load induced cracks in pavement slabs are usually caused by the force of aircraft tires near the edges of the slabs. The cracks normally originate at a slab edge and migrate toward the interior. Crack propagation is promoted by repeated stresses caused by aircraft loads.

The ability of a slab to resist the spread of fractures may be characterized as fracture toughness K_{1c}. Equation 2.3 on page 44 defines K_{1c}.
By substituting the radius (a) of the tire contact area for the variable R and defining $\underline{t}$ to be the pavement thickness in equations 2.3 through 2.5, the minimum pavement thickness to inhibit the spread of cracks is:

$$t = F(s)\ F(g)\ C^{1/2}\ \frac{P}{K_{1c}\ a} + M \qquad (6.19)$$

where

$$F(s) = 6.530078e^{4.30577\ (C\ /\ a)^{2.475}} \qquad (6.20)$$

$$F(g) = 3.950373e^{-3.07103\ (C\ /\ a)^{0.25}} \qquad (6.21)$$

and

C = Length of pavement cracks
M = Margin of safety
p = Applied load (pounds)
t = Slab thickness (inches)

6.5 MARGIN OF SAFETY

The values selected for the allowable stresses should be low enough to allow for uncertainties that are unavoidably present. Some of the uncertainties may be due to:

- Variations in the chemical properties of the constituent components used to mix the LCF,
- Lack of homogeneity and uniformity in the construction of the pavement,
- Deterioration due to wear, and/or
- Deterioration due to the action of chemicals in the subgrade or spilled on the pavement.

Although the values of the allowable stresses should be taken sufficiently low to allow for the many inaccuracies, they should be high enough to permit efficient and economical use of the material. Tests conducted in this study resulted in variations of up to 50 percent in the measured stress levels. A 50 percent margin of safety is suggested for use in the design of LCF pavements.

CHAPTER 7 - RECOMMENDATIONS

The following recommendations result from the LCF test and analysis activities:

1. It is recommended that a pavement design approach that recognizes the variability of LCF properties be developed using methods similar to those described in Chapter 6.

2. Fatigue tests should be used that more nearly approximate the stresses encountered when exposed to moving traffic in the field, as discussed in section 3.8.4. It is recommended that a new method of fatigue testing be established and that the new method load the test samples using cyclical stress reversal.

3. In order to be able to accurately determine the time of onset of cracks during fatigue testing, it is recommended that more sensitive methods of observation be used, such as stress coating, trip gages, or acoustic signature techniques.

BIBLIOGRAPHY

1. George, K.P., "Development of a Freeze-Thaw Test for Evaluating Stabilized Soils," Master's Thesis, Iowa State University, Ames, Iowa (1961).

2. Robinett, Q.L. and Thompson, M.R., "Soil Stabilization Literature Reviews," Civil Engineering Studies, Highway Engineering Series No. 34, June 1969, University of Illinois, Urbana, Illinois.

3. Yang, Nai C., Design of Functional Pavements, McGraw-Hill Book Company, New York, 1972, Page 130.

4. Viskochil, R.K., Handy, R.L., and Davidson, D.T., "Effect of Density on Strength of Lime-Flyash Stabilization Soil," Highway Research Board Bulletin 183, pp. 5-30, 1957, National Academy of Sciences - National Research Council, Washington, D.C.

5. Towsend, F.C. and Donaghe, R.T., "Investigation of Accelerated Curing of Soil-Lime and Lime-Flyash-Aggregate Mixtures," Report S-76-9, August 1976, U.S. Army Engineer Waterways Experiment Station, CE, Vicksburg, Mississippi.

6. Hollen, G.W. and Marks, B.A., "A Correlation of Published Data on Lime-Pozzolan-Aggregate Mixtures for Highway Base Course Construction," Circular 72, 1962, Engineering Experiment Station, University of Illinois, Urbana, Illinois.

7. "Lime-Flyash-Stabilized Bases and Subbases," Synthesis 37, National Cooperative Highway Research Program, 1976.

8. Halstead, W.J., "Quality Control of Highway Concrete Containing Fly Ash," Virginia Highway and Transportation Research Council Report VHTRC 81-R38, 1981, National Ready Mixed Concrete Association, Silver Spring, Maryland.

9. Dempsey, B.J. and Thompson, M.R., "Interim Report - Durability Testing of Stabilized Materials," Civil Engineering Studies, Transportation Engineering Series No. 1, Illinois Cooperative Highway Research Program, Series No. 132, University of Illinois at Urbana Champaign, Sept. 1972.

10. Dempsey, B.J. and Thompson, M.R., "A Vacuum Saturation Method for Predicting the Freeze-Thaw Durability of Stabilized Materials," Record No. 442, Highway Research Board, 1973.

11. Terrel, R.L., Epps, J.A., Barenberg, E.J., Mitchell, J.K., and Thompson, M.R., "Soil Stabilization In Pavement Structures A User's Manual Volume 1 Pavement Design and Construction Considerations," Report DOT-FH-11-9406, U.S. Department of Transportation, Federal Highway Administration, 1975.

12. MacMurdo, F.D., and Barenberg, E.J., "Determination of Realistic Cutoff Dates for Late-Season Construction with Lime-Flyash and LCF Mixtures," Highway Research Record No. 442 (1973) pp. 92-101.

13. Thompson, M.R., and Dempsey, B.J., "Final Report - Durability Testing of Stabilized Materials," Civil Engineering Studies, Transportation Engineering Series No. 11, Illinois Cooperative Highway Research Program, Series No. 152, University of Illinois, Urbana, Ill. (June 1974)

14. Terrel, R.L., Epps, J.A., Barenberg, E.J., Mitchell, J.K., and Thompson, M.R., "Soil Stabilization In Pavement Structures A User's Manual Volume 2 Mixture Design Considerations," Report DOT-FH-11-9406, U.S. Department of Transportation, Federal Highway Administration, 1979.

15. Barenberg, E.J., "Lime-Flyash Aggregate Mixtures in Pavement Construction," Process and Technical Data Publication, National Ash Association (1974).

16. Ahlberg, H.L., and Barenberg, E.J., "Pozzolanic Pavements," Bulletin 473, Eng. Experiment Station, University of Illinois, Urbana, Illinois (1965).

17. Callahan, J.P., Morrow, J., and Ahlberg, H.L., "Autogenous Healing in Lime-Pozzolan-Aggregate Mixtures," Report No. 631. Department of Theoretical and Applied Mechanics, College of Engineering, University of Illinois, Urbana, Illinois (1962).

18. Ahlberg, H.L., and McVinnie, W.W., "Fatigue Behavior of a Lime-Flyash-Aggregate Mixtures," HRB Bulletin 325 (1962) pp. 1-10.

19. Miller, R.H., and Couturier, R.R., "Measuring Thermal Expansion of Lime-Flyash-Aggregate Compositions Using SR-4 Strain Gages," Highway Research Record No. 29 (1963) pp. 83-94.

20. Ahlberg, H.L., and Barenberg, E.J., "The University of Illinois Pavement Test Track - A Tool for Evaluating Highway Pavements," Highway Research Record No. 13 (1963) pp. 1-21.

21. Barenberg, E.J., "Behavior and Performance of Asphalt Pavements with Lime-Flyash-Aggregate Bases," Proc. Second International Conference on the Structural Design of Asphalt Pavements, Ann Arbor, Michigan (1967) pp. 619-633.

22. McLaughlin, A.L., The Performance of Civil Airport Pavements with LCF Base Course, FAA Report No. DOT/FAA/PM-84/10; April, 1984.

23. "Observations of Field Performance of Continuously Reinforced Concrete Pavements in Ohio," Ohio DOT-12-77, September, 1978.

24. Montgomery, D.C., Design and Analysis of Experiments, 2nd Edition, John Wiley and Sons, 1976.

25. Yang, Nai C.. "Systems of Pavement Design and Analysis," Proceedings,

47th Annual Meeting of Committee on Theory of Pavement Design.

26. Roark, Raymond J., Formulas for Stress and Strain, 4th Edition, McGraw-Hill Book Company, 1965.

27. Specification for "LCF Stabilized Fill Sand Base", Port of New York Authority.

28. Specification No. 26-00029-040, "LCF Pavement Base", City of Houston, Airport Engineer Office.

29. Airport Pavement Design and Evaluation, FAA Advisory Circular AC 150/5320-6C, December, 1978.

30. Bergstrom, S.G., "Curing Temperature, Age and Strength of Concrete," Magazine of Concrete Research, December, 1953.